KATHMANDU UNIVERISTY

SCHOOL OF ENGINEERING

DEPARTMENT OF CIVIL& GEOMATICS ENGINEERING

DISSERTATION

TUNNEL CLOSURE ANALYSIS OF HYDROPOWER TUNNELS IN LESSER HIMALAYAN REGION OF NEPAL THROUGH CASE STUDIES

In Partial Fulfillment of the Requirements for the Doctor of Philosophy Degree in

Civil Engineering

by

Shyam Sundar Khadka

January 2019

ACKNOWLEDGEMENT

I express my sincere gratitude to the Department of Civil & Geomatics Engineering, School of Engineering of Kathmandu University for support to me in pursuing this doctoral work through the Faculty Development Program. I express my sincere thanks to Prof. Dr. Ramesh Kumar Maskey, Kathmandu University, Prof. Dr. Seokwon Jeon, Seoul National University, South Korea for their support and encouragement during my thesis work.

My special thanks go to Prof. Dr. Antonio Topa Gomes for accepting me to supervise my PhD work as a Local supervisor at University of Porto, Portugal, during Erasmus Mundus Scholarship. I am very grateful to him for his support, encouragement, and correction of the thesis from the very beginning. I am also thankful to Seoul National University- Woongjin Scholarship for providing a scholarship to study at the Department of Energy Systems Engineering, Seoul National University, Korea. Similarly, Erasmus Mundus- Leader Project for providing a scholarship to do research work at the University of Porto, Portugal for one year.

I am very much thankful to Prof. Dr. Bhola Thapa, former Registrar, Kathmandu University, for his encouragement and support to do my PhD work in underground structures. I am also thankful to Dr. Damber Bahadur Nepal, Dean, Dr. Prachand Man Pradhan, Head of Department of Civil & Geomatics Engineering, Dr. Rabindra Bista, and Prof. Dr. Bhupendra Bimal Chhetri, former Dean, School of Engineering for their help. I am thankful to Prof. Dr. Subodh Sharma, Registrar, Kathmandu University for his support to complete PhD. I am also thankful to Mr. Tore Skeie for his support during the coursework of Tunneling & Underground structure and his valuable suggestion during the PhD work. I would also like to thank all my colleagues and friends at Kathmandu University, Nepal, Seoul National University, Korea and the University of Porto, Portugal.

And lastly but not least I thank my mother Sumitra Khadka, my father Shree Krishna Khadka for their countless effort what they did and are doing for future. My special thanks go to my brothers, Shekhar and Bhasker, sister, Vijaya, and especially my wife Deepa, and my son Amush for their understanding while I was abroad during for my research work and also the newly born my daughter Anika.

ABSTRACT

In the Lesser Himalayan region of Nepal, medium to mega-size hydropower projects, road tunnels for short and effective route in steep terrain and other underground structures are under construction day-by-day. It is found that most hydropower tunnels undergo excessive deformation and support failure during and after construction as it passes through very weak rock masses with high overburden pressure. The estimation of rock support pressure and selection of tunnel support are carried out by empirical methods since basically rock mass classification approaches are not adequate to encounter stability problems. To understand the behavior of weak and jointed rock mass, a detailed 2D finite element analysis has been performed for different qualities of rock masses of six hydropower tunnels located in the Lesser Himalayan region. Geological Strength Index (GSI) system is used to estimate the peak strength of jointed rock mass based on the geological conditions.

In the numerical modeling, the rock mass is characterized by the GSI method and the rock mass parameter are estimated using generalized Hoek Brown failure criteria. The numerical analysis is carried out for unsupported and supported tunnels with elastic-perfectly plastic and strain-softening (residual strength) constitutive models. The disturbance factor (D) is also considered for the analysis. In the elastic-perfectly plastic analysis, the peak GSI is used only, that is, there is no reduction of GSI. It is assumed that the GSI remains the same before and after tunnel excavation while the strain-softening constitutive model is assumed in which the residual strength is accounted by the reduction of the peak GSI.

Based on the rock mass conditions, different rock mass models are presented which can address the real behavior of rock mass. For extremely poor rock mass, i.e. GSI less than 30, the elastic-plastic failure characteristic is more appropriate with the disturbance factor taken as zero. It is found that the disturbance factor has a great influence on the modeling of such weak rock mass in the Himalayan region.

For very poor to poor rock mass, moderately jointed, (30<GSI<50), the strain-softening failure characteristics is more appropriate. In this case, the disturbance factor is taken as 0.5. The residual strength parameters are taken as between 60 and 70 % of the peak value. Similarly, for fair to good rock mass (50<GSI<65), the strain- softening failure characteristics is suitable when the residual strength parameters are taken as between 40 and

50 % of the peak value which represented crushing of the intact rock and wearing joint surface roughness.

3D numerical analysis is carried out for two case studies; namely Kulekhani III and Chameliya hydropower tunnel. Both hydropower tunnels pass through extremely poor, poor, fair and good quality of rock masses at different cross-sections along their route. The preliminary conclusion from the 2D analysis is used for modeling such rock mass. It is concluded that the appropriate numerical models are suitable for analysis and design of tunnel supports in such geological conditions. There is no significant stability problem as the tunnel passes through fair and good rock quality. But as the tunnel section passes through extremely poor and poor rock quality, there could be stability problems of support at the lower corner of the wall and invert. Rock support around the tunnel suggests by the rock mass classification approach is uniform support around the excavation, but from the numerical analysis, it is observed that the lower corners of wall and invert are more critical than the crown.

TABLE OF CONTENTS

LIST OF FIGURES

LIST OF TABLES

1 INTRODUCTION

1.1 Background

Nepal has the longest division of the Himalaya occupying the central sector of the Himalayan arc. Its extension is about 880 km from east to west and has a width ranging from 150 to 250 km. Nepal has tremendous potential for hydropower development because its steep terrain and fast flowing rivers originating from the glaciers fulfill the basic need. Construction of underground structures like tunnels and caverns are useful for achieving such development activities with a thorough understanding of the geological condition.

Due to active tectonic movement and dynamic monsoon, the rock mass in the Himalayan is relatively weak and highly deformed, weathered and altered. The major tectonic thrust faults such as Main Central Thrust (MCT) and Main Boundary Thrust (MBT) have a significant influence on the high degree of shearing and fracturing to the rock mass. Predicting rock mass quality, analyzing stress-induced problems, in particular, tunnel squeezing, and predicting water inflow and leakage often have been found extremely difficult. Considerable discrepancies have been found between predicted and real rock mass conditions, resulting in significant cost and time overrun for most of the tunneling projects (Panthi & Nilsen, 2007).

From the last decade, the construction of underground structures, like tunnel and caverns, has considerably increased day-by-day in the Lesser Himalaya. Due to a few detailed studies on ever-changing Himalayan region and geological condition in Nepal, it has been difficult to predict the effect of geology on underground structures. The need of study is not only relevant to underground structures such as tunnels but also to the sound structural stability of small to large-scale projects.

This research mainly focuses on the tunnel closure analysis of hydropower tunnel in the weak geology. The study area lies within the Lesser Himalaya of Nepal where rock masses are weak, highly jointed, weathered, faulted, folded and tectonically disturbed with high overburden. High mountainous topography causes high overburden pressure in the underground structures causing squeezing and other stability problems. This geological difficulty resulted in a huge financial burden because of heavily reinforced support in the squeezed section.

1.2 Problem Statement

Nepal lies in a highly seismically vulnerable region by its proximity to the young Himalayan range and the ongoing neo-tectonic activities in the region. The seismicity of the country is attributed to the location of the region in the subduction zone of Indian and Asian tectonic plate (Khadka, 2013). Due to this active tectonic movement, the rock masses in Nepal are fragile. Weak rock mass quality with high rock stress is one of the major stability problems during tunneling in the Lesser Himalayan region of Nepal (Panthi, 2006). Tunnel failure is mainly due to the failure of weak rock mass around a tunnel and the influence of high overburden pressure or tectonic stresses. Almost all tunnels constructed in this region experienced excessive deformation (Panthi, 2006). In general, tunneling through such weak rock mass may cause severe squeezing problems.

On the basis of tunnel closures, the squeezing ground conditions have been classified into four classes by Hoek (2001) as minor, severe, very severe and extreme squeezing ground conditions as shown in Figure 2-8 (Singh & Goel, 2011). Tunnel closure is defined as the ratio of the wall displacement of the tunnel with respect to tunnel radius. It depends significantly on the method of excavation. In extreme squeezing ground conditions, tunnel closure may lead more than 8% and more than 4% of tunnel span should not allow, otherwise support pressure is likely to build up rapidly due to the failure of rock arch (Singh & Goel, 2011).

Existing hydropower tunnels from different hydropower projects like Kaligandaki, Middle Marsyangdi, Modi and Khmiti have a considerable amount of squeezing occurred while tunneling. Similarly, the headrace tunnel of Chameliya hydroelectric project, located in the western part of the lesser Himalayan region of Nepal, has faced severe squeezing problem resulted into a huge financial loss because of heavily reinforced support in the squeezed section. Therefore, the knowledge on squeezing or non-squeezing ground plays an important role in designing the support system.

1.3 Objectives of Study

The primary objective of this study is to do tunnel closure analysis of hydropower tunnels located in the Lesser Himalayan region of Nepal. To achieve the primary objective, the following secondary objectives are studied in detailed.

1. Tunnel closure analysis of different case studies.
2. Different rock models are used to predict appropriate numerical modeling
3. Stability analysis of tunnels of the case studies using existing empirical, semi-empirical and analytical methods.
4. 2D and 3D numerical modeling of tunnels.

To fulfill the above objectives, a detailed literature survey has been carried out and two hydropower tunnels have been studied in detail with available data. For numerical modeling, Rocscience finite element analysis software RS2 and RS3 (Rocscience, 2016) has been used for analysis of tunnels in 2D and 3D modeling, respectively.

1.4 Scope of Research

From the experience of tunneling in this region, the rock mass classification approaches are not adequate to estimate the tunnel support. Most of the hydropower tunnels experienced excessive deformation due to poor rock mass and high in-situ stress. Tunnels from Kaligandaki, Modi, Chameliya hydropower projects experienced the severe tunnel deformation due to squeezing of rock around the tunnel. It is difficult to tackle the severe squeezing in tunneling through Himalaya rock mass. Till date, no uniform solution exists that may control instability caused by tunnel squeezing of such magnitudes (Panthi, 2006). Therefore, the existing empirical, semi-empirical and analytical methods are not sufficient for analysis and design of support. Proper numerical modeling should be carried out to predict the excessive deformation of rock mass around the tunnel. From this research work, the following questions could be addressed:

- What are the driving forces and factors that cause squeezing problems in the Himalayan region of Nepal?
- Are the existing support design methods sufficient to address the squeezing phenomenon of tunnels in different rock masses?
- What types of support elements and arrangement of supports are necessary to design underground structures in the Himalayan region?

In Nepal, it is very difficult to get published and recorded data from the hydropower projects due to cost, lack of knowledge of the investigation and not measuring tunnel deformation for the future and others. Hence, it is not possible to get much more sources and information. Therefore, case studies are selected on the basis of the information regarding site investigation, laboratory testing, rock mass quality logs, tunnel support details can be obtained as more as possible.

Based on the tunnel closures, Goel et al. (1994) defined the degree of squeezing of the tunnel as very mild, mild, mild to moderate, moderate, high and very high squeezing, presented in Table 2.3 and Figure 2-7. The available data related to the ground conditions of the selected case projects are studied. Numerical analysis is carried out to predict real ground behavior while tunneling. Different non-linear stress-strain constitutive model is adopted to represent the ground surrounding the tunnel. The results are predicted in terms of the tunnel closure around the opening. Therefore, an only time-independent analysis is considered.

1.5 Research Methodology

Limited research has been conducted in context to the stability analysis of underground structures in the Nepal Himalaya. Stress-induced failure is the common failure in the Himalayan geology having high overburden and poor rock mass quality. Six hydropower tunnels are selected for the 2D numerical modeling. The output from 2D numerical modeling is used for 3D modeling of two hydropower tunnels, namely Khulekhani III and Chameliya, taken as case studies in this PhD work. These are nearing completion.

To meet the above-mentioned research questions, the following research methodology is applied in this study as presented in Figure 1-1.

1. Literature review related:
    - To geology of the Himalaya regarding stress regime, rock types, weathering effect on rock mass and tectonic influence.
    - To rock mass classification and support design methods.
    - To the existing empirical, semi empirical and analytical methods to evaluate the squeezing potential and design of undergrounds structures.
    - To numerical modeling and analysis of underground structures.

2. Data collection: It includes the project details and engineering geological information on the rock mass condition. Geological properties of rock masses will be referred from the as provided.
3. Stability analysis: The stability analysis is carried out by empirical, semi-empirical and analytical methods. Support system requirement will be proposed accordingly in terms of different rock mass classification.

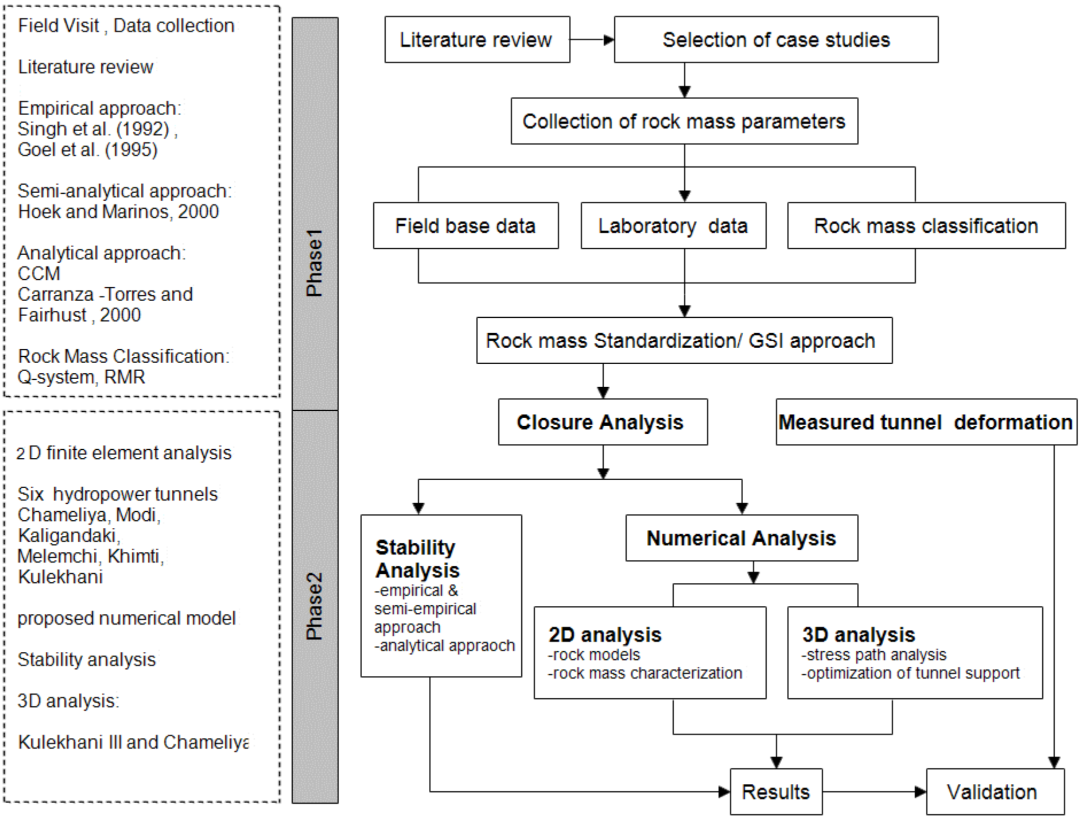

Figure 1-1 General methodology used in the study

4. Numerical Analysis:
   - Commercially available finite element software, from RocScience, RS3 and RS2 are used for 3D and 2D analysis, respectively.
   - The parameters calculated by empirical methods will be used as input parameters for the finite element analysis.
5. Based on the existing empirical, semi- empirical, analytical and numerical methods, design supports are recommended for the stability analysis of underground structures.

1.6 Organization of Dissertation

The study is divided into six chapters. In Chapter 2, various literature related to the research works is surveyed in detail. Literature related to the geology of Himalaya, empirical and semi-empirical methods for assessing the tunnel stability in terms of squeezing, rock mass classification system are studied, an analytical method, i.e. Convergence Confinement Method, is discussed and also literature related to numerical methods is also discussed in detail.

Chapter 3 discusses the different rock failure models, Mohr-Coulomb failure criterion and Generalized Hoek-Brown failure criterion are discussed in detail. It discusses 2D numerical modeling in tunnels and its suitability for the design of tunnels.

Chapter 4 presents the study of case studies with description.

Chapter 5 presents 3D numerical modeling of case tunnels in details.

Chapter 6 presents the overall conclusions of the study.

2 COMMON DESIGN PRACTICE OF UNDERGROUND STRUCTURES

2.1 General

This chapter presents the available literature related to the description of Himalayan geology of Nepal, design practice of tunnel support by rock mass classification, closed-form solution for analyzing circular tunnel using Hoek-Brown criterion. Extensive researches and works have been carried out to design and assessing the squeezing behavior of tunnel in different parts of the world. A brief description of such research works is presented in this chapter which is relevant for this research work in terms of empirical and semi-empirical methods. It also briefly describes the numerical methods and its application to underground structures to access the stability.

2.2 General Review of Himalayan Geology

The Himalayan range is young and weak mountain system of the world. It is a broad continuous arc along the northern fringes of the Indian subcontinent, from the end of the Indus River in the northwest to the Brahmaputra River in the east. Many scientists believe that at that time the northward-moving Indian plate first touched the southern edge of Tibetan (Eurasian) Plate. The mountain building (orogenic) process continues from the collision and the mountain is still on making process.

Nepal has the longest division of the Himalaya. Its extension is about 800 km and starts from the west at the Mahakali River and ends at the east by the Mechi River. Nepal occupying the central sector of Himalayan arc similar topographic division can be seen throughout. Basically, the geology of Nepal is divided into following five zones; the Gangetic plain (Terai zone), the Sub-Himalayan zone, the Lesser Himalayan zone, the Higher Himalayan zone, and the Tibetan-Tethys zone as shown in Figure 2. The main rock types found in these regions are shown in Table 2.1.

Table 2.1 Geomorphic units of Nepal and main types of rocks (Upreti, 1999)

Geomorphic Unit	Width(km)	Altitudes (m)	Main rock types
Gangetic plain (Terai zone)	20-50	100-200	Alluvium deposits ,coarse gravel in the north near the foot of mountains
Siwaliks (Churia Group)	10-50	200-1000	Sandstone, mudstone, shale and Conglomerate etc
Lesser Himalayan Zone	70-165	1000-5000	Schist, Phyllite, gneiss, quartzite, granite, marble and dolomite.
Higher Himalayan Zone	10-60	> 5000	Gneisses schists and marbles
Tibetan-Tethys zone	-	2500 – 4000	Gneisses schists and marbles of Higher Himalayan Zone and Tethyan sediments (limestone, shale, sandstone etc)

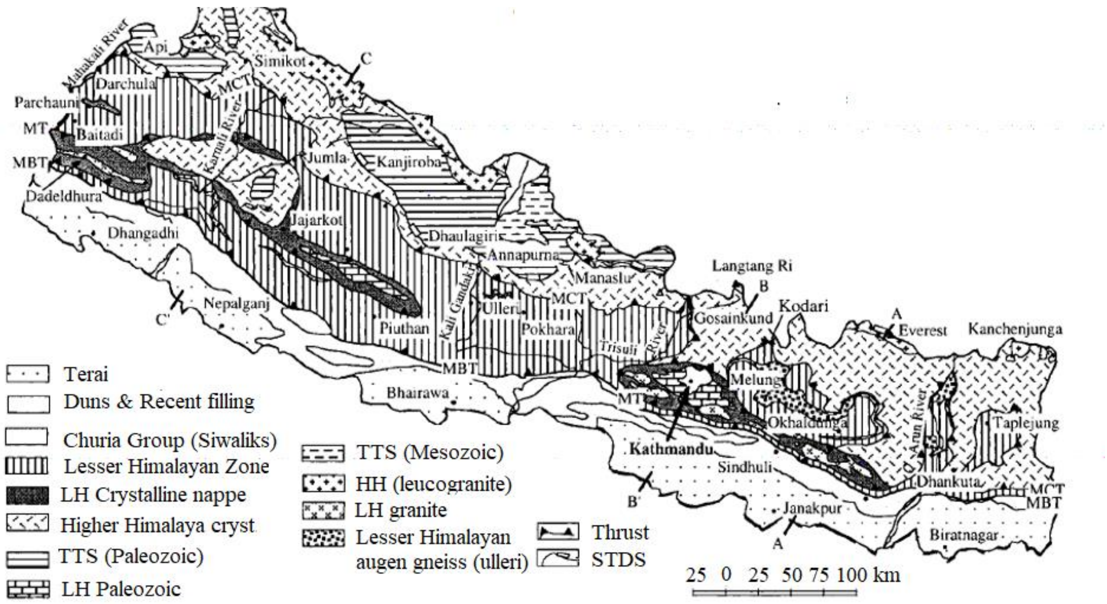

Figure 2-1 Geological map of Nepal (Upreti, 1999)

This can be summarized as the major 3-tectonic zones: - Main Central Thrust (MCT): tectonic contact between Higher Himalayas and Lesser Himalayas, Main Boundary Thrust (MBT): active tectonic contact between the Lesser Himalayas and the Siwaliks and Himalayan Frontal Thrust (HFT), or Main Frontal Thrust (MFT): tectonic feature located between the boundary of Siwaliks and the Terai. Those are active faults, as shown in Figure 2-2.

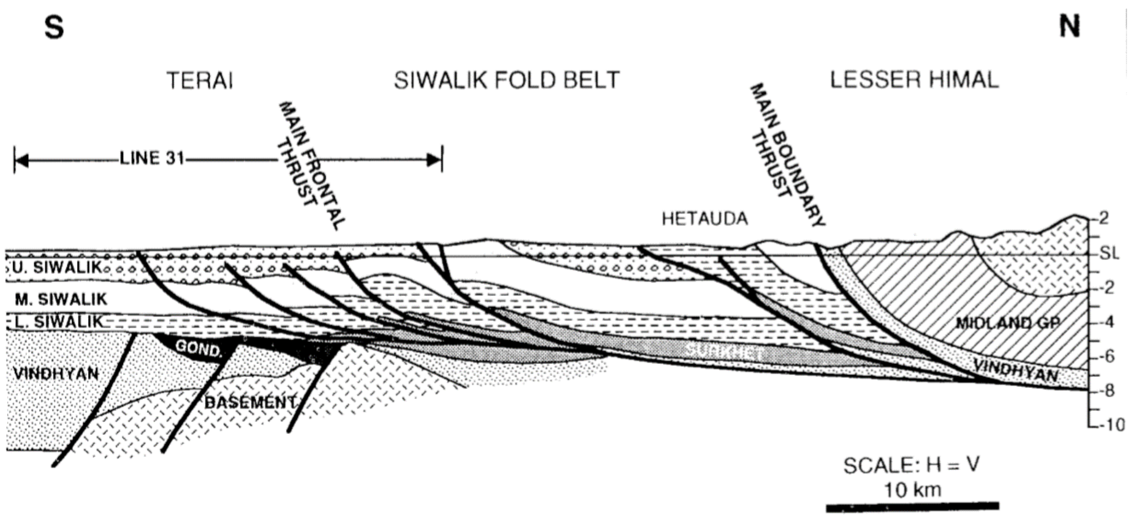

Figure 2-2 Structural cross section across Terai, Siwaliks, Lesser Himalaya Nepal (Upreti, 1999)

2.3 Rock Mass Classification

Extensive researches have been done in the rock mass classification for the design of underground structures. The most common empirical methods for tunneling are Rock Mass Rating (RMR) (Bieniawski 1989), Rock Mass Quality (*Q* system) (Barton et al. 1974) and Geological Strength Index (GSI) (Hoek, 1994; Hoek et al, 1995; Hoek & Marinos, 2000; Marinos et al, 2005; Hoek et al, 2005) in the Himalayan region of Nepal. These three methods incorporate geological, geometric and design/engineering parameters in arriving at a quantitative value of their rock mass quality.

The similarities between RMR and Q- system come from the use of identical, or very similar, parameters in calculating the final rock mass quality rating. The differences between the systems lie in the different weightings given to similar parameters and in the use of distinct parameters in one or the other scheme. RMR uses compressive strength directly while Q only considers strength as it relates to in situ stress in competent rock. Both schemes deal with the geology and geometry of the rock mass but in slightly different ways. The greatest difference between the two systems is the lack of a stress parameter in the RMR system.

2.3.1 Rock Mass Rating (RMR)

Bieniawski (1989) published the details of a rock mass classification called the Geomechanics Classification or the Rock Mass Rating (RMR) system. Over the years, this system has been successively refined as more case records have been examined and it should be noted that Bieniawski has made significant changes in the ratings assigned to different parameters. The discussion which follows is based upon the 1989 version of the classification (Bieniawski, 1989).

Table 2.2 Guidelines for excavation and support of rock tunnels in accordance with the RMR system (Bieniawaski, 1989)

Rock mass class	Excavation	Supports		
		Rock bolts (20 mm dia. Fully grouted)	Conventional shotcrete	Steel sets
Very good rock RMR =81-100	Full face 3 m advance	Generally, no support required except for occasional spot bolting		
Good Rock RMR= 61-80	Full face 1.0-1.5 m advance. Complete support 20 m from face	Locally, bolts in crown 3 m long, spaced 2.5 m, with occasional mesh	50 mm in crown where required	None
Fair rock RMR= 41-60	Heading and bench. 1.5 -3 m advance in heading. Commence support after each blast. Complete support 10 m from face.	Systematic bolts 4 m long, spaced 1.5-2 m in crown and walls with wire mesh in crown	50-100 mm in crown and 30 mm in sides	None
Poor rock RMR= 21-40	Top heading and bench. 1.0 -1.5 m advance in top heading. Install support concurrently with excavation 10 m from face.	Systematic bolts 4-5 m long, spaced 1-1.5 m in crown and wall with wire mesh.	100-150 mm in crown and 10 mm in sides	Light to medium ribs spaced 1.5 m where required.
Very poor rock RMR<20	Multiple drift 0.5-1.5 m advance in top heading. Install support concurrently with excavation. Shotcrete as soon as possible after blasting	Systematic bolts 5-6 m long, spaced 1-1.5 m in crown and walls with wire mesh. Bolt invert	150-200 mm in crown 150 mm in sides and 50 mm on face	Medium to heavy ribs spaced 0.75 m with steel lagging and forepoling if required. Close invert

To apply the geomechanics classification system, a given site should be divided into several geological structural units in such a way that each type of rock mass is represented by a separate geological unit. The following six parameters are used to classify a rock mass using the RMR system: i) uniaxial compressive strength of rock material, ii) Rock Quality Designation (RQD), iii) joint or discontinuity spacing, iv) joint conditions, v) groundwater conditions, and vi) joint orientation. The rating from each six parameters is used for evaluating the RMR of rock mass.

Guidelines for selection of tunnel support is presented in Table 2.2, based on the RMR values, which is applicable to tunnels excavated with conventional drilling and blasting method. These guidelines depend upon the factors like depth below surface (to take care of overburden pressure or in situ stress), tunnel size and shape and method of excavation.

2.3.2 Rock Mass Quality (Q- system)

Barton et al. (1974) at the Norwegian Geotechnical Institute (NGI) proposed the Rock Mass Quality (Q) System of rock mass classification on the basis of about 200 case histories of tunnels and caverns. It is a quantitative classification system, and it is an engineering system enabling the design of tunnel supports. The numerical value of the index Q varies in logarithmic scale from 0.001 to a maximum of 1000.

The concept upon which the Q system is based upon three fundamental requirements:

a. Classification of the relevant rock mass quality,
b. Choice of the optimum dimensions of the excavation with consideration given to its intended purpose and the required factor of safety,
c. Estimation of the appropriate support requirements for that excavation.

The Q-System is based on a numerical assessment of the rock mass quality using six different parameters:

$$Q = \frac{\mathrm{RQD}}{J_n} . \frac{J_r}{J_a} . \frac{J_w}{\mathrm{SRF}} \tag{2.1}$$

where, RQD is the Rock Quality Designation, J_n is the joint set number, J_r, is the joint roughness number, J_a, is the joint alteration number, J_w, is the joint water reduction factor and SRF is the stress reduction factor.

The three quotients in the Q system can be explained as follows: the quotient RQD/J_n is a crude measure of the block or particle size, the second quotient J_r/J_a represents the roughness and frictional characteristics of the wall or filling materials, and the third quotient J_w/SRF consists of two parameters. While J_w can be directly related to water pressure values across the joint, while SRF bears more complicated relationship with a number of factors such as 1) loosening load in the case of an excavation through shear zones and clay bearing rock, 2) rock stress in competent rock, and 3) squeezing loads in plastic incompetent rock.

For various rock conditions, the rating (numerical values) to these six parameters are assigned. The details of rating can be found in Barton et al, 1974. The goal of Q-system is preliminary empirical design of support system for tunnels and caverns. There are 1260 case records to prove efficacy of this design approach.

The ratings of these parameters obtained for a given rock mass is substituted in above equation to get rock mass quality Q. In addition to the Q- value two other factors are decisive for the support design in underground openings. These factors are the safety requirements and the dimension, i.e., the span or height of the underground opening. Generally, there will be an increasing need for support with increasing span and increasing wall height. Safety requirements will depend on the purpose of the excavation.

The Q-value and the equivalent dimension will be decisive for the permanent support design. In the support chart shown in Figure 2-3, the Q values are plotted along the horizontal axis and the Equivalent dimension along the vertical axis on the left-hand side. For the given combination of Q- value and Equivalent dimension, a given type of support has been used and the support chart has been divided into areas according to type of support.

In sections with very poor rock mass quality ($Q<1$), Reinforced Ribs Shotcrete (RRS) in many cases is a preferred alternative to cast concrete, Figure 2-3, the ribs are constructed with a combination of steel bars (usually with a diameter of 16 mm or 20 mm), sprayed concrete and rock bolts. The thickness of the ribs, the spacing between them as well as the number of ribs and diameter of the steel bars must vary according to the dimension of the underground opening and the rock mass quality.

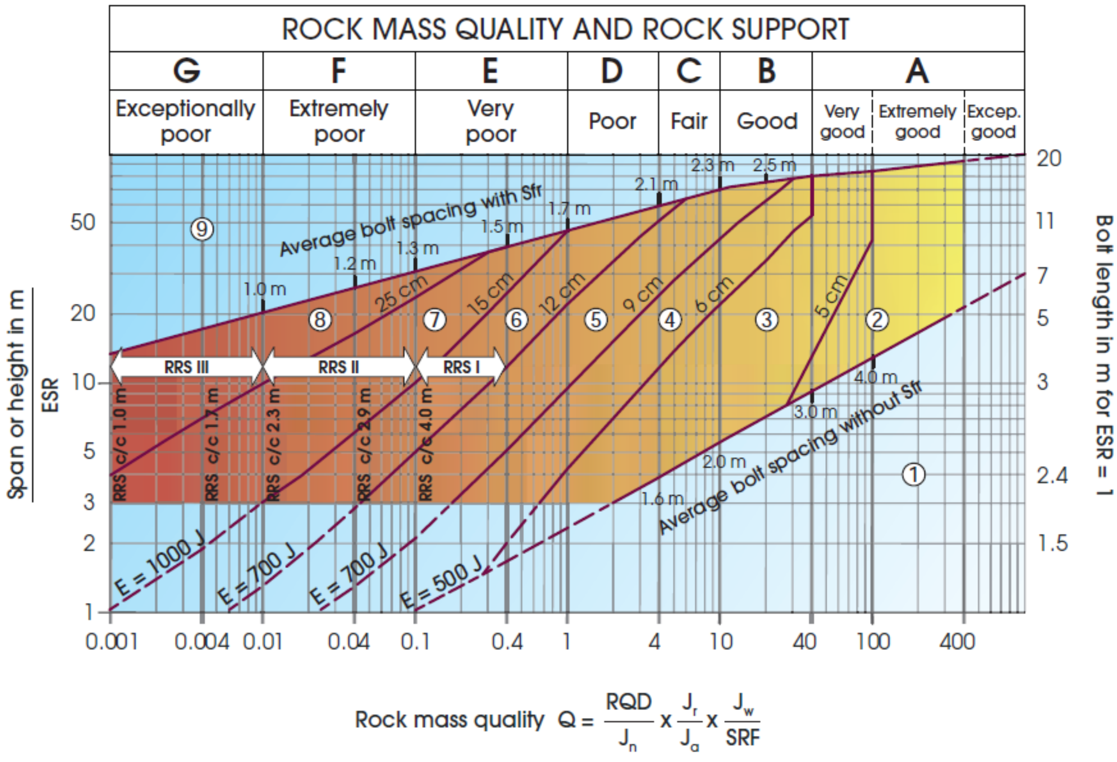

Figure 2-3 Permanent support recommendations based on Q values and span/ESR (NGI, 2013)

Singh & Goel (2006), concluded that in-situ stress and water pressure are should be considered in rock mass classification in Q system because they are external and internal boundary conditions which are taken into account in all software packages. Stress reduction factor (SRF) depends upon the depth of tunnel, external boundary conditions, and needs to be consider in the rock mass classification system. It helps to develop the total concept of rock mass quality. It is the best among all the classification system for support in tunnels. Q-system is very useful for empirical design of support system for tunnels and caverns and it has been extended to the rock mass characterization successfully (Barton, 2002).

2.3.3 Geological Strength Index (GSI)

The geological strength index (GSI) is a system of rock-mass characterization, initially proposed by Hoek (1995), that has been developed in engineering rock mechanics to meet the need for reliable input data, particularly those related to rock-mass properties required as inputs into numerical analysis or closed form solutions for designing tunnels, slopes or foundations in rocks. The geological character of rock material, together with the visual assessment of the mass it forms, is used as a direct input to the selection of parameters relevant for the prediction of rock-mass strength and deformability. This approach enables a rock mass to be considered as a mechanical continuum without losing the influence geology has on its mechanical properties. It also provides a field method for characterizing difficult-to-describe rock masses. Figure 2-5 presents the general chart for GSI to estimate the rock mass parameters for poor and weak rock mass.

Marinos et al., 2005 commented and compared GSI with RMR and Q methods. These approaches (RMR and Q) are less reliable for squeezing, swelling, clearly define structural failures or spalling, slabbing and rock bursting under very high stress conditions. More importantly, these classification systems are of little help in providing information for the design of sequentially installed temporary reinforcement and the support required to control progressive failure in difficult tunneling conditions. Both the RMR and the Q classification include and are heavily depended upon the RQD. Since RQD in most of the weak rock mass is essentially zero or meaningless it became necessary to consider an alternative classification system. The required system would not include RQD, would place greater emphasis on basic geological observation of rock mass characteristics, reflect the material, its structure and geological history and would be developed specially to estimate rock mass properties rather than for tunnel reinforcement and support.

The general approach adopted for design and estimation of tunnel support in the Himalayan region of Nepal is shown in the Figure 2-4. Rock mass classification approaches, basically Q-system and RMR are very popular for the initial estimation of tunnel support. After excavation, the tunnel support may be revised based on the tunnel face. From the past experience, it is also found that the re-estimation of tunnel support is also not adequate for stability.

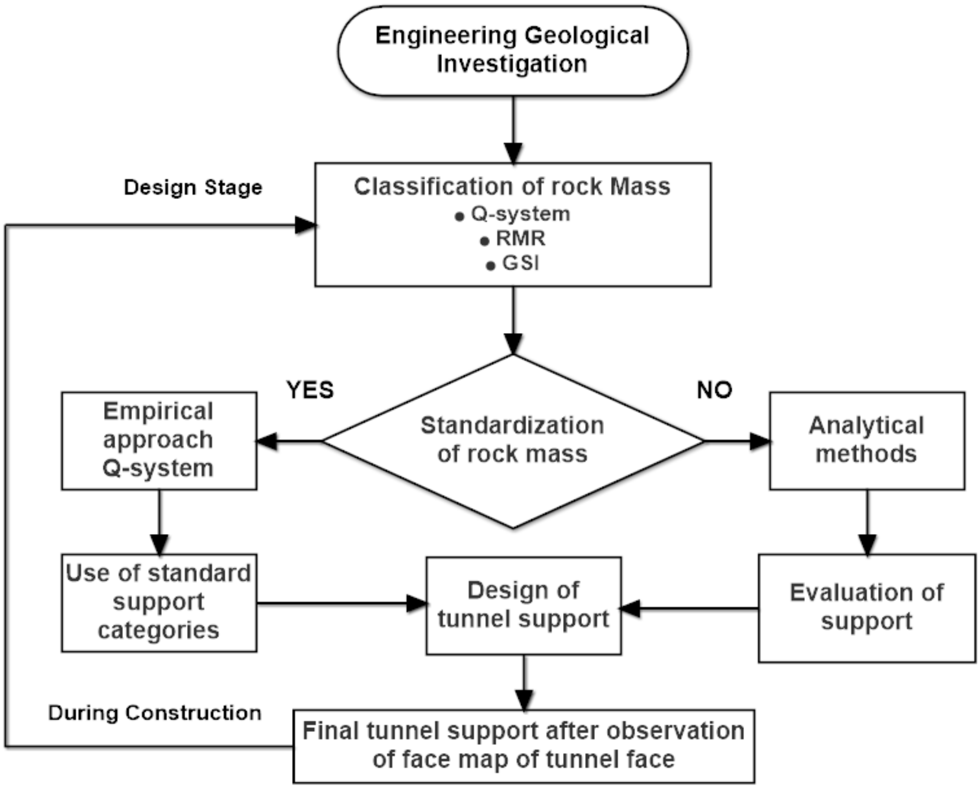

Figure 2-4 General flow chart for design of tunnel support in the Himalayan region of Nepal

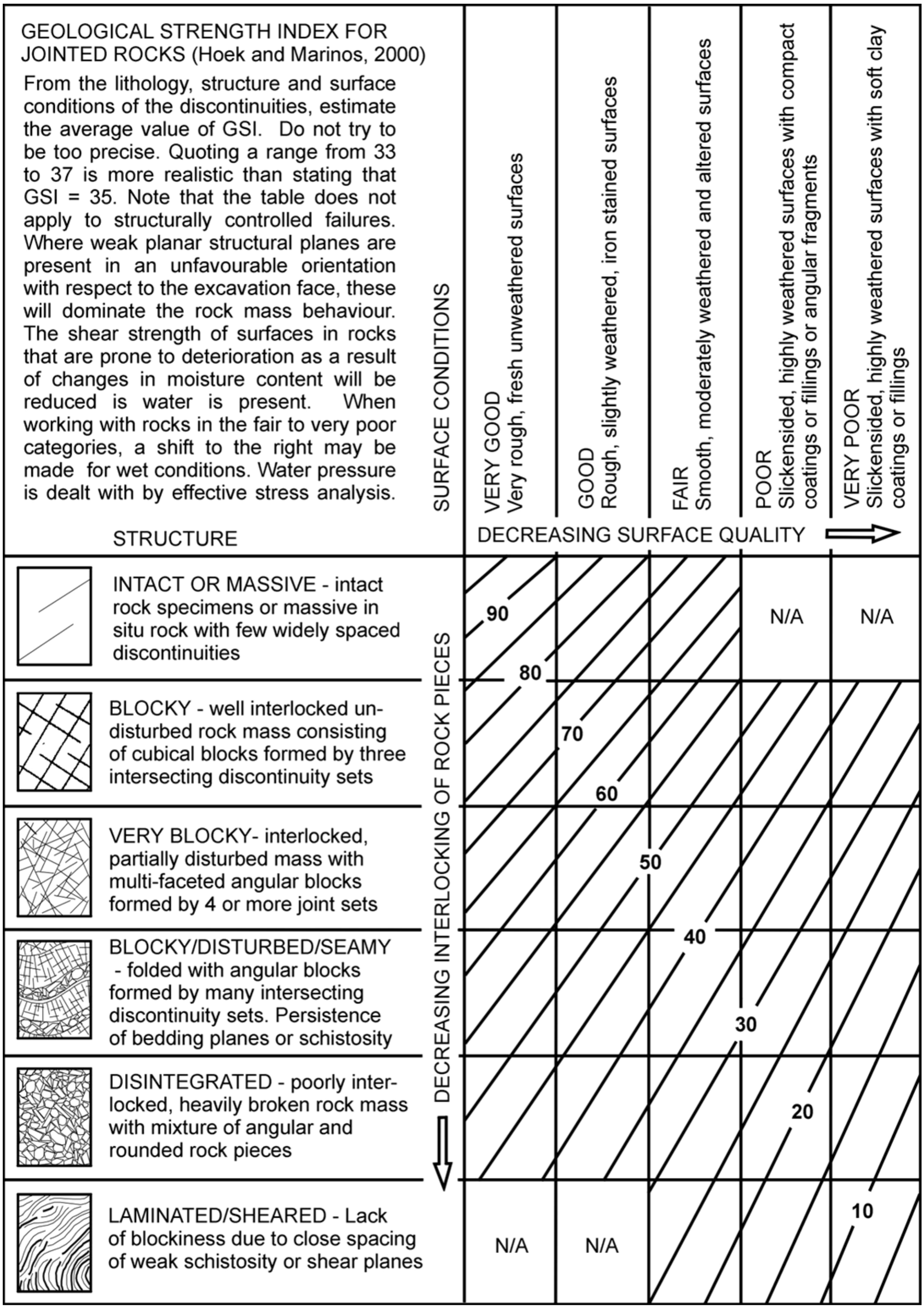

Figure 2-5 General chart for GSI estimates from geological observation (Marinos et al., 2005)

2.4 Squeezing Assessment

Extensive researches have been carried out for the assessment of squeezing and support design of underground structures through case studies in different parts of the world. Many researchers and authors have proposed a number of empirical and semi-empirical approaches for quantifying the squeezing behavior and support design. These approaches can be classified in the following manner:

2.4.1 Empirical Approaches

These empirical approaches are based on the rock mass classification schemes through the study of different case histories of tunneling in weak and squeezing ground conditions.

Singh et al. (1992) plotted a clear cut demarcation line to differentiate squeezing cases from non-squeezing cases as shown in Figure 2-6.This approach based on 39 case histories, by collecting data on rock mass quality Q (Barton et al. 1974) and overburden depth H. The data points lying above the line represents squeezing conditions, whereas those below this line represent non squeezing conditions. The equation of demarcation line is $H= 350Q^{1/3}$ (m). This can be summarized as for squeezing condition: $H > 350Q^{1/3}$ (m) and for non-squeezing conditions:$H < 350\ Q^{1/3}$ (m).

Based on the back analysis of several tunnels, Singh et al. (1997) have suggested the relation for rock mass strength as, $\sigma_{cm} = 7\gamma Q^{1/3}$ (MPa), where σ_{cm} is the uniaxial compressive strength of rock mass in MPa and γ is rock mass unit weight in gm/cc and Q is the rock mass quality.

Goel et al (1995) approach: Goel et al. (1995) defined the rock mass number, denoted by N, as stress-free rock mass quality Q. Stress effect has been considered indirectly in the form of overburden height H. Thus N can be defined as with stress reduction factor (SRF) is equal to 1 of Q system of Barton et al. (1974). Rock mass number, N, is needed because of the problem and uncertainties in obtaining the correct rating of Barton’s SRF parameter and it is given by

$$N = \left[\frac{RQD}{J_n}\right]\left[\frac{J_r}{J_a}\right][J_w] \tag{2.2}$$

where, N is the rock mass number, RQD is the Rock Quality Designation, $J_n$is the joint set number, J_r, is the joint roughness number J_a, is the joint alteration number, and J_w, is the joint water reduction factor

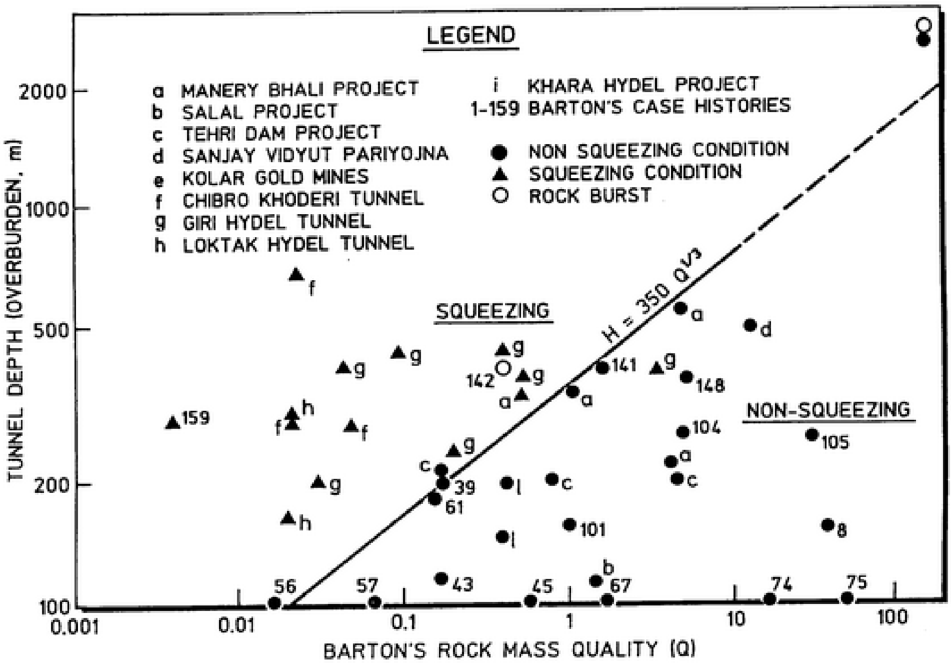

Figure 2-6 To predict squeezing condition (Singh et al., 1992)

Considering the overburden depth H, the tunnel span or diameter B, and the rock mass number N from 99 tunnel sections, Goel et al. (1995) plotted the available data on log-log diagram, as shown in Figure 2-7, between N and $HB^{0.1}$. Out of 99 tunnel section data, 39 data were taken from Barton's case histories and 60 from projects in India. Out of those 60 data 38 data were from 5 projects in Himalayan region. All the 27 squeezing tunnel sections were observed in those 5 projects in Himalayan region. Other 72 data sets were from non-squeezing sections. As shown in the same figure, a line AB distinguishes the squeezing and non-squeezing cases.

The equation of that line is H = 275 $N^{0.33}B^{-0.1,}$ where H is in m. The data points lying above the time represents squeezing conditions, whereas those below this line represent non-squeezing condition.

This can be summarized as for *squeezing conditions* the overburden depth is given by $H>275\ N^{0.33}B^{-0.1}$ and for non-squeezing conditions, the overburden depth is given by $H < (275\ N^{0.33}B^{-0.1}$, where N is rock mass number, B is width of tunnel in m and H is overburden depth in m.

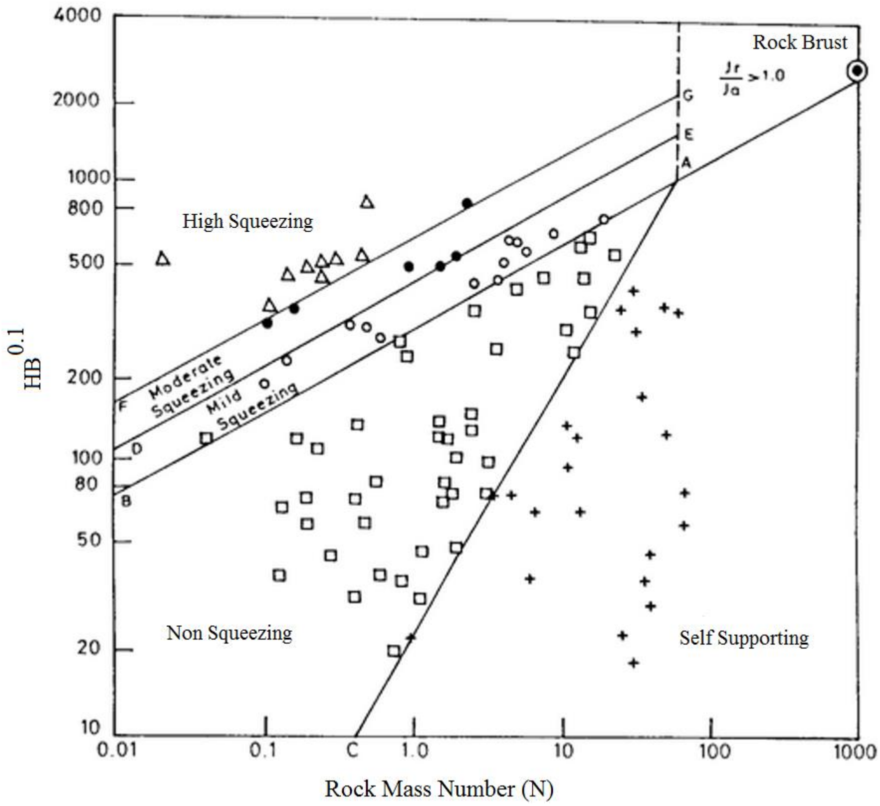

Figure 2-7 Criteria for predicting squeezing ground conditions using rock mass number N (Goel et al., 1995)

Estimation of support pressure and tunnel deformation in squeezing ground conditions:

Different authors predicted support pressure and tunnel deformation in squeezing ground conditions based on the measured in situ data in different support conditions.

In 1993, Grimstad and Barton suggested an empirical approach using Q-value for estimation of roof support pressure in tunnels. Accordingly, the support pressure is independent of the span or diameter of the tunnel and is given by

$$P_u = \frac{0.2\sqrt{J_n}}{J_r} Q^{-1/3} \tag{2.3}$$

where P_u is the ultimate roof support pressure, in MPa, J_n, the joint set number, J_r, the joint roughness number, and Q, the rock quality index.

In 1994, Goel developed two sets of empirical relation to estimate the support pressure for both squeezing and non-squeezing ground conditions. The relation was developed using Rock Mass Number (N) and the measured values of support pressures, the tunnel depth H, the tunnel radius a, and the expected tunnel closure u_a from 25 tunnel sections (Goel et al., 1995a; Singh et al., 1997).

For non-squeezing conditions

$$p_v(el) = \left(\frac{0.12H^{a0.1}a^{0.1}}{N^{0.33}}\right) - 0.038 \tag{2.4}$$

For squeezing ground condition

$$p_v(sq) = \left(\frac{f(N)}{30}\right)10^{\left(\frac{H^{0.6}a^{0.1}}{50N^{0.33}}\right)} \tag{2.5}$$

where, p_v (el) is the ultimate support pressure in non-squeezing ground conditions, p_v(sq)is the ultimate support pressure in squeezing ground condition in MPa, f(N) is the correction factor for tunnel closure given in Table 2.3, H is the depth of tunnel (m), *a* is the radius of tunnel (m), and N is the rock mass number.

Table 2.3 Correction factor for tunnel closure in equation (Singh & Goel, 2011)

SN	Overburden depth, H (m)	Degree of squeezing	Normalized tunnel closure (%)	f(N)
1	$275N^{0.33}B^{-0.1}<H<360N^{0.33}B^{-0.1}$	Very mild	1-2	1.5
2	$360N^{0.33}B^{-0.1}<H<450N^{0.33}B^{-0.1}$	Mild	2-3	1.2
3	$450N^{0.33}B^{-0.1}<H<540N^{0.33}B^{-0.1}$	Mild to moderate	3-4	1.0
4	$540N^{0.33}B^{-0.1}<H<630N^{0.33}B^{-0.1}$	Moderate	4-5	0.8
5	$630N^{0.33}B^{-0.1}<H<800N^{0.33}B^{-0.1}$	High	5-7	1.1
6	$800N^{0.33}B^{-0.1}<H$	Very high	>7	1.7

Note: Tunnel closure depends significantly on the method of excavation. In highly squeezing ground condition, heading and benching method of excavation may lead to tunnel closure >8%

Goel (1994) also developed an empirical correlation to estimate the tunnel deformation on the basis of measured tunnel closures from 60 tunnel sections, for both non-squeezing and squeezing ground condition. The correlations are given below:

Non-squeezing ground conditions

$$\frac{u_a}{a} = \frac{H^{0.6}}{28N^{0.4}K^{0.35}}\% \tag{2.6}$$

Squeezing ground condition

$$\frac{u_a}{a} = \frac{H^{0.8}}{10N^{0.3}K^{0.6}}\% \qquad (2.7)$$

where u_a/a is the normalized tunnel closure in percent, K is the effective support stiffness(=$p_v.a/u_a$), H is the tunnel depth and a is the tunnel radius.

These correlations can also be used to obtain desirable effective support stiffness so that the normalized tunnel closure is contained within 4 percent (in squeezing ground ground).

Using rock mass quality (Q), Bhasin and Grimstad (1996) developed a relation to predict ultimate roof support pressure by considering the span of tunnel for poor quality rock mass. They used the data of Singh et al. (1992), Goel et al. (1995) and also included the case studies from Scandinavian tunnels. The correlation is as follows:

$$P_b = \frac{0.04}{J_r}.D.Q^{-1/3} \qquad (2.8)$$

Where P_b defines the ultimate roof support pressure in MPa, D is the diameter or span of the tunnel in m, Jr is the joint roughness number, and Q isthe rock quality index.

Dwivedi et al.,(2013) analyzed the 52 tunnel sections along the Himalayan region including 16 tunnel sections from Lesser Himalayan region of Nepal. These sections have high in-situ stress, poor rock mass quality being excavated in squeezing ground. They developed a dimensionally correct empirical correlation for assessment of support pressure in tunnels which are excavated in squeezing ground conditions. The correlation uses the concept of 'joint factor' as a measure of rock mass quality, allowable closure, depth and radius of opening as the governing parameters. The predicted results have been compared with the results obtained via existing approaches, discussed above, based on rock mass quality (Q) and rock mass number (N). It was observed that the proposed correlation fits better the collected data with a correlation coefficient of 0.92.

$$P_s = 9.23 \times 10^{-3}\sigma_v \left(\frac{J_f^3 \sigma_h^{0.1}}{10^7 \sigma_{ci}^{0.1} \left(d^{0.2} + \frac{J_f}{1434} \right)} \right)^{1.7} \tag{2.9}$$

where, P_s is ultimate support pressure in MPa, J_f is the joint factor, σ_v is the vertical in-situ stress, σ_{ci} is the uniaxial compressive strength of intact rock in MPa, σ_h is horizontal in situ stress in MPa and *d* is the radial tunnel deformation (= *u/a**100, *u* is the radial tunnel deformation and *a* is the tunnel radius).

In equation 2.17, the ultimate support pressure should be increases with in-situ stress and decrease with allowed tunnel deformation. Also a competent rock will exert a small support pressure and low value of J_f will result in lower support pressure. It is an handy tool to predict the support pressure in squeezing ground conditions and take appropriate measures for the stability of underground structures.

Similarly, Dwivedi et al., (2013) predicted the tunnel closure by analyzing 63 tunnel sections including 37 tunnel sections from Lesser Himalayan region of Nepal. The dimensionally correct empirical correlation has been developed with correlation factor of 0.94 to predict tunnel deformation for squeezing ground,

Using J_f:

$$\frac{u_p}{a} = \frac{5 * 10^{-10} \sigma_v J_f^3}{K + 0.5} + 0.0052 \tag{2.10}$$

Using Q:

$$\frac{u_p}{a} = \frac{0.0191 \sigma_v Q^{-0.2}}{K + 1} + 0.0025 \tag{2.11}$$

where u_p is the predicted radial deformation of tunnel in m, *a* is the radius of tunnel in m, J_f is the joint factor, σ_v is the vertical in-situ stress in MPa, K is the support stiffness, MPa, and Q is the rock mass quality.

2.4.2 Semi- empirical approach

The semi-empirical approaches not only give indicator for predicting squeezing, but also provide some tools for estimating the expected deformation around the tunnel and/or the support pressure required, by using closed form analytical solution for a circular tunnel in hydrostatic stress field. The common starting point of all these methods for quantifying the squeezing potential of rock is the use of "competency factor", which is defined as the ratio of uniaxial compressive strength of rock mass, σ_{cm},to overburden stress γH. This competency factor was initially proposed by Muirwood (1972), and later used by Nakano (1979), Barla (1995) and Hoek (1999).

2.4.2.1 Aydan et al. (1993) approach

Aydan et al. (1993), proposed to relate the strength of the intact rock σ_{ci} to the overburden pressure γH. In which the uniaxial compressive strength of intact rock $\sigma_{ci}$and of the rock mass $\sigma_{cm\ are}$ the same. The fundamental concepts of the method based on the analogy between the stress-strain responses of the rock in laboratory testing and tangential stress-strain response around tunnels. Based on a closed form analytical solution, which has been developed for computing the strain level ε_θ^a around a circular tunnel in a hydrostatic stress field, five different degree of squeezing are defined as shown in Table 2.4 with some comments on expected tunnel behavior.

Table 2.4 Classification of the degree of squeezing (Aydan et al.,1993)

Class No.	Squeezing Degree	Theoretical Expression	Comments on tunnel behavior
1	No-squeezing	$\varepsilon_\theta^a/\varepsilon_\theta^e \leq 1$	The rock behaves elastically and the tunnel will be stable as the face effect ceases
2	Light-squeezing	$1 < \varepsilon_\theta^a/\varepsilon_\theta^e \leq \eta_p$	The rock exhibits a strain-hardening behavior. As a result, the tunnel will be stable and the displacement will converge as a face effect ceases
3	Fair-squeezing	$\eta_p < \varepsilon_\theta^a/\varepsilon_\theta^e \leq \eta_s$	The rock exhibits a strain-softening behavior, and the displacement will be larger. However, it will converge as the face effect ceases
4	Heavy-squeezing	$\eta_s < \varepsilon_\theta^a/\varepsilon_\theta^e \leq \eta_f$	The rock exhibits a strain-softening behavior at much higher rate. Subsequently, displacement will be larger and it will not take to converge as the face effect ceases
5	Very heavy-squeezing	$\eta_f < \varepsilon_\theta^a/\varepsilon_\theta^e$	The rock flows which will result in the collapse in the medium and the displacement will be very large and it will be necessary to re-excavate the opening and install heavy support

2.4.2.2 Hoek and Marinos (2000) approach

Based upon a simple closed form solution for a circular tunnel with hydrostatic stress field, the support is assumed to act uniformly on the entire perimeter of the tunnel. These conditions are seldom met in the field in reference to the excavation method, tunnel shape and in situ stress conditions. A plot of tunnel strain ε_t (defined as the percentage ratio of radial tunnel wall displacement to tunnel radius, i.e. the same strain as ε_θ^a given by Aydan et al., 1993) against the ratio σ_{cm}/ p_0 could be used effectively to assess squeezing conditions as shown in Figure 2-8.

Based on the above and consideration of different case histories for several tunnels in Venezuela, Tiwan and India, Hoek (2000) gave a curve of Figure 2-8to be used as a first estimate of tunnel squeezing. To compare with the previously reported classes of squeezing conditions as given by Aydan et al., (1993), Table 2.5 gives the range of tunnel strains expected in two cases.

Table 2.5 Comparasion of the approaches (Singh et al. 2007)

Class no	Aydan et al. (1993)		Hoek (2000)	
	Squeezing level	Tunnel strain (%)	Squeezing level	Tunnel strain (%)
1	No-squeezing	$\varepsilon_\theta^a \leq 1$	Few support problems	$\varepsilon_t \leq 1$
2	Light-squeezing	$1 < \varepsilon_\theta^a \leq 2.0$	Minor squeezing	$1 < \varepsilon_t \leq 2.5$
3	Fair-squeezing	$2.0 < \varepsilon_\theta^a \leq 3.0$	Severe squeezing	$2.5 < \varepsilon_t \leq 5.0$
4	Heavy-squeezing	$3.0 < \varepsilon_\theta^a \leq 5.0$	Very severe squeezing	$5.0 < \varepsilon_t \leq 10.0$
5	Very heavy-squeezing	$\varepsilon_\theta^a \leq 5.0$	Extreme squeezing	$\varepsilon_t > 10.0$

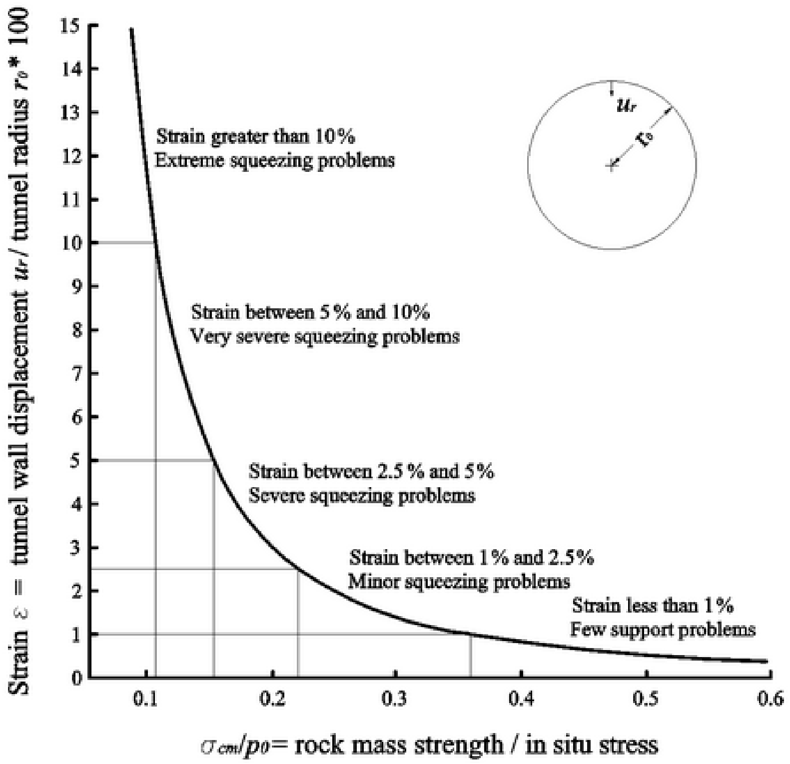

Figure 2-8 Classification of squeezing behavior (Hoek and Marinos,2000)

2.4.3 Analytical Methods: Rock Support Interaction

The rock support interaction curves, suggested by Carranza-Torres and Fairhust (2000), as shown in Figure 2-9, is one of the simple and useful method to design tunnel support. It can be drawn by assuming the tunnel is circular with radius R through a rock mass that is to be subject initially to a uniform far field stress σ_o as shown in Figure 2-10 (b). For the simplicity, it is assumed that all the deformation occurs in a plane perpendicular to the axis of tunnel. Radial displacement u_r and internal pressure p_i i.e. the reaction of support on the walls of the tunnel are uniform at the section. Figure 2-10 (c) shows that the circular annular support of thickness t_c and external radius R is installed at the section A-A'. The pressure P_s represents uniform load transmitted by rock-mass to the support.

Carranza-Torres and Fairhurst (2000) concluded that the Longitudinal Displacement Profile (LDP), the Ground Reaction Curve (GRC) and the Support Characteristics Curve (SCC) are the three basic components of Convergence Confinement Method (CCM). The application of CCM requires the knowledge of the deformation characteristics of the ground and of the support. CCM is the procedure that allows the load imposed on support installed behind the face of tunnel to be estimated. If the support is installed immediately near face, it does not carry out full load to which it is supposed to. The part of load is carried by face itself.

As tunnel face advance away from the support, face effect decreases, and support must carry more loads. When the tunnel moves well away from face, the support will be subjected to full design load. LDP is the graphical representation of radial displacement that occurs along the axis of unsupported cylindrical excavation i.e. for the sections located ahead of and behind tunnel face. The upper diagram in Figure 2-9 represents the typical LDP. The diagram indicates that at some distance behind tunnel face the effect of face is negligibly small, so that beyond this distance the tunnel has converged by final value i.e. u_r^M. At some distance ahead of face, the tunnel excavation has no effect on the rock mass and the radial displacement is zero. Hence, it provides insight into how quickly the support begins to interact with rock mass behind the face of tunnel. GRC is the relationship between decreasing internal pressure p_i and increasing radial displacement of tunnel wall u_r. The relationship depends upon mechanical properties of rock mass and can be obtained from the elasto-plastic solution of rock deformation around an excavation (Carranza-Torres and Fairhurst, 2000). The curve OEM in Figure 2-9 is the typical diagram of GRC. SCC is defined as the relationship between increasing pressure p_i on the support and increasing radial displacement u_r of the support.

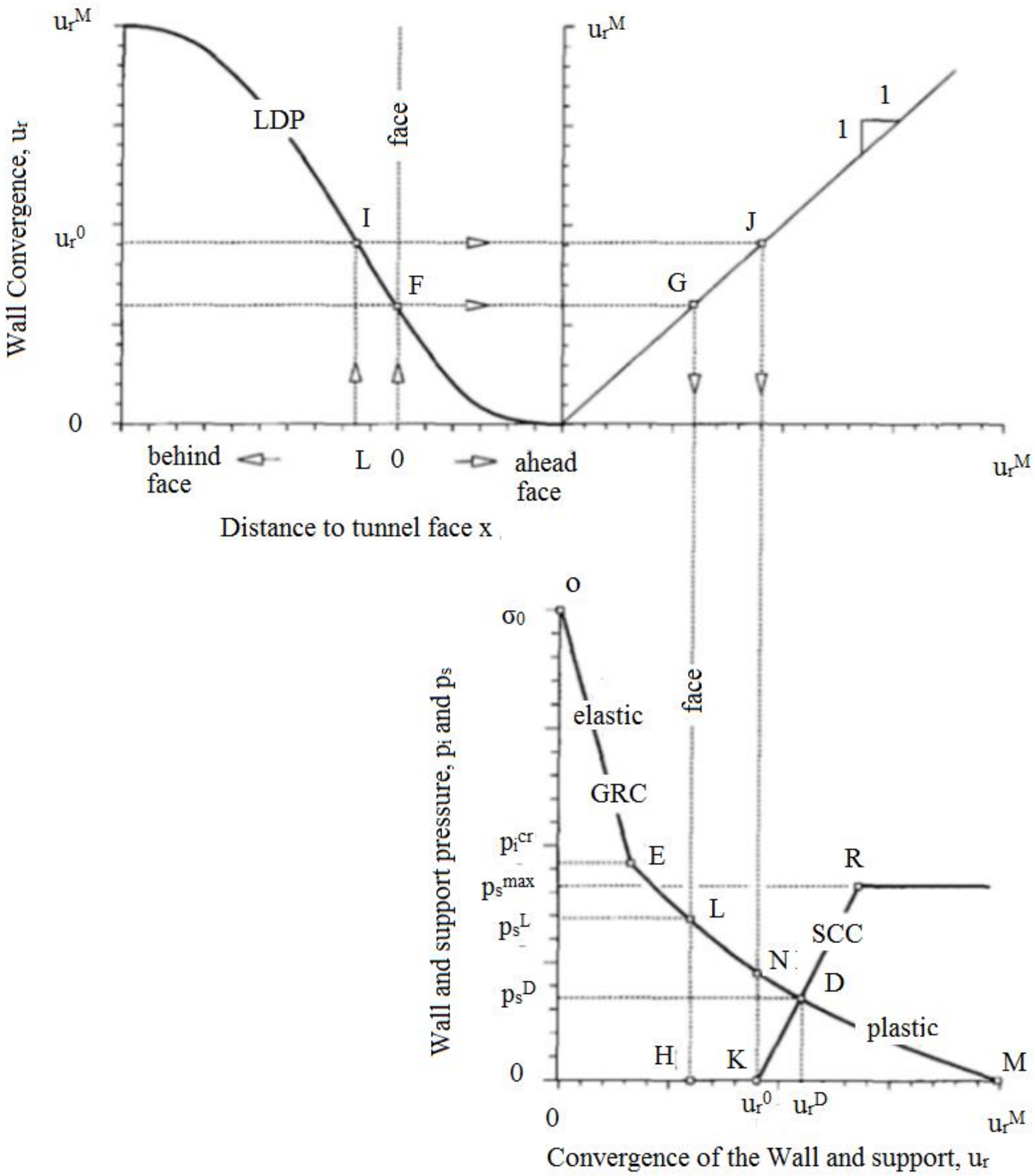

Figure 2-9 Rock support interactions curves: Longitudinal Displacement Profile (LDP), Ground Reaction Curve (GRC) and Support Characteristics Curve (Carranza-Torres and Fairhurst, 2000)

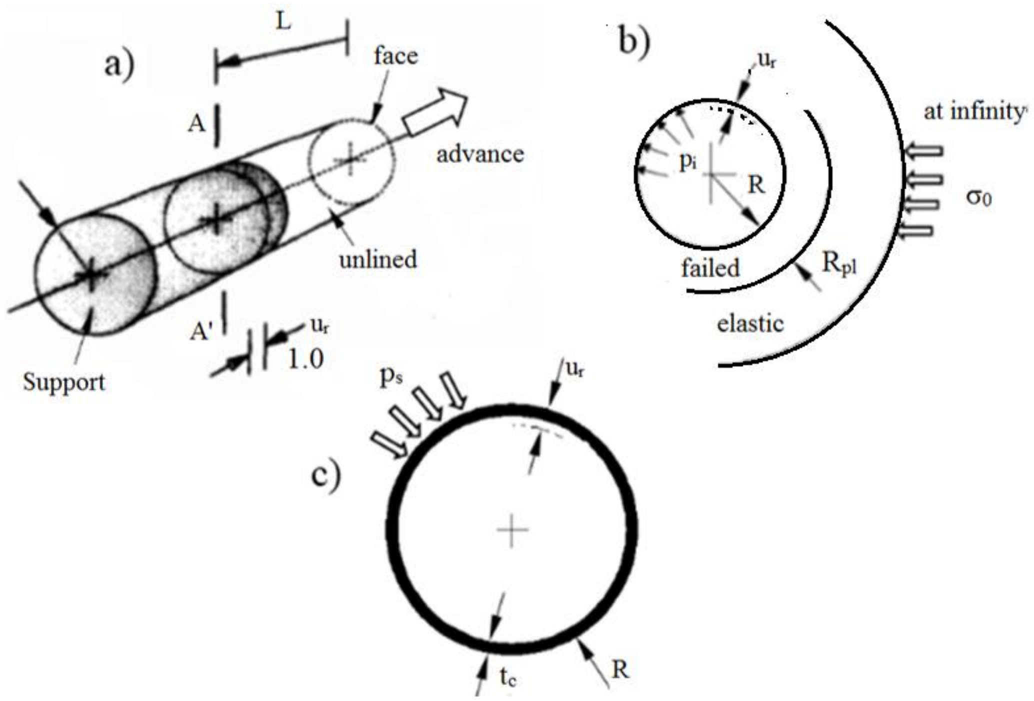

Figure 2-10 a) Cylindrical tunnel of radius R driven in the rock mass. b) Cross-section of the rock mass at the section A-A'. c) Cross-Section of the circular support installed at section A-A' (Carranza-Torres and Fairhurst, 2000)

It can be constructed form the elastic relationship between applied pressure and resulting displacement for the section of support of unit length in the direction of tunnel. The applied stress p_s can be expressed in terms of elastic stiffness of the support K_s and resulting closure u_r in the following way;

The plastic part of the SCC i.e. horizontal segment starting at point R in Figure 2-9, is defined by the maximum pressure p_s^{max} that the support can accept before collapse. For different support system such as; concrete or shotcrete linings, ungrouted bolts and cables, steel ribs, lattice girders etc, the main task is to find the maximum pressure and elastic stiffness for the construction of SCC.

2.5 Numerical Analysis

The use of numerical analysis is advisable in cases where the σ_{cm}/p_0 ratio is below 0.3, and it is highly recommended if this ratio falls below about 0.15, when the stability of the tunnel may become a critical issue. Significant advantages are envisaged by using numerical analysis at the design stage, when very complex support/excavation sequences, including pre-support/stabilization measures are to be adopted, in order to stabilize the tunnel during construction (Barla, 2002). The most commonly applied numerical methods for rock mechanics problems are: i) continuum methods- finite difference method (FDM), finite element method (FEM), and the boundary element method (BEM), ii) discrete methods- the discrete element methods (DEM), discrete fracture network (DFN) methods, iii) Hybrid continuum/discrete method (Jing et al.,2002). Rock mass can be modeled either by the continuum approach or the discontinuum approach (Unteregger et al., 2015). The continuum approach can be used if only a few fractures are present and if fracture opening and complete block detachment are not significant factors. The discontinnum approach is most suitable for moderately facture rock masses where the number of fractures is too large for the continuum-with-fracture-elements approach, or where large-scale displacements of individual blocks are possible. There are no absolute advantages of one method over another (Jing et al.,2002). Unteregger et al., (2015) suggested that the choice of the appropriate approach depends on many problem specific factors, and mainly on the problem scale and facture system geometry. Discontinnum approach would be appropriate to shallow tunnels since failures of the rock mass are often controlled by the discontinuities present in rock mass. Continuum approach is commonly employed in underground excavation with high overburden exhibits large stress changes accompanied by plastic deformation.

3 MODELING OF WEAK ROCK

3.1 General

Most of the hydropower tunnels in the Lesser Himalayan region of Nepal undergo excessive deformation due to rock squeezing and it would be a high probability for newly proposed tunnels. Rock squeezing is mainly failure of a weak rock mass around a tunnel under influence of high overburden pressure or tectonic stresses. These tunnels pass through jointed weak rock mass and high overburden. From the experience, it was experienced a huge financial loss and time because of the necessity of heavily reinforced support in the squeezed section. The heavily reinforced concrete ring around the cross-section tunnel is not a good option always. Therefore, the knowledge of rock mass strength, including their peak and residual strengths, and deformation behavior is required for the economic design of tunnel in such geological conditions.

Extensive researches have been done by various researchers to develop a constitutive model to describe the strength and deformation behaviors of such rock masses with so many parameters. It is generally impossible to develop a universal model that can be used to prior to predicting the strength of rock mass and traditional methods including plate-loading testing and in-situ block shear test for determining these parameters are costly in initial stages of the project (Cai et al. 2007). Hoek et al. (1995), developed the Geological Strength Index (GSI) system to estimate the peak strength of jointed rock mass based on the geological conditions of the rock mass. It provides the complete set of mechanical properties for both Hoek-Brown failure criteria and equivalent Mohr-Coulomb failure criteria. GSI itself, or by any other system, is not able to give the guidelines for estimation of residual strength that yield consistent results.

In this chapter a proper rock modeling approach is proposed for modeling the jointed weak rock mass in the Lesser Himalayan region of Nepal by use of field data of different hydropower tunnels and laboratory data, which is able to predict the real behavior of the rock mass during tunneling.

3.2 Peak and Residual strength of Rock Mass

Peak strength is the maximum shear strength or shear stress at yield point given by a curve obtained by plotting shear displacement against shear stress at constant normal stress. Residual strength is the shear strength that levels out at a constant value with increasing shear displacement in a shear test at a constant normal stress (Goodman, 1989). The peak and residual strength are shown in Figure 3-1.

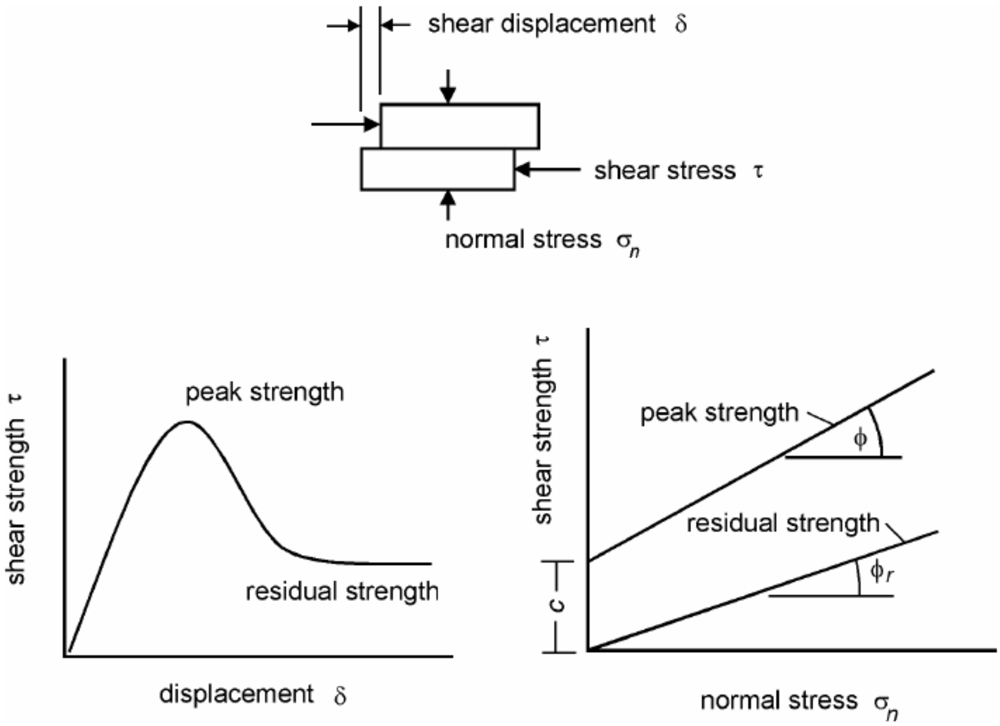

Figure 3-1 Peak and residual strength (Hoek, 2007)

Cai, et al. (2007), suggested that understanding of the rock mass strength behavior, including the peak and residual strength, will facilitate the cost-effective design of tunnel support. Hoek, (2007) had suggested post failure characteristics for different quality of rock masses. Elastic-brittle, strain-softening, and elastic-plastic failures are characteristics for very good quality hard rock mass, average quality rock mass and very poor-quality rock mass respectively, shown in Figure 3.2.

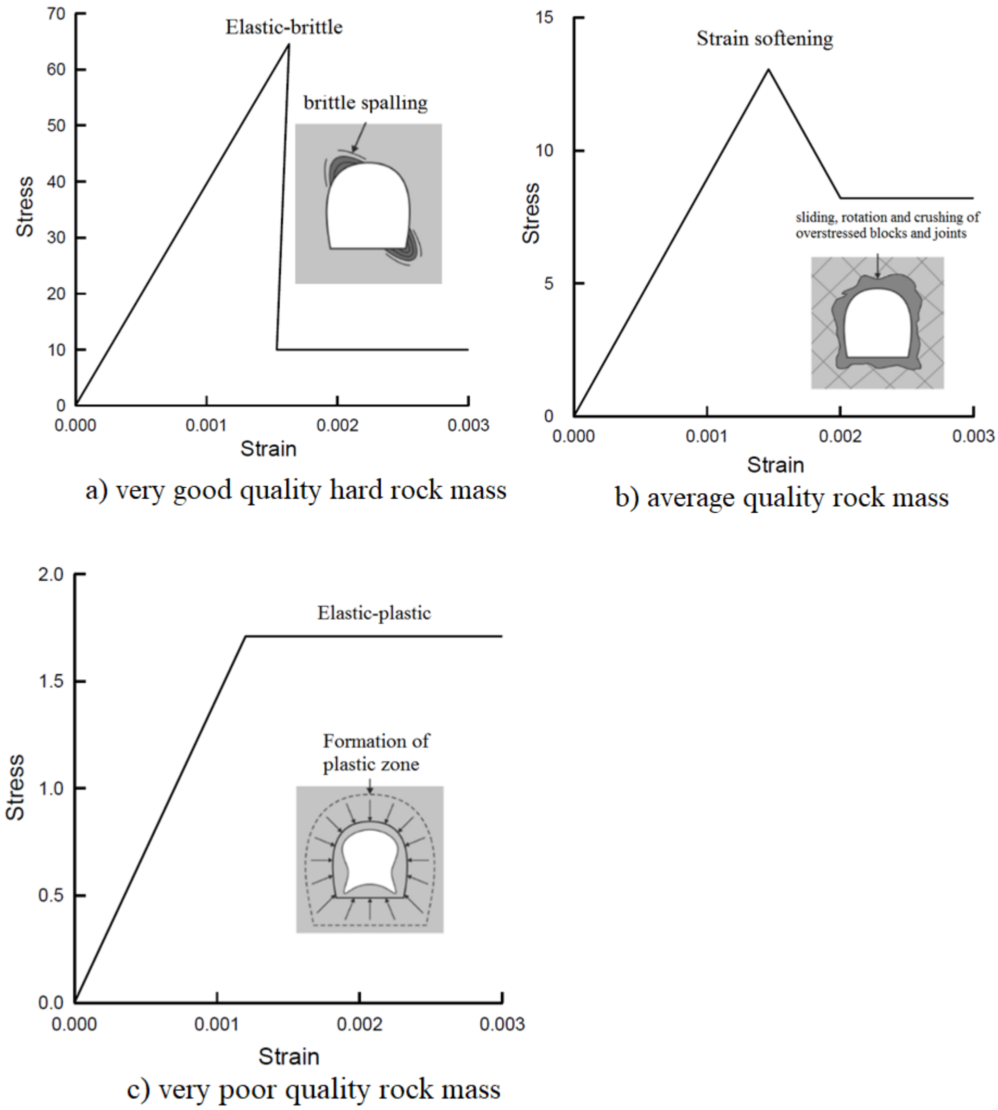

Figure 3-2 Suggested post failure characteristics for different quality of rock mass and tunnel behavior (Hoek, 2007 and Lorgi, et al. 2013)

Cai, et al. (2007) mentioned that rock masses, in general, exhibit Strain-softening behavior, except when highly disturbed, so that the residual strength parameter are lower than the peak parameters. Peak and residual strength parameters are required for design. Strain-softening behavior describes the gradual loss of load bearing capacity of a material. They also mentioned that for hard rocks, the term, “strain weakening” seems more appropriate than the term “Strain-softening” because softening refers to reduction of rock stiffness.

In case of elastic-perfectly- plastic behavior of rock, the residual strength of rock mass parameter is considered as equal to the peak strength of rock mass parameters as suggested by Hoek et al.

Similarly, Cai, et al. (2007) also discussed on the importance, necessity and existing approach for estimating of the residual strength of rocks on design support for the underground excavation.

Influence of residual strength of rock mass to design underground structure:

- The post –peak behavior of rock is important in the design of underground excavation because it has significant influence upon the stability of the excavation.
- The rocks retain some strength even when their maximum load-carrying capacity has been exceeded.
- The peak and residual strength of rocks increase with increasing confining pressure as shown in Figure 3-3, triaxial test on marble (after Cai. et al, 2007). At low confinement stresses, the loss of cohesive strength component around peak load leads to strain localization with significant stress drop, which is traditionally called strain-softening behavior.

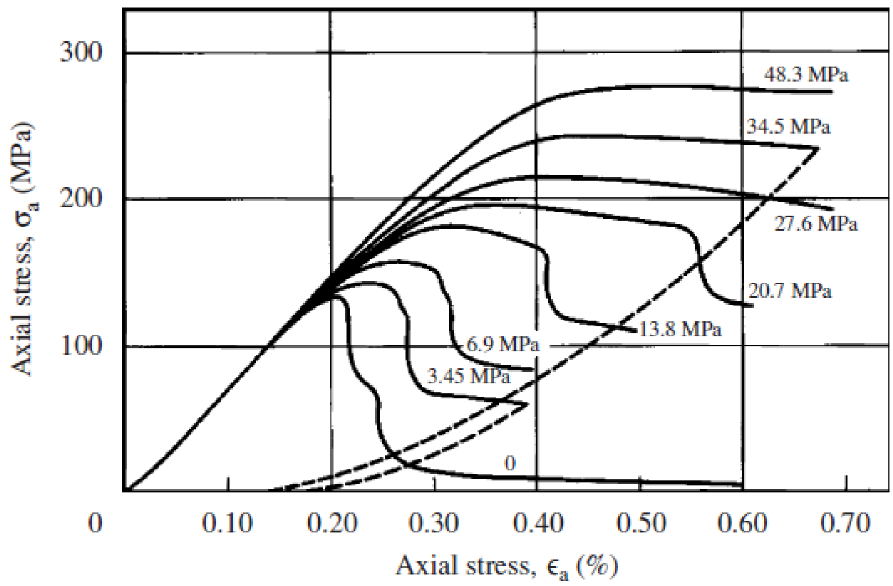

Figure 3-3 Stress–strain curves for Tennessee Marble at different confining stresses (Cai, et al. 2007)

Need of accurate determination of the residual strength of rock mass:

- The post-peak strength depends on the resistance developed on the failure plane against further straining. Initially, the fracture orientation, degree of interlocking, surface irregularity or roughness will affect the level of resistance. However, as strain increases, the residual strength will be less.
- In the field, the post-peak strength will be influenced by the boundary conditions as well. If further straining is constrained, then, the residual strength level cannot be reached and the rock mass can thus support a higher load than the residual strength would suggest.
- It is very challenging and difficult task to correctly represent the strain-softening behavior of rock masses due to a lack of large scale test data.
- Most numerical tools designed for the rock engineering application, however, provide strain-softening constitutive models of varying sophistication to describe the behavior of jointed rock masses.
- In these models, the residual strength of rock mass and the rate of the post-peak strength degradation play an important role in the determination of the size of the plastic zone and the associated rock mass deformation, affecting the final rock support system design.
- If the residual strength is not determined appropriately, an optimal rock support design can never be achieved. Therefore, the basic guidelines are that the residual strength of rock masses has to be properly determined in order to design the appropriate rock support system.

Existing methods to determine the residual strength of rock masses:

- Hoek also suggested that in the case of an average quality rock mass, it is reasonable to assume that the post-failure characteristics can be estimated by reducing GSI value from the in-situ value to a lower which characterizes the broken rock mass.
- Cai, et al. (2007) mentioned, in 1998 Russo et al. proposed to set the residual GSI value at 36% of the peak GSI value. This empirical relation may underestimate the residual GSI values for poor quality rock masses on the other hand, for very good quality rock masses, it may overestimate the residual GSI values.

- Cai, et al. (2007) mentioned, in 2000 Ribacchi suggested to use the following relation to estimate the residual strength of jointed rock masses: m_b= 0.65m_r, s_r= 0.04s or $(\sigma_c)_r$ = 0.2 σ_c, where m_b and s are the Hoek–Brown peak strength parameters, the subscript ‘‘r’’ indicates residual values, and σ_c is the uniaxial compressive strength of the intact rock. Taking into account the structure of the tested rock, these relations may be valid only for rock masses in which joints are characterized by a thin infilling or slightly weathered to unweathered joint walls. The corresponding GSI reduction that would fit such parameters is approximately GSI_r = 0.7GSI.
- Several attempts have been made to estimate the residual strength of the jointed rock mass. The reduction of GSI to its residual value is a logic choice because the failure of rock masses is associated with the crushing of intact rock and the wearing of the joint surface roughness.

3.3 Failure Criteria and Strength Parameter Estimation Using GSI

Squeezing of tunnels are mainly governed by weak rock mass and high overburden pressure (Singh et al. 2007). Boundary conditions (geological, stress state and hydrogeology) must be identified to be able to analyze the system and to classify the condition. Estimation of the ground properties is one of the most difficult tasks, which are based on the GSI. An empirical relation/classification system cannot be applied to identify the complex non-linear relationship between the grounds conditions involved in squeezing rock conditions. Opening at greater depth, the extent and depth of failure is predominantly a function of the in-situ stress and rock mass strength. Traditional approaches of modeling rock mass failure are often based on a linear Mohr-Coulomb failure criterion or on non-linear criteria such as the Hoek-Brown failure criterion (Hajiabdolmajid et al., 2002). In this chapter both failure criteria are studied in detail through case study.

3.3.1 Mohr- Coulomb failure criterion

The Mohr-Coulomb failure criterion is a set of linear equations in the principal stress space describing the conditions for which an isotropic material will fail, with any effect from the intermediate principal stress σ_2. Mohr’s condition assumes that failure envelope, the loci of σ, τ acting on a failure plane, can be linear or non-linear (Mohr, 1900).

Coulomb's conditions are based on a linear failure envelope to determine the critical failure on some plane (Labuz and Zang, 2012). The Mohr-Coulomb strength criterion is one of the most widely used strength criteria in geotechnical engineering applications, including in rock engineering modelling and design (Zhao, 2000). The basic concept of this criterion suggests that the shear strength of a rock material is made up of two parts: a constant cohesion; and a friction varying with normal stress.

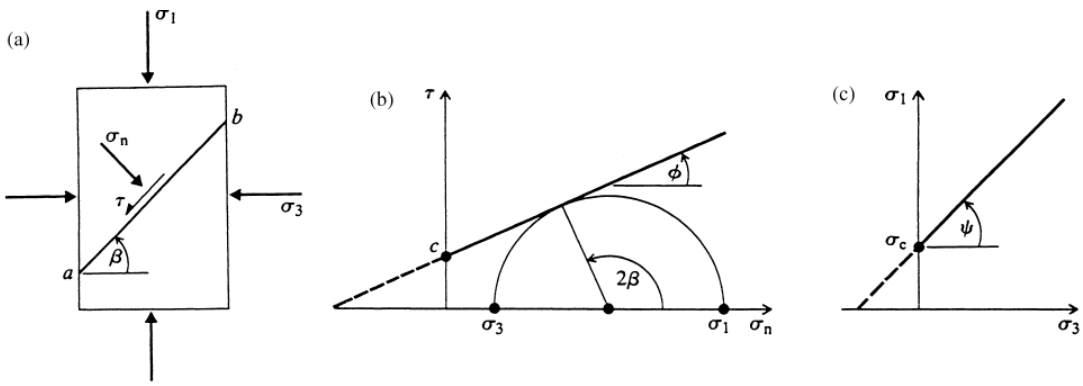

Figure 3-4 The Mohr- Coulomb strength criterion: (a) shear failure on plane *a-b*, (b) strength envelope of shear and normal stresses, and (c) strength envelope of principal stresses (Zhao, 2000)

As shown in Figure 3-4, the shear strength, τ, that can be developed on a plane such as a-b in Figure 3-4(a)is given by

$$\tau = c + \sigma_n \tan \phi \tag{3.1}$$

where c is cohesion, σ_n is the normal stress acting on plane a-b, and ϕ is the angle of internal friction.

Applying the stress transformation equations gives

$$\sigma_n = \frac{1}{2}(\sigma_1 - \sigma_3) + \frac{1}{2}(\sigma_1 - \sigma_3)\cos 2\beta \tag{3.2}$$

$$\tau = \frac{1}{2}(\sigma_1 - \sigma_3)\sin 2\beta \tag{3.3}$$

Substituting for σ_n and τ from equations (3.2) and (3.3) in equation (3.31) and rearranging gives the limiting stress condition on any plane defined by β as

$$\sigma_1 = \frac{2c + \sigma_3[\sin 2\beta + \tan \emptyset(1 - \cos 2\beta)]}{\sin 2\beta - \tan \emptyset(1 + \cos 2\beta)} \tag{3.4}$$

There will be a critical plane on which the available shear strength will be first reached as σ_1 is increased. The Mohr circle construction of Figure 3-4 (b) gives the orientation of this critical plane as

$$\beta = \frac{\pi}{4} + \frac{\emptyset}{2} \tag{3.5}$$

For the critical plane, sin 2β = cos ϕ, cos 2β = - sin ϕ, and equation (3.4) reduces to

$$\sigma_1 = \frac{2c\ \cos \emptyset + \sigma_3(1 + \sin \emptyset)}{1 - \sin \emptyset} \tag{3.6}$$

This linear relation between σ3 and the peak value of σ_1 is shown in Figure 3-4 (c) .Note that the slope of this envelope is related to ∅ by the equation

$$\tan \psi = \frac{1 + \sin \emptyset}{1 - \sin \emptyset} \tag{3.7}$$

and that the uniaxial compressive strength (σ_c) and uniaxial tensile strength (σ_t) are related to *c* and ϕ by

$$\sigma_c = \frac{2c \cos \emptyset}{1 - \sin \emptyset} \tag{3.8}$$

and,

$$\sigma_t = \frac{2c\ \cos \emptyset}{1 + \sin \emptyset} \tag{3.9}$$

It can be noted that σ_c, σ_t and c are proportionally related if ∅ is constant. For practical purposes, in rock mechanics, the uniaxial tensile strength (σ_t) often has a cut-off value that is frequently assumed as null (0).

3.3.2 Generalized Hoek Brown failure criterion

The Hoek–Brown strength criterion is an empirical criterion which was developed by trial and error and is based on the observed behavior of rock masses, model studies to simulate the failure mechanism of jointed rock, and triaxial compression tests of fractured rock (Hoek et al., 2002). Hoek–Brown follows a non-linear that distinguishes it from the linear Mohr–Coulomb failure criterion as shown in Figure 3-5. The criterion includes companion procedures developed to provide a practical means to estimate rock mass strength from laboratory test values and field observations. Hoek–Brown assumes independence of the intermediate principal stress.

The original non-linear Hoek–Brown strength criterion for intact rock is defined by (Hoek and Brown, 1980) as:

$$\sigma_1' = \sigma_3' + \sigma_c \left(m \frac{\sigma_3'}{\sigma_c} + s \right)^{0.5} \tag{3.10}$$

where σ_c is the unconfined compressive strength of the intact rock; σ_1' and σ_3' are the major and minor effective principal stresses, respectively; and m and s are material constants.

This criterion was later updated (Hoek & Brown, 1988) and modified (Hoek et al., 1992) to the current generalized form as follows:

$$\sigma_1' = \sigma_3' + \sigma_c \left(m_b \frac{\sigma_3'}{\sigma_c} + s \right)^{a} \tag{3.11}$$

where m_b is the reduced value of material constant m_i for the rock mass; and s and a are constants that depend on the characteristics of the rock mass.

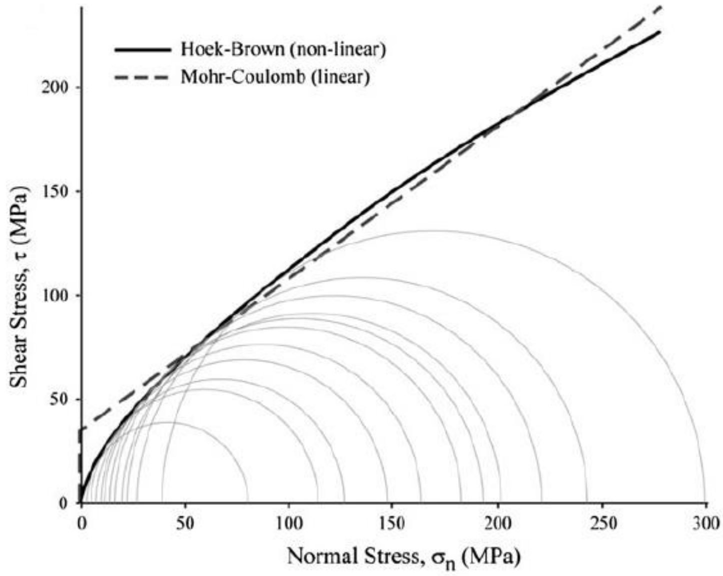

Figure 3-5 Comparison of the linear Mohr–Coulomb and nonlinear Hoek–Brown failure envelopes plotted against triaxial test data for intact rock (Eberhardt, 2012)

The parameters m_b, s and a can be estimated from the Geological Strength Index (GSI) as follows (Hoek et al., 2002):

$$m_b = m_i exp\left(\frac{GSI - 100}{28 - 14D}\right) \tag{3.12}$$

$$s = exp\left(\frac{GSI - 100}{9 - 3D}\right) \tag{3.13}$$

$$a = \frac{1}{2} + \frac{1}{6}\left(e^{\frac{-GSI}{15}} - e^{\frac{-20}{3}}\right) \tag{3.14}$$

D is a factor which depends upon the degree of disturbance to which the rock mass has been subjected by blast damage and stress relaxation. It varies from 0 for undisturbed in situ rock masses to 1 for very disturbed rock mass. The unconfined compression strength is obtained by setting σ'_3=0 in equation (3.11), giving

$$\sigma_c = \sigma_{ci} s^a \tag{3.15}$$

and, tensile strength is

$$\sigma_t = -\frac{s\sigma_{ci}}{m_b} \tag{3.16}$$

Priest (2005), suggested that the Hoek–Brown criteria has been used widely in rock engineering practice for the following reasons:

- It has been developed specifically for rock materials and rock masses.
- It has been applied for almost three decades by practitioners in rock engineering and has been applied successfully to a wide range of intact and fractured rock types.

3.4 Previous Research Works in Nepal Himalaya

The estimation of rock support pressure and selection of tunnel supports are carried out by empirical approaches based on the rock mass classification in the Himalayan region of Nepal. Among them, Q- system, proposed by Barton et al. (1974), is mostly used to design the tunnel support. The Q-system is not able to predict the deformation of the tunnel and the proposed support system was inadequate to control deformation in tunnels in weak rock mass conditions.

In 2003, Nepal Electricity Authority (NEA) conducted the in-situ rock test for Kulekhani III hydropower project. The tests were performed in the exploratory adit to obtain rock mechanics data for the design of underground tunnel and cavern. The exploratory adit was planned to check the actual condition of siliceous dolomite at excavation face. Plate load and block shear test were performed. Plate load testing was performed for determining moduli of the deformation and Deformation Modulus. Block shear test was performed to measure the peak and residual direct shear strength as a function of normal stress to the sheared plane. The adopted normal stresses were 0.5 MPa, 0.75 MPa, and 1 MPa.

Shrestha (2005), analyzed two hydropower tunnels situated in the Lesser Himalayan region of Nepal namely Khimti hydropower tunnel and Melemchi water supply tunnel project. The first one was completed and had stability problems during and after the construction and the second one was the proposed water supply tunnel at that time.

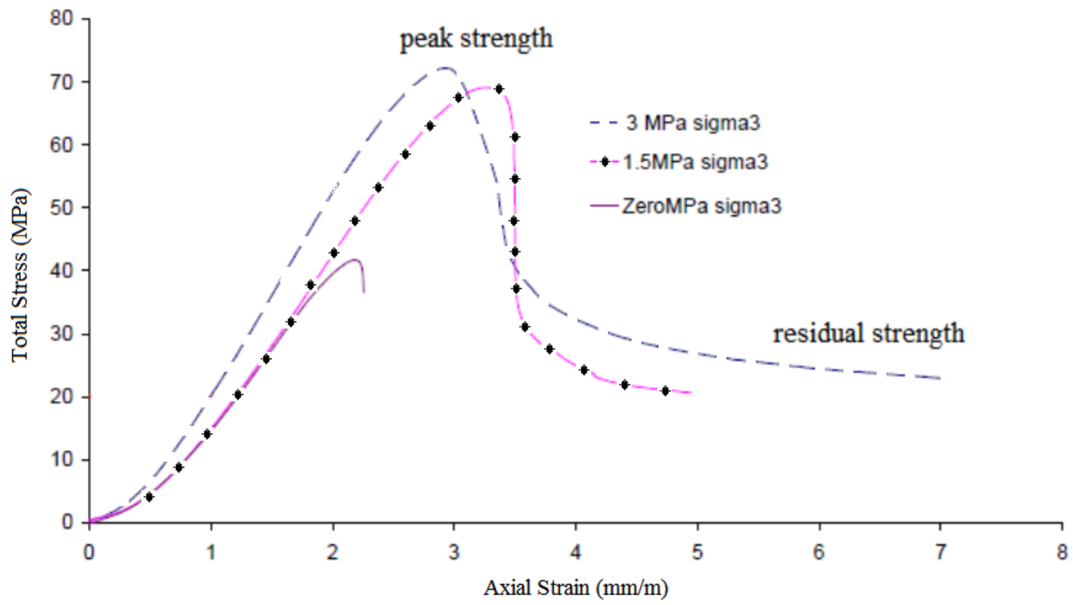

Figure 3-6 Stress-strain curves for different confining stresses of augen gneiss of Melemchi Project (Shrestha, 2005)

From that study, it was concluded that existing empirical, analytical and semi-analytical methods are more convenient for accessing stability of tunnel in jointed rock mass of Lesser Himalayan region of Nepal through case studies and found that there were good agreements on the convergence obtained by the analytical and measured values. In the case of the Melemchi tunnel, tunnel deformation obtained by numerical modeling was larger than that obtained by the analytical methods. The lab test was conducted for complete stress-strain curves for the Augen Gneiss. The complete stress-strain curve containing both peak and residual strength at different confining stress as shown in Figure 3-6.

3.5 GSI Reduction Base Approach

In the year 1995, Hoek et al. proposed Geological Strength Index (GSI) for estimation of rock mass strength and the rock mass deformation based on the two factors, rock structure and the block surface conditions. GSI gives the guidelines to estimate the peak strength parameters of jointed rock masses and no guidelines given by the GSI, or by any other system, for the estimation of the rock mass residual strength (Cai et al., 2007).

Cai et al. (2007) proposed a method to adjust the peak GSI to the residual GSI_r value based on the two main factors in the GSI system- the residual block volume V_b^r and the residual joint conditions factor J_c^r. They presented the methods to estimate the residual block volume and joint conditions factor, described later. They also validated the proposed method for the estimation of rock mass' residual strength with in-situ block shear test from three large scale cavern construction site and from a back analysis of rock slopes. It was found that the estimated residual strengths, calculated using the reduced residual GSI_r value, were in good agreement with field test or back analysis data. Based on the proposed quantification chart of GSI developed by Cai et al. 2007, and using surface technique, the following equation for the calculation of GSI from joint condition factor (J_c) and block volume (V_b) was developed

$$GSI(V_b, J_c) = \frac{26.5 + 8.75 \ln J_c + 0.9 \ln V_b}{1 + 0.0151 \ln J_c - 0.025 \ln V_b} \tag{3.17}$$

where J_c is dimensionless factor and V_b in cm^3.

Block Volume: Block size, which is determined from the joint spacing, joint orientation, number of joint sets and joint persistence, is an extremely important indicator of rock mass quality. Block size is a volumetric expression of joint density. The block volume spectrum from massive to very blocky rock masses ranges from 10^3 to 10^7 cm^3, and for disturbed to sheared rock from 0.1 to 10^3 cm^3. As an estimate, if the peak block volume V_b is greater than 10 cm^3, then, the residual block volume V_b^r in the disintegrated category can be taken to be 10 cm^3. If V_b is smaller than 10 cm^3, then, no reduction to the residual block volume is recommended, i.e., $V_b^r = V_b$.

Joint condition factor: The joint condition factor is defined as

$$J_c = \frac{J_W J_S}{J_A} \tag{3.18}$$

where J_c, J_W J_s, and J_A are joint condition factor, joint large-scale waviness factor, small scale smoothness factor, and alternation factor respectively.

Failure process affects the joint surface condition, especially the joint roughness then residual joint surface condition factor J_c^r is calculate as

$$J_c^r = \frac{J_W^r J_S^r}{J_A^r} \tag{3.19}$$

where J_W^r J_S^r, and J_A^r are residual values large scale waviness factor, small scale smoothness factor, and alteration factor respectively.

3.5.1 Residual GSI Value and Strength Parameters

According to the logic of the original GSI system, the strength of rock mass is controlled by its block size and joint surface conditions. The same concept is valid for the failed rock masses at the residual strength state (Cai et al. 2007). Therefore, the residual GSI_r is a function of V_b^r and J_c^r ,i.e.,

$$GSI_r = f(J_{c,}^r V_b^r) \tag{3.20}$$

Then above equation is rewritten as

$$GSI_r(V_b^r, J_c^r) = \frac{26.5 + 8.79 \ln J_c^r + 0.9 \ln V_b^r}{1 + 0.0151 \ln J_c^r - 0.0253 \ln V_b^r} \tag{3.21}$$

As for the intact rock properties, fracturing and shearing do not weaken the intact rock (even if they are broken into smaller pieces) so that the mechanical parameters (σ_c and m_i) should be unchanged. What has changed are the block size and joint surface conditions (especially the roughness).

Therefore, the generalized Hoek-Brown criterion for the residual strength of jointed rock masses can be written as

$$\sigma_1 = \sigma_3 + \sigma_c \left(m_r \frac{\sigma_3}{\sigma_c} + s_r \right)^{a^r} \tag{3.22}$$

Where m_r, s_r, a_r are the residual Hoek Brown constants for the rock mass. It is postulated that these constants can be determined from a residual GSI_r value using the same equations for peak strength parameters. This simply means that the equations for the peak strength parameter calculation hold true to the residual strength parameter calculation.

This statement is supported by the fact that the rock mass in its residual state represents one kind of rock mass spectrum in the GSI chart shown in Figure 3-7.Once the reduced GSI_r is obtained, the residual Hoek- Brown strength parameters or the equivalent residual Mohr-Coulomb strength parameters can be calculated, if other parameters such as σ_c and m_i are unchanged.

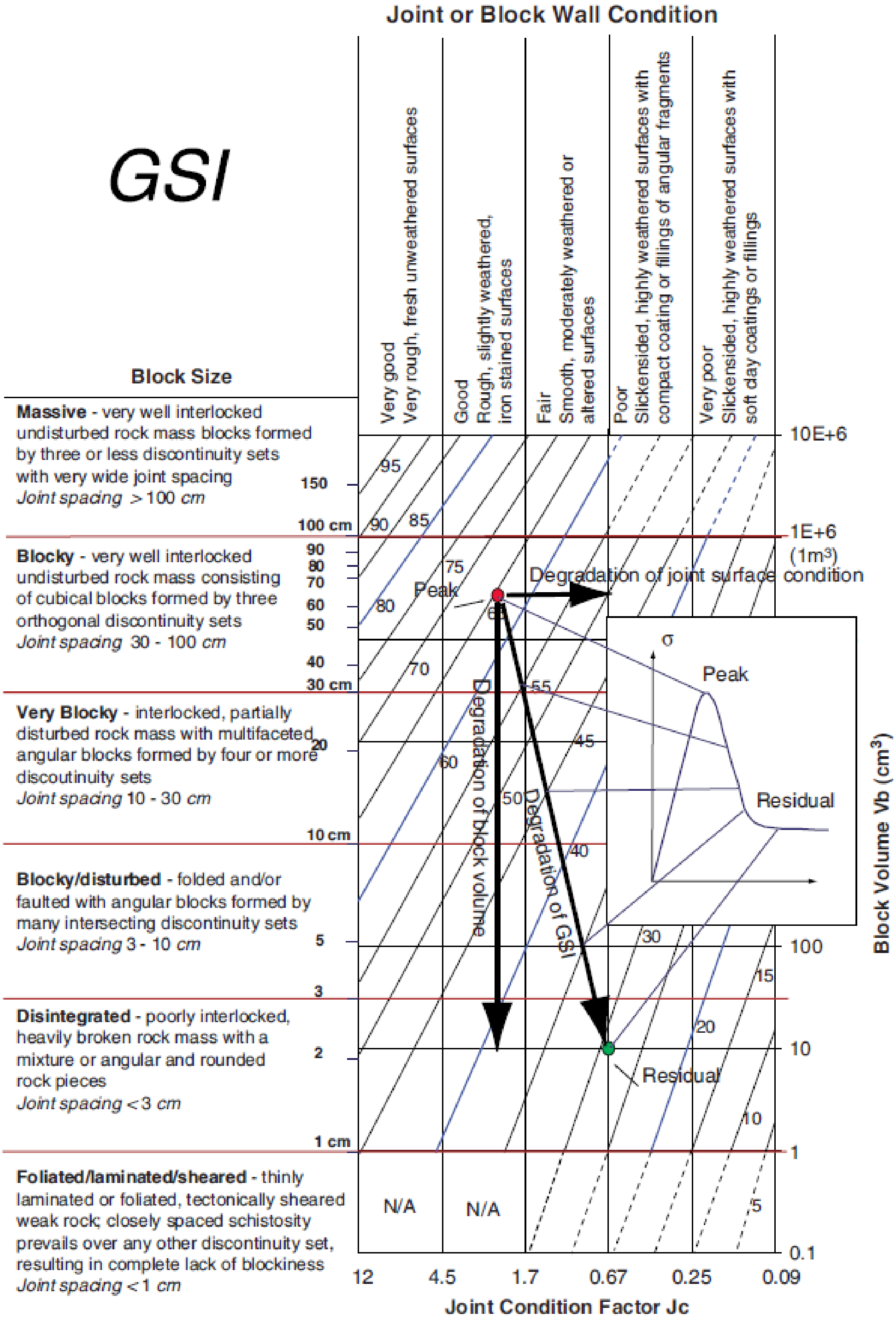

Figure 3-7 Degradation of the block volume and joint surface condition rock mass from peak to residual state (Cai et al., 2007)

3.6 Selection of Case Study

In this study six different tunnels are selected for the study, Figure 3-8. All these tunnels located in the Lesser Himalayan region of Nepal. The Lesser Himalayan zone constitutes a relatively broad tectonic zone, especially in western Nepal, a sandwiched between the Churia range, in the south, and the High Himalayan, in the North. It contains many major thrust as well as other types of faults. The main types of rocks are: schist, phyllite, gneiss, quartzite, granite, limestone geologically belonging to the Lesser Himalayan zone. Out of six selected projects, Chameliya and Kulekhani III hydroelectric project a field visit has been conducted because these projects are in under-construction. The information regarding rock mass quality, support details and some of the laboratory testing are collected from the previous published research works and reports from the concerned authority.

The input data for the analysis has been obtained from different published research works, feasibility reports of projects. From different authors like Panthi, 2006; Shrestha & Panthi, 2014; Shrestha, 2005; Basnet, 2013 published the data on their research work of Kaligandaki, Modi, Khimti, Melemchi and Chameliya respectively. For Kuleknani III hydropower project, the data are referred from the Geotechnical investigation reports published by Nepal Electricity Authority. Data from the published reports, tunnel logs has been collected and by using RocLab software developed by Rocscicence is used to generate the complete set of input data required for numerical modeling for 2D and 3D analysis and shown in Table 3.4.

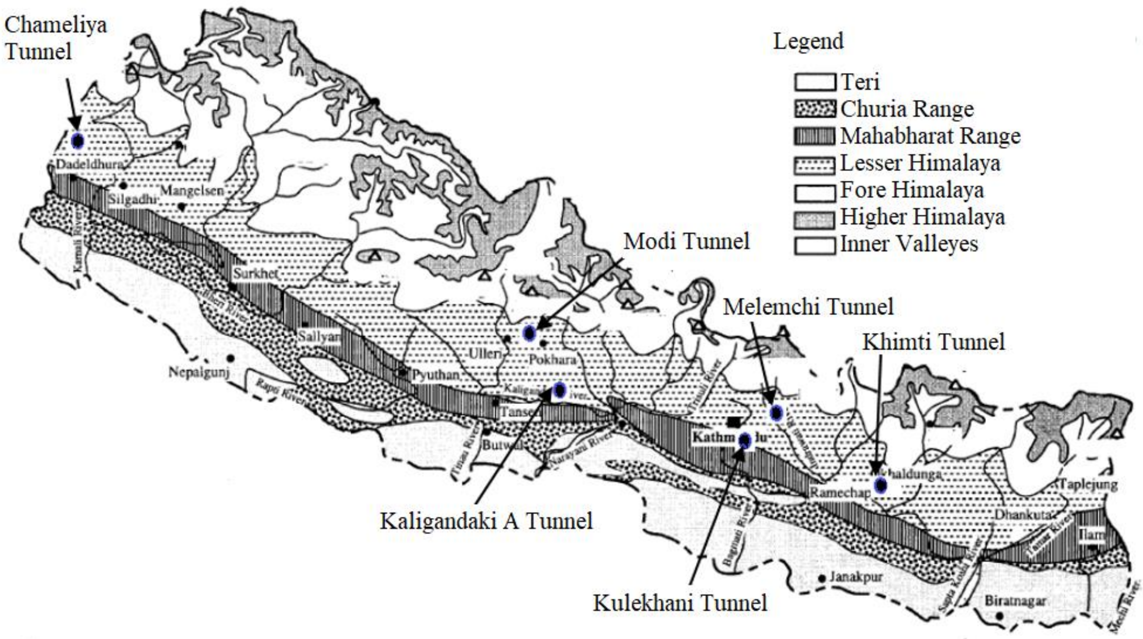

Figure 3-8 Location of studied tunnels in Lesser Himalayan region of Nepal(added on the geological map of Nepal Upreti and Le Fort, 1999)

In the following sections it will be presented a brief description of the selected case studies.

3.6.1 Kaligandaki Hydropower Tunnel

The Kaligandaki A hydropower tunnel was built between 1997 and 2000, with a total length of 5950 m (Figure 3-9) and a transversal cross section of approximately 60 m^2. The headrace tunnel mainly passes through highly deformed siliceous and poor quality, thinly foliated and highly weathered graphitic phyllite. Because of tectonic movement, the rock mass in the area has been subjected to shearing, folding and faulting. The maximum overburden above the tunnel is about 600 m and more than 80% of the tunnel alignment has overburden exceeding 200 m. The headrace tunnel faced severe squeezing due to weak rock mass and high overburden pressure. (Panthi & Nilson, 2007). There were considerable deviations between predicted and actual rock mass quality found and the provided tunnel rock support was not sufficient to control the excessive deformation (Panthi, 2006). There were mainly two types of tunnel stability problems: (i) the existing rock mass had not sufficient capacity to self-supporting the opening as shown in Figure 3-10 (a); and (ii) the second was related to the rock squeezing. Due to the squeezing, there were cracks in concrete lining as shown in Figure 3-10(b) and tunnel squeezed at many locations (Panthi, 2006).

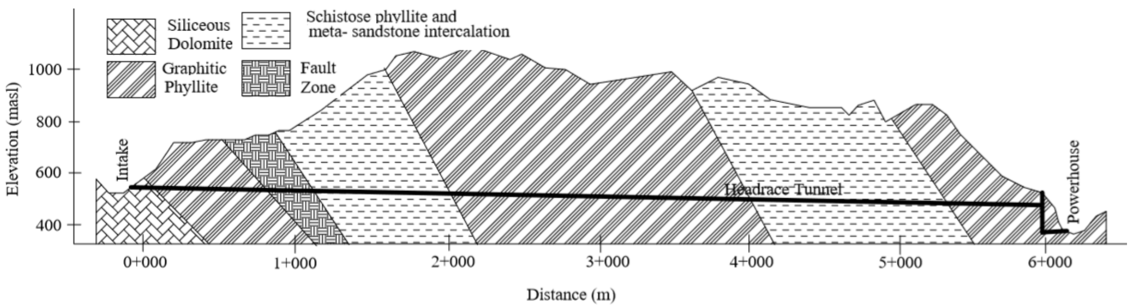

Figure 3-9 Longitudinal geological profile of Kaligandaki "A" hydropower tunnel (Panthi & Nilsen, 2007)

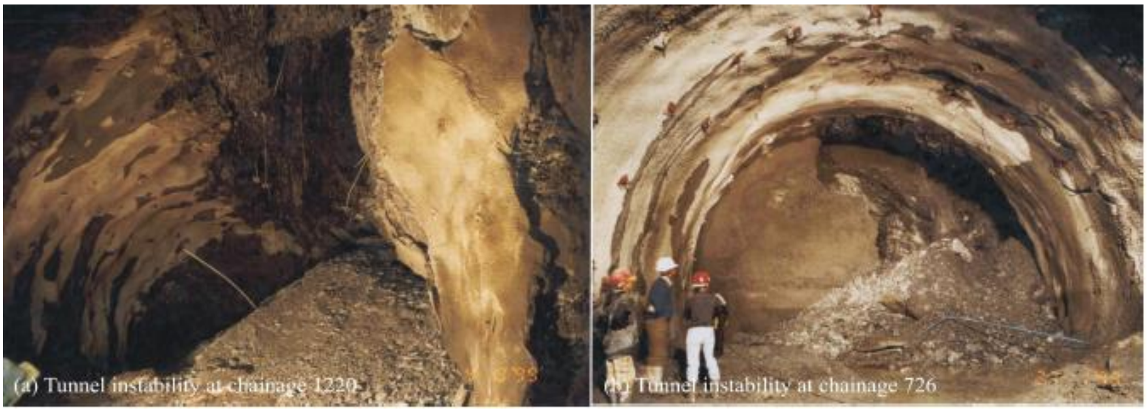

Figure 3-10(a) collapse due to strength and stress anisotropy and (b) cracks formed by high squeezing pressure (Panthi, 2006).

3.6.2 Modi Hydropower Tunnel

The Modi hydropower tunnel is located on the Lesser Himalayan region of Nepal about 270 km west of Kathmandu. The transversal cross section of tunnel is approximately 15 m^2, with a total length of 1500 m. The tunnel area lies in the Precambrian sequence of the Lesser Himalayan meta-sedimentary rock formation and nearly close to the Main Central thrust (MCT).

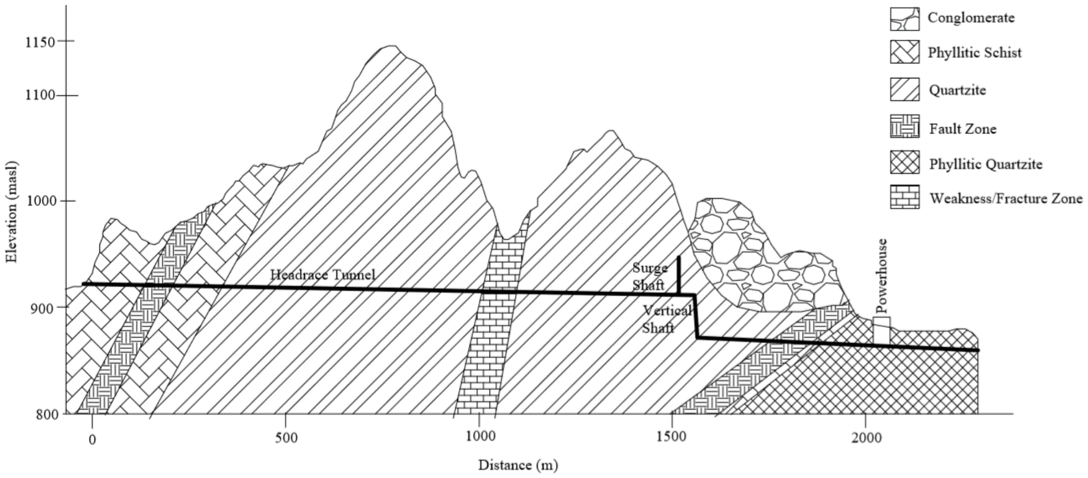

Figure 3-11 Plan and geological longitudinal profile of heardeace tunnel of Modi (Panthi, 2006).

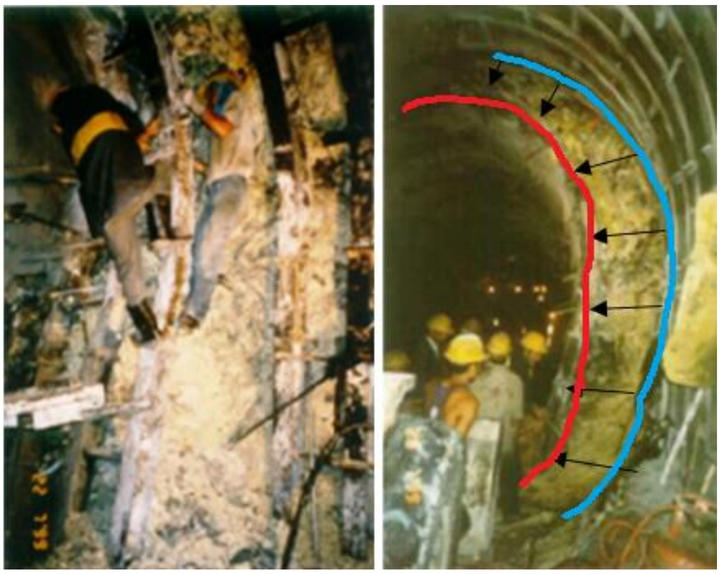

Figure 3-12 Squeezing and remedial works in Modi hydropower tunnel (Shrestha & Panthi, 2014)

The area has many local faults and the rock mass is fractured and deformed. The tunnel passes through the highly fractured greenish quartizite and highly sheared and deformed phyllitic green schists,Figure 3-11(Panthi, 2006). As the tunnel passes through very faulty zones, severe tunnel instabilities related to rock squeezing and increasing water inflow occurred during excavation between chainage 1700 m to 1800 m, Figure 3-11.

Severe squeezing was observed at several locations of headrace tunnel as the excavation proceeded across the fault as shown in Figure 3-12 (Shrestha & Panthi, 2014). Squeezing initiated with failure of joints in steel ribs; along the spring line of tunnel; and continued throughout the fault zone (Figure 3-12). The severity of squeezing reached its maximum at the hill side wall-bottom compare to the riverside wall. The tunnel lost considerable dimensions due to squeezing, thus, re-excavation of the squeezed tunnel was carried out, and the tunnel invert was lowered. Damaged steel ribs were removed in pieces and crown was excavated with due care, additional shotcrete was applied, and new steel ribs were installed. Horizontal H-beam struts were also provided at the lowered tunnel invert (Shrestha & Panthi, 2014).

3.6.3 Chameliya Hydropower Tunnel

The Chameliya hydropower tunnel is an under-construction tunnel, located to western part of Lesser Himalayan region. The main rock types within the project area are dolomite, sandstone, slate, dolomite intercalated with slate, talcosis dolomite and dolomite interbedded with phyllite (Basnet, 2013). The total length of horseshoe headrace tunnel is 4067 m, with transversal cross section area of 21 square meter. The longitudinal geological profile of headrace tunnel is shown in Figure 3-13. The maximum rock cover above the headrace tunnel is nearly 470 m in between the adit-1 and adit-2.

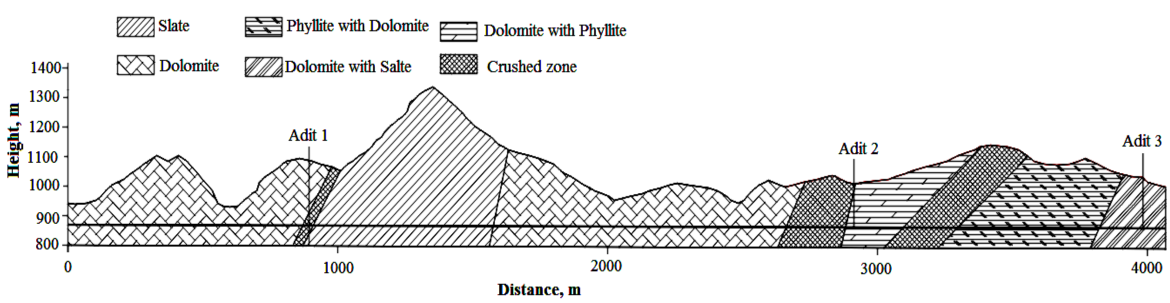

Figure 3-13 Longitudinal geological profile of Chameliya headrace tunnel (Source: Chameliya Hydropower Project)

The rock cover between adit -2 and adit -3 is nearly 275 m and rock mass are poor compared to the rest of tunnel alignment. It had been found that nearly 800 m length of tunnel, from chainage 3+102 m to 3+922 m, of tunnel is severely squeezed, Figure 3-13. The main rock type around the squeezed tunnel consists of kaoline and very poor talcosic phyllite, Figure 3-14 (b). In the squeezed section of tunnel, heavy reinforced concrete ring beam is provided to control the deformation of tunnel, Figure 3-14 (a).

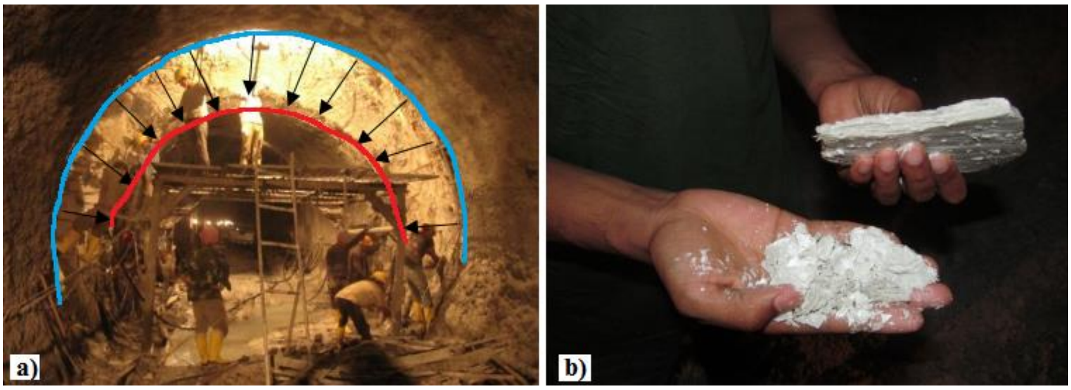

Figure 3-14 a) Treatment of squeezing tunnel, b) talcosic phyllite in squeezed tunnel of Chameliya (Photo taken by author during visit to tunnel)

3.6.4 Kulekhani III Hydropower Tunnel

The Kulekhani III hydropower tunnel is under construction and located southern part from Kathmandu. The total length of tunnel is 4221 m, with transversal cross section is approximately 10 m^2. The headrace tunnel passes across marble, schists, quartzite phyllite, siliceous dolomite and slaty phyllite.

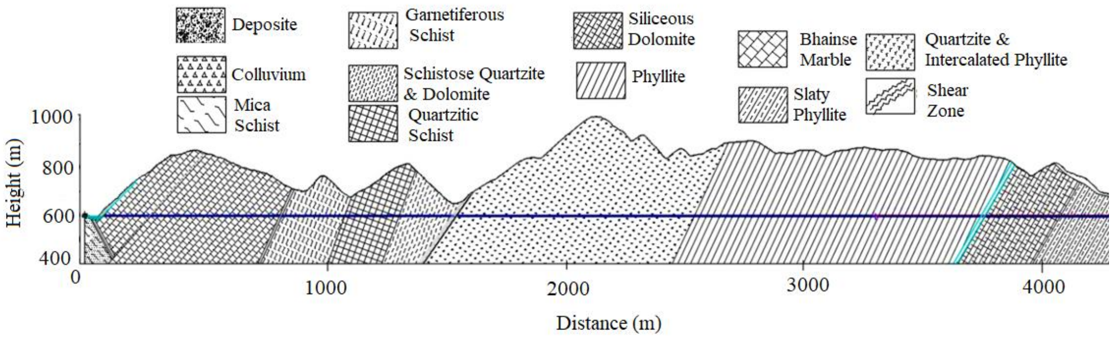

Figure 3-15 Longitudinal geological section of Kulekhani III tunnel (Source: Kulekhani III hydropower Project)

The tunnel passes across shear zones and thrusts. Mahabharat thrust is the main structure at 1450 m chainage. Seismic refraction survey shows about 12-25 m wide weak zones (velocity 1600m /s) along the thrust (NEA, 1997). The longitudinal geological section is shown in Figure 3-15. The roof of the tunnel gets collapsed after the application of support as shown in Figure 3-16 (a) and highly deformed Figure 3-16 (b).

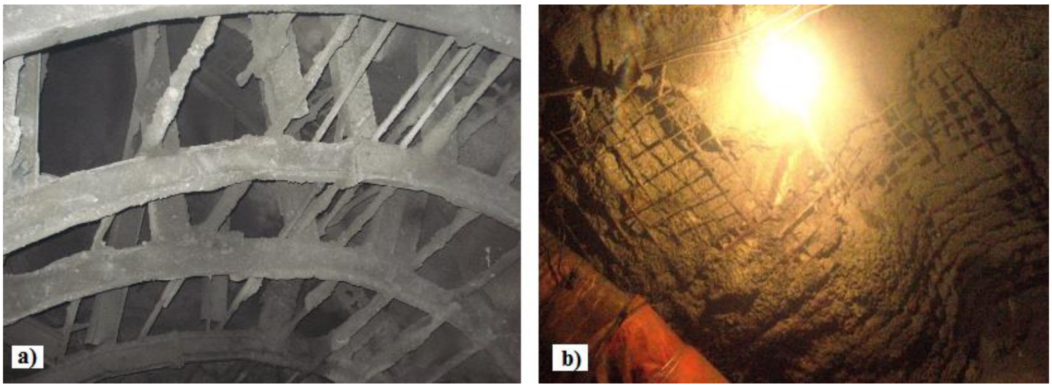

Figure 3-16 Tunnel stability problems a) fall of concrete lining, b) deformation of concrete lining (Photo taken by author during visit to tunnel)

3.6.5 Khimti Hydropower Tunnel

The Khimti hydropower tunnel was completed in 2000. It is located about 100 km from the Kathmandu, eastern part of Lesser Himalaya. The total length of headrace tunnel is 7900 m with inverted D-shape and 14 squarer meter cross section area. The project area mainly comprised by banded granite gneiss and augen mica gneiss. The headrace of tunnel passes through augen gneiss Figure 3-18. The area is also influenced by several minor thrust faults characterized by very weak rocks (Panthi, 2006). Adits and headrace tunnel faced the squeezing problems at various location especially at the sections where schists or decomposed Gneiss with 80 m to 420 m overburden depths was present.

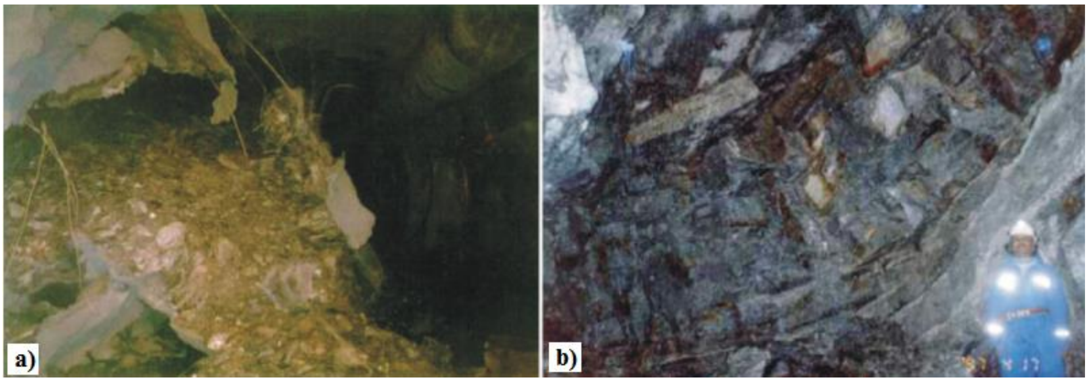

Figure 3-17 Tunnel instability: a) tunnel collapse after application of support, b) open and permeable joints within gneiss (Panthi, 2005)

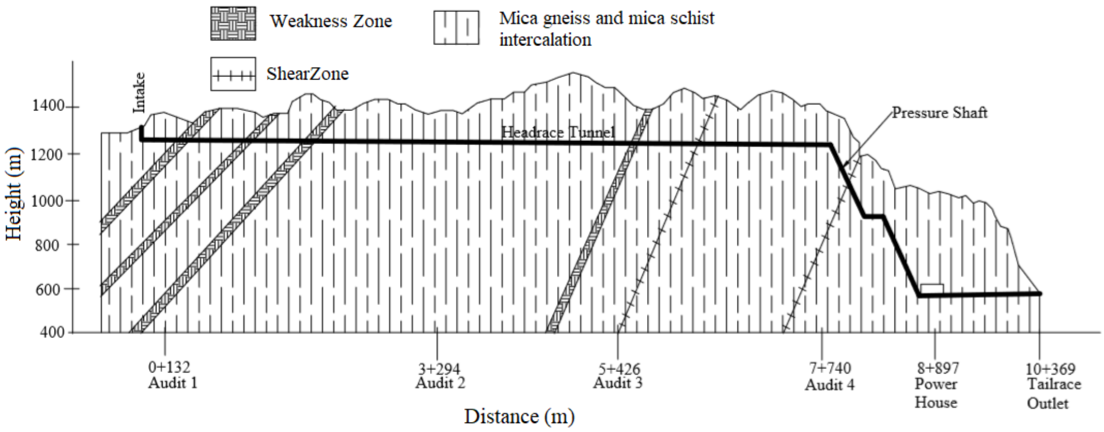

Figure 3-18 Longitudinal geological profile of headrace tunnel of Khimti (Panthi, 2006)

Two types of stability problems were observed in Khimti tunnel. The first one was related to tunnel support collapse caused by the presence of thick bands of highly weathered and sheared chlorite and talcose mica schist intercalated between relatively strong but fractured gneiss that allowed ground water to move into such bands as shown in Figure 3-17(a).

The second one was related to large leakage through open and permeable joints present in the gneisses and loss of valuable water from the tunnel during operation, as shown in Figure 3-17 (b). Such possible loss of water also may cause tunnel instability due to weakening and disintegration of weak rock mass strata consisting of mica schist (Panthi, 2006).

3.6.6 Melemchi Watersupply Tunnel

The Melemchi Watersupply tunnel is under construction tunnel and located in the Lesser Himalayan region of Nepal. It is one of the longest tunnel in Nepal with total length of 26 km and transversal cross section are is 12.7 m^2 (Shrestha,2005). The headrace tunnel passes through banded gneiss, intensely deformed and folded, augen gneiss, bolde quartizite (Figure 3-19).

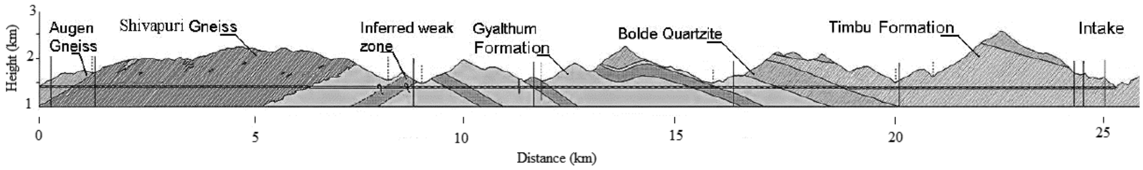

Figure 3-19 Longitudinal geological profile of Melemchi water supply tunnel (Shrestha, 2005)

3.7 Numerical Modeling

Numerical modeling is highly recommended to analyze the stability of tunnel passes through weak rock mass quality and high overburden (Shrestha & Panthi, 2014). It is therefore possible to predict tunnel behavior reliably, provided a proper understanding as observed in practice (Barla 2002).

3.7.1 Used Software

For numerical modeling finite element software RS^2 developed by Rocscience is used. It is used for 2-dimensional analysis and design of underground tunnels in hard rock, weak rock, jointed rock, and soft ground and other geotechnical works. Multi-stage analysis and advance support design tools simplify the design of tunnel lining system. It has, among other models, Mohr-Coulomb and Generalized Hoek-Brown failure criteria for material model (Rocscience, 2016). Both generalized Hoek Brown failure criteria and Mohr-Coulomb failure criteria are widely used for numerical modeling of weak rock mass of tunnel. The rock mass properties were evaluated by the empirical methods proposed by Hoek et al. (2002). Hsiao et al., (2009) mentioned that, these empirical methods have been widely used in design practice and verified by back analysis of case histories.

3.7.2 2D Model

Consider a circular tunnel of radius R, excavated in an elasto-plastic rock mass subjected to a hydrostatic initial stress of initial stress of P_0 as shown in Figure 3-20. If the support pressure p_i is less than a critical pressure p_e, then a plastic zone of radius r_e is formed around the opening. For such a tunnel, the lower value of the minor principal stress in the yielded zone occurs at the tunnel boundary and is equal to the support pressure p_i.

The upper value of the minor principal stress, when a plastic zone is formed around the opening, occurs on the elastic-plastic zone interface (Sofianos & Nomikos, 2006).

Hydrostatic stress field is assumed for analysis in which vertical and horizontal stress are equal. The rock mass is modelled by elastic perfectly plastic material and strain-softening. The length and width of model is taken as six times the diameter of circular tunnel respectively. The dimension of the 2D model is illustrated in Figure 3-21.

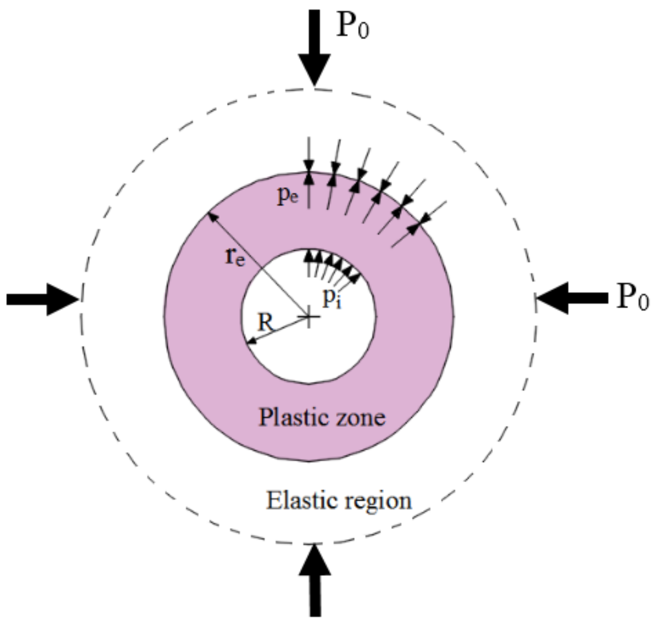

Figure 3-20 Circular tunnel in an elasto-plastic rock mass subjected to hydrostatic initial stress field (Sofianos & Nomikos, 2006)

At the outset of numerical modeling of rock mass for underground structures like tunnels and cavern in the Lesser Himalayan region of Nepal, six different cases are modeled to understand the nature of the rock mass. The rock mass properties of tunnel sections are given in Table 3.4. For tunnel support, concrete lining is modeled as an elastic material. The material properties of the concrete lining are given in Table 3.2.

The numerical analysis is carried out for an unsupported and supported tunnel with elastic- plastic and strain-softening (residual strength) constitutive models. The disturbance factor (D) is considered for the analysis. In the elastic-perfectly plastic analysis, the peak GSI is used only, that is, there is no reduction of GSI. It is assumed that the GSI remains the same before and after tunnel excavation. Another calculation, the strain-softening constitutive model is assumed in which the residual strength is accounted by the reduction of the peak GSI. There will be a reduction of the surrounding rock mass strength after excavation. The details of the numerical model are given in Table 3.1. Both constitutive models are used for all eight tunnel section, shown in Table 3.4 and analyzed by both failure criteria.

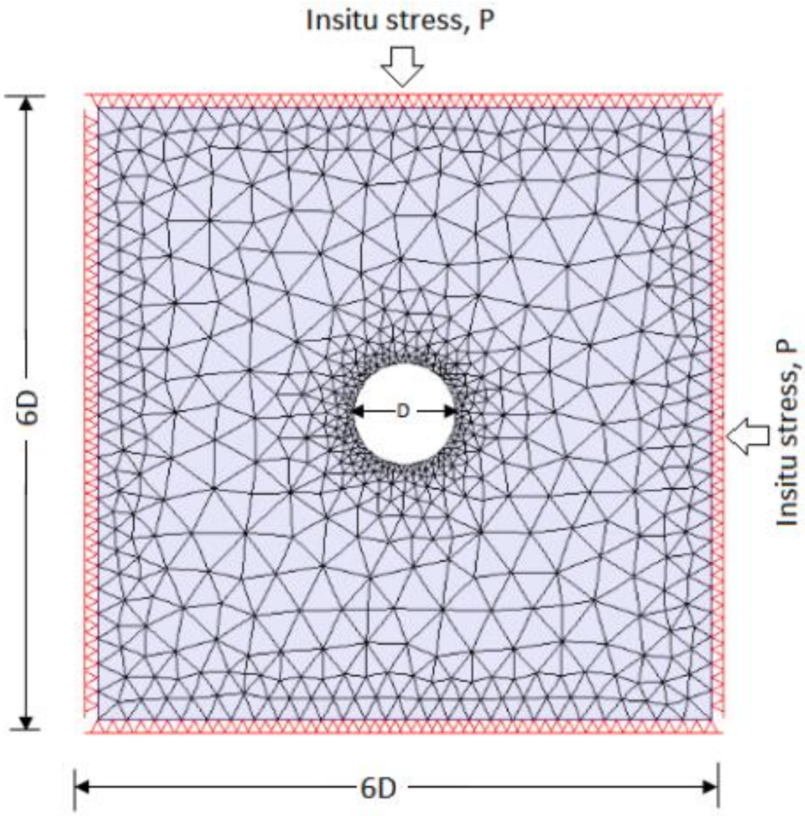

Figure 3-21 2D model for circular tunnel analysis

3.7.3 Numerical Steps

The following steps of modeling are used for modeling and analysis are as follows:

1. In this study full face tunnel excavation has been considered by drill and blast method. The hydropower tunnels are relatively smaller in cross section in Nepal Himalaya due to naturally available of high head for power generation.
2. A plane strain model has been developed in RS^2, as shown in Figure 3-21, and that relaxes an internal pressure on the tunnel boundary from a value equal to the applied in-situ stress to zero. The final stage, with zero internal pressure is used to determine the amount of deformation prior to support installation. The deformation is determined by the empirical relation proposed by Vlachopoulos and Diederichs (Rocscience, 2016).

3. The factoring of the applied internal pressure over several stages is used to determine the pressure that yields the amount of the tunnel wall deformation at the point of support installation. The support in the tunnel is installed and activated at a distance 2 m behind the tunnel face.
4. The tunnel closure is determined by knowing the maximum displacement of tunnel, at zero internal pressure, and radius of plastic zone.

Table 3.1 Selected numerical models for investigation of tunnel sections

SN	Tunnel	Constitutive Model	support	D	Remarks
1	All section	Elastic perfectly plastic	unsupported	0	Support install behind face
2	All section	Elastic perfectly plastic	supported	0	Support install behind face
3	All section	Elastic perfectly plastic	unsupported	0.5	Support install behind face
4	All section	Elastic perfectly plastic	supported	0.5	Support install behind face
5	All section	Strain-softening	unsupported	0	Support install behind face, Reduce peak GSI value
6	All section	Strain-softening	supported	0	Support install behind face, Reduce peak GSI value
7	All section	Strain-softening	unsupported	0.5	Support install behind face, Reduce peak GSI value
8	All section	Strain-softening	supported	0.5	Support install behind face, Reduce peak GSI value

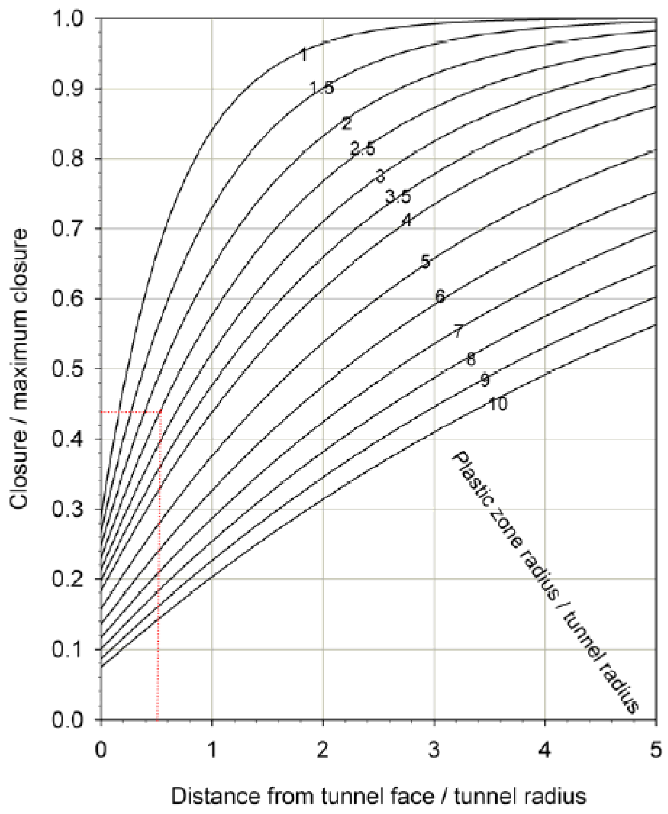

Figure 3-22 Plot to determine the tunnel closure prior to support installation suggested by Vlachopoulos and Diederichs (Rocscience)

3.7.4 Analyzed Tunnel Sections

In this study, eight different types of rock masses are modeled which are very common in the Lesser Himalayan region of Nepal. The rock masses are selected from the six different hydropower tunnels located in this region. These rock masses are classified into extremely poor, very poor, poor, fair and good based on the rock mass quality, as presented in Table 3.2. Due to weak rock mass quality and high overburden, these tunnels have experienced rock squeezing problems with excessive rock deformation. Melemchi and Kulekhani tunnels have not experienced such problems yet during the construction despite weak rock formation. Generalized Hoek-Brown failure criterion is used for the estimation of the rock mass properties which is also used for numerical modeling.

The numerical modeling is carried out by both Generalized Hoek- Brown and Mohr-Coulomb failure criterion. In numerical modeling, the disturbance factor, D, has been considered which depends upon the degree of disturbance due to blast damage and stress relaxation, as drill and blast is a common method for tunnel excavation in Nepal Himalaya. The degree of disturbance of the surrounding rock mass depends upon the method of excavation and rock mass quality. It varies from 0, for undisturbed in situ rock masses, to 1 for very disturbed rock mass (Hoek, 2007). Therefore, the numerical analysis is carried out by taking disturbance factor as 0 and 0.5.

Table 3.2Material properties of concrete lining

Description	Concrete
Young’s modulus (GPa)	30
Poisson’s ratio	0.15

Table 3.3 Tunnel support

Tunnel Project	concrete thickness (mm)
Kaligandaki	600
Chameliya	300
Modi	300
Kulekhani	100
Khimti	100
Melemchi	100

Table 3.4Rock mass properties of tunnel section used for numerical analysis

Rock Mass	Extremely poor			Very Poor		Poor	Fair	Good
Project tunnel	Kaligandaki	Chameliya	Modi	Khimti	Melemchi	Kulekhani	Melemchi	Kulekhani
Rock type	Graphite Phyllite	Talcosic Phyllite	Phylliti c Schist	Augen Gneiss Schist	Augen Gneiss	Phyllite	Augen Gneiss	Quartzit e
σci (MPa)	29.1	15	16	30	39	55	39	75
Ei (MPa)	7500	8250	10000	13700	34000	6000	20475	9000
ν	0.2	0.3	0.1	0.1	0.21	0.2	0.2	0.2
Q	0.018	0.01	0.008	0.25	0.45	2	7.18	13
H (m)	620	275	80	276	300	315	300	330
r (m)	4.35	2.7	2.5	2.5	2.5	2	2.5	2
GSI	20	20	15	35	40	50	57	62
D=0								
Hoek Brown Parameter								
mi	7	7	9	26	23	7	23	20
m_b	0.402	0.402	0.432	2.551	2.698	1.174	4.95	5.148
s	1.38E-04	1.38E-	7.91E-	7.30E-	1.00E-	4.00E-	8.00E-03	1.50E-
a	0.544	0.544	0.561	0.516	0.511	0.506	0.504	0.502
Mohr-Coulomb								
c (MPa)	0.671	0.36	0.361	1.604	2.166	2.46	2.746	5.451
Φ (^{0})	18.81	18.8	19.012	34.24	34.687	27.53	39.827	40.102
σ_{cm} (MPa)	0.223	0.119	0.08	0.722	1.29	3.312	3.512	8.99
E_{rm} (MPa)	959.1	376.8	554.02	2041.3	3580.2	3686.2	9259.66	5087.96
D=0.5								
Hoek Brown Parameter								
m_b	0.155	0.155	0.157	1.177	1.321	0.647	2.968	3.275
S	2.33E-05	2.33E-	1.19E-	1.70E-	3.35E-	1.00E-	3.00E-03	6.00E-
Mohr-Coulomb								
c (MPa)	0.445	0.238	0.23	1.229	1.7	1.955	2.319	4.674
Φ (^{0})	12.77	12.77	12.416	27.601	28.57	22.92	35.418	36.225
σ_{cm} (MPa)	0.085	0.045	0.028	0.343	0.652	1.88	2.178	5.881
E_{rm} (MPa)	627.95	246.36	399.6	1028.5	1724.34	1763.3	4678.1	2728.4

3.8 Results and Discussion

The numerical modeling has been carried out to investigate the tunnel deformation which predicts squeezing behavior of tunnel in the Lesser Himalayan region of Nepal. Based on the measured from 60 tunnel sections, for both non-squeezing and squeezing ground conditions, from several Indian tunnels, located in the Himalaya, the degree of tunnel squeezing has been classified as per tunnel closure (Singh & Goel, 2006). The classification of tunnel squeezing shown in Table 3.5. The different selected models used in this study are shown in Table 3.1. The numerical analysis is carried out by reducing the peak GSI value of rock mass, as suggested by Cai et at. (2007), for the strain-softening model. In the elastic-plastic model, there is no reduction of peak GSI.

Hoek and Brown (1997) confirm that fact the dilation angle is lower than the friction angle. For very good they suggest that the dilation angle is about ¼ of the friction angle, for the average quality rock, the value suggested is 1/8 and poor rock seems to have a negligible dilation angle. Modular ratio (MR) is used for the estimation of deformation modulus using the relation. When no direct values of the intact modulus are available or where completely undisturbed sampling for measurement of E_i is difficult.

The input data for the analysis has been obtained from different published research works, feasibility reports of projects. From different authors like Panthi, 2006; Shrestha & Panthi, 2014; Shrestha, 2005; Basnet, 2013 published the data on their research work of Kaligandaki, Modi, Khimti, Melemchi, and Chameliya respectively. For Kuleknani III hydropower project, the data are referred from the Geotechnical investigation reports published by the Nepal Electricity Authority. Data from the published reports, tunnel logs have been collected and by using RocLab software, developed by Rocscicence, is used to generate the complete set of input data required for numerical modeling for 2D and 3D analysis and shown in Table 3.4.

Table 3.5 Classification of tunnel squeezing based on the tunnel closure (after Singh & Goel, 2006)

SN	Degree of Squeezing	Tunnel Closure (%)
1	Very mild squeezing	1-2
2	Mild squeezing	2-3
3	Mild to moderate squeezing	3-4
4	Moderate squeezing	4-5
5	High squeezing	5-7
6	Very high squeezing	>7

3.8.1 Elastic- Plastic Analysis

Eight tunnel sections are analyzed considering elastic-perfectly plastic analysis in which both peak and residual GSI are the same during the analysis. The analysis is carried out for different disturbance factor as described above with two failure criteria namely generalized Hoek- Brown and Mohr-Coulomb. The tunnel deformation and percentage of tunnel closure, for these elasto-plastic calculations, are shown in Table 3.6.

Table 3.6 Tunnel deformation by elastic perfectly plastic analysis

Peak GSI	Tunnel	Tunnel radius (mm)	Tunnel Deformation (mm)				Tunnel Closure (%)			
			D=0		D=0.5		D=0		D=0.5	
			GHB	MC	GHB	MC	GHB	MC	GHB	MC
20	Kaligandaki	4350	270	250	1310	1170	6	6	30	27
20	Chameliya	2700	170	250	360	500	6	9	13	19
12	Modi	2500	30	20	90	80	1	1	4	3
50	Kulekhani	2000	8	6	20	20	0.4	0.3	1	1
62	Kulekhani	2000	4	4	8	7	0.2	0.2	0.4	0.35
35	Khimti	2500	30	10	30	30	1	0.4	1	1
40	Melemchi	2500	30	7	30	20	1.2	0.28	1	0.8
57	Melemchi	2500	4	3	7	4	0.16	0.12	0.28	0.16

Note: GHB: Generalized Hoek Brown, MC: Mohr-Coulomb, D=Disturbance factor

Disturbance factor is taken as 0

- In case of extremely poor rock masses like graphitic phyllite, talcosic phyllite and phyllitic schists of Kaligandaki, Chameliya and Modi hydropower tunnel respectively, the peak GSI is 20 and less than 20, the tunnel deformations are given by both failure criteria are not significantly different.
- The tunnel closure of extremely poor rock masses with high overburden like Kaligandaki and Chameliya tunnel is 6% of tunnel radius and for the same rock mass but low overburden of Modi tunnel is 1%. Therefore, high rock stress plays a vital role in the rock squeezing in poor rock mass conditions. Similarly, the tunnel closure for rock masses, GSI greater than 40, like Kulekhani and Melemchi tunnel, is less than 1%. But when the GSI lies between 30 and 40, the tunnel closure is within 1%, as shown in Table 3.6.
- If GSI is greater than 50, that is the rock masses of Melemchi Augen gneiss, Kulekhani phyllite, and Kulekhani quartzite, the tunnel closure is less than 1%, as shown in Table 3.6.

Disturbance factor is taken as 0.5

When the tunnel is modeled by considering D=0.5, assuming the surrounding rock mass is disturbed during tunneling.

- The tunnel is highly deformed in cases of the extremely poor rock mass like Kaligandaki, Chameliya and Modi tunnel. The tunnel closure is more than 10 %, which signifies a very high squeezing tunnel. The tunnel closure for extremely poor rock masses, GSI is less than 30, like Kaligandaki and Chameliya tunnels, are 30 % and 13 % respectively and for Modi it is 4% of the tunnel radius.

- If GSI is greater than 50, the tunnel closure is below 1% and if it is lies between 30 and 40, the tunnel closure is within 1 % of tunnel, that is mild squeezing.
- There are no significant effects on tunnel deformations to consider disturbance factor for modeling the rock masses whose peak GSI is greater than 30 in case of an elastic-plastic material. It suggests that the rock mass around the tunnel periphery is not disturbed during tunneling. But in reality, the rock mass around the tunnel gets disturbed in such geological conditions. Therefore, the elastic-plastic analysis would not be appropriate to model such rock masses.

3.8.2 Strain-Softening Analysis

In case of strain- softening analysis, it is assumed that the rock mass will take some field stress before it reaches maximum deformation. It will have some residual strength to take the field stress. During the modeling of the rock mass the peak GSI is reduced to some extent as a residual value. This is achieved by reducing the peak GSI value to residual, which is estimated by the guidelines provided by the Hoek et al., (1995). In case of Kulekhani Phyllite, the peak GSI reduced from 50 to 30, as shown in Table 3.7, means that the rock mass is poorly interlocked, heavily broken with mixture of angular and rounded rock pieces from very well interlocked undisturbed rock mass as per the quantification of GSI chart, see Figure 3-7, (Cai et al., 2007). It is due to the blasting of rock during the excavation of tunnel and also the poor quality of rock mass in the Himalayan region.

Table 3.7 Tunnel deformation by strain-softening analysis

Peak GSI	Residual GSI	Tunnel name	Tunnel radius (mm)	Tunnel Deformation (mm)				Tunnel Closure (%)			
				D=0		D=0.5		D=0		D=0.5	
				GHB	MC	GHB	MC	GHB	MC	GHB	MC
20	15	Kaligandak	4350	400	350	2200	19	9	8	51	44
20	15	Chameliya	2700	240	350	520	76	9	13	19	28
15	10	Modi	2500	30	30	70	70	1.2	1	3	3
50	30	Kulekhani	2000	20	10	70	50	1	0.5	4	3
62	30	Kulekhani	2000	20	4	60	7	1	0.2	3	0.3
35	25	Khimti	2500	30	20	70	70	1.2	1	3	3
40	25	Melemchi	2500	20	10	60	30	0.8	0.4	2	1
57	25	Melemchi	2500	10	4	30	20	0.4	0.1	1	1

Note: GHB: Generalized Hoek Brown, MC: Mohr-Coulomb, D=Disturbance factor

Disturbance factor is taken as 0

In case of the extremely poor rock mass like Kaligandaki, Chameliya, the tunnel closure is increased form 6 % to 9% for both tunnels when the peak GSI is reduced by 75 % as shown in Table 3.7. This signifies that the tunnel undergoes very high squeezing, Table 3.5. For the Modi tunnel it is only 1% because it has low overburden, 80 m, as compare to Kaligandaki and Chameliya.

When the peak GSI is reduced, the tunnel deformation is increased because the surrounding rock mass is degraded during the tunneling. The tunnel closure is increased by 1 % of tunnel radius showing very mild squeezing, as compared to the elastic-plastic analysis for the rock masses whose peak GSI is more than 50, Table 3.7. There is no significant difference in tunnel deformation obtained from both elastic-perfectly plastic and strain-softening constitutive models of the rock masses having the peak GSI is greater than 30.

Disturbance factor is taken as 0.5

- In case of extremely poor rock mass, the tunnel closure is 51% and 19% of tunnel radius for the Kaligandaki and Chameliya tunnel respectively, shown in Table 3.7. It showed that the tunnels undergo very high squeezing.
- Poor to very poor rock mass like Khimti, Melemchi and Khulekhani tunnel, GSI is lies between 30 and 50, the tunnel deformation is increased from 1 % to 3% of tunnel radius when the peak GSI is reduced in between 60 and 70 %, as shown in Table 3.7. This showed that tunnels undergo mild squeezing problem, Table 3.5 which is likely to occur in such geological conditions.
- Fair to good rock mass where, GSI lies between 50 and 65, the tunnel deformation increased from less than 1 % to up to 2%. This showed that tunnel undergo very mild squeezing. In this case the peak GSI is reduced in between 50 and 40 %, as shown in Table 3.7.

There are very few measured tunnel sections in this region. In Kaligandaki, Khimti and Modi tunnel, the tunnel deformation was measured in different sections during the construction, as shown in Table 3.8. For numerical modeling, these sections are considered for analysis. The averaged measured tunnel deformation of Khimti tunnel is 65 mm, as shown in Table 3.8, and it is closer to the deformation from numerical analysis analyzed by the strain-softening considering disturbance factor as 0.5, as shown in Table 3.7, using generalized Hoek-Brown failure criterion. Similarly, for Kaligandaki tunnel, the averaged measured tunnel deformation is 292 mm, as shown in Table 3.8, which is closer to the deformation obtained from the elastic-plastic analysis considering disturbance factor as 0. The deformation obtained from the elastic plastic analysis is 270 mm as shown in Table 3.6. The tunnel deformation obtained from the strain-softening analysis is 400 mm when the disturbance factor is taken to 0 and it is 2200 mm when the disturbance factor is taken to 0.5 shown in Table 3.7. From this comparison, it is suggested that, for extremely poor rock mass, the elastic plastic analysis is more appropriate. Strain softening analysis is the good for poor to good rock mass considering the different value of the disturbance factor. Based on the numerical analysis and measured deformation of the tunnel, the different types of rock mass have been characterized for the numerical analysis which is able to show real behavior as shown in Table 3.9.

Table 3.8 Measured tunnel deformation from case studies located in Lesser Himalayan region

SN	Tunnel, location	Rock Type	H (m)	Q	a (m)	U_{obs}(mm)	Average (mm)	Reference
1	Khimti, Adit1	Augen Gneiss	98	0.08	4.0	30.9	65.4	Shrestha, 2005
2	Khimti, Adit1	Augen Gneiss	100	0.01	4.2	160		
3	Khimti, Adit1	Augen Gneiss	111	0.00	4.3	32.3		
4	Khimti, Adit3	Augen Gneiss	276	0.25	5.0	38.7		
5	Kaligandaki	Graphitic	620	0.02	8.7	213	292.8	Shrestha & Panthi, 2014
6	Kaligandaki	Graphitic	620	0.00	8.7	370		
7	Kaligandaki	Graphitic	620	0.00	8.7	334		
8	Kaligandaki	Graphitic	620	0.00	8.7	356		
9	Kaligandaki	Graphitic	620	0.01	8.7	191		
10	Modi,50 m	Phyllitic schist	80	0.01	5.0	205	379	Shrestha & Panthi, 2013
11	Modi,60 m	Phyllitic schist	80	0.01	5.0	465		
12	Modi,70 m	Phyllitic schist	80	0.01	5.0	467		

Note: H, overburden depth; Q, rock mass quality; a, tunnel radius; U_{obs}, measured tunnel deformation

Table 3.9 Rock mass characterization in terms of peak and residual strength in Lesser Himalayan region using GSI system

Rock mass quality	GSI	Tunnel name	Rock Types	Peak GSI	Residual GSI
Extremely poor rock mass, Highly Jointed and weathered rocks	20<GSI<30	Kaligandaki	Graphitic phyllite	20	No reduction in peak GSI
		Chameliya	Talcosic phyllite	20	
		Modi	Phyllitic schists	15	
Very poor to Poor, Moderately Jointed and weathered rocks	30<GSI<50	Khimti	Augen gneiss schists	35	Reduce between 60 and 70% of peak GSI
		Melemchi		40	
		Kulekhani	Phyllite	50	
Fair to good rock, Jointed rocks	50<GSI<65	Melemchi	Augen gneiss	57	Reduce between 40 and 50% of
		Kulekhani	Quartzite	62	

3.9 Conclusions

This chapter focuses on modeling of weak rock mass which exhibits squeezing behavior common during tunneling in the Lesser Himalayan region of Nepal. It has composed with extremely poor to a good quality of rock masses. It is due to the active tectonic movement and high degree of weathering. Most of the tunnels in this region pass through weak rock mass and a high in-situ stresses and suffered from rock squeezing problems.

In numerical modeling, the rock mass is characterized by the GSI method and the rock mass parameter are estimated using generalized Hoek-Brown failure criteria. Generalized Hoek-Brown and Mohr-Coulomb failure criteria are used for numerical analysis. Kaligandaki, Modi and Chameliya hydropower tunnels are located in the western part of the Lesser Himalayan region and rock masses are characterized as extremely poor with high overburden.

These tunnels experienced moderate to severe squeezing. Khimit and Melemchi tunnels are located in the eastern part of the region and rock masses are more competent comparatively better than the western part. They are classified very poor to fair rock mass. Similarly, Kulekhani hydropower tunnel located in the Southern part of the Lesser Himalayan region has fair to good quality rock mass. The location of tunnels is shown in Figure 3-8.

From this study the following point are concluded:

A) General

- Disturbance factor played an important role in the analysis of underground structures in Lesser Himalayan of Nepal which composed of very poor and poor rock mass conditions in high in-situ stress. Disturbance factor is considered in each analysis and it is taken as 0 for the controlled blasting, that is, minimal disturbance to the surrounding rocks and 0.5 is taken for the potential of squeezing.
- Different types of rock masses, that is, extremely poor, very poor, poor, fair and good quality of rock mass, of different six hydropower tunnels, are analyzed by both generalized Hoek-Brown and Mohr-Coulomb failure criteria.
- The western part of this region is characterized with extremely poor to poor rock mass while the eastern and the southern parts are characterized by the comparatively good quality of rock mass than the western part, Figure 3-8. Talcosic phyllite, graphitic phyllite and phyllitic schists of Chameliya, Kaligandaki and Modi hydropower tunnels respectively are extremely poor rock mass. The GSI for these rock mass is 20 or below. Banded augen gneiss and augen gneiss schist of Khimti and Melemchi are poor to fair quality rock masses and have GSI more than 30. Similarly, the phyllite and quartzite of Kulekhani

hydropower tunnels are fair to good quality of rock mass and the GSI is greater than 50.

- The deformation given by both failure criteria are close to each other. The deformation is given by the generalized Hoek-Brown slightly more than the Mohr- Coulomb.
- It is advisable to model this kind of jointed rock masses with generalized Hoek-Brown because it characterized by the GSI.

B) Elastic-perfectly plastic model

- For the extremely poor rock mass, GSI is less than 30, an elastic-perfectly plastic constitutive model would predict the actual behavior of the tunnel in this region. These tunnels were highly squeezed during construction. Due to extremely poor rock and high in-situ stress conditions, it is suggested that during the tunneling control blasting should be carried out and during the modeling, the disturbance factor 0 is taken for analysis and design of tunnel.
- In the case of elastic-perfectly plastic analysis, rock mass having GSI greater than 30, like Khimti and Melemchi, the tunnel closure is within 1% by generalized Hoek-Brown and it is less than 1% as analyzed by the Mohr-Coulomb failure criteria, Table 3.6, considering the disturbance factor 0 and 0.5. It is clear that for rock masses having GSI greater than 30, the disturbance factor has no significant role in the elastic-plastic analysis. Similarly, for the rock masses having GSI greater than 50, like Kulekhani quartzite and Melemchi gneiss, the tunnel deformation given by both failure criteria are less than 1% of tunnel radius. This indicates that the tunnel undergoes very mild squeezing in such geological conditions but it is not able to predict the real behavior of tunnels in this region.
- In the case of Modi tunnel, the in-situ stress is comparatively less than the Kaligandaki and Chameliya tunnel, it is appropriate to take disturbance factor 0.5 for numerical modeling in the elastic-plastic model.

C) Strain-softening model

- In case of strain-softening analysis, the extremely poor rock masses, GSI is less than 30, gives higher tunnel deformation by both failure criteria. Disturbance factor significantly effects on the tunnel deformation, Table 3.7. Therefore, extremely poor rock mass and have high in-situ stress, a strain-softening model may not be appropriate for numerical modeling.
- For rock masses GSI is greater than 30, a strain-softening model is more appropriate to predict the real tunnel behavior during tunneling by taking account of disturbance factor as 0.5 in such geological conditions, shown in Table 3.9.

4 DESCRIPTION OF THE CASE STUDIES

4.1 General

In this chapter, two hydropower tunnels from the Lesser Himalayan region of Nepal, shown in Figure 4-1, are discussed and analyzed as case studies. Kulekhani III hydropower project and Chameliya hydropower project are taken as case studies. Both projects are near to completion and lie in the same geological region. In Figure 4-1, the project locations are shown with geological formation.

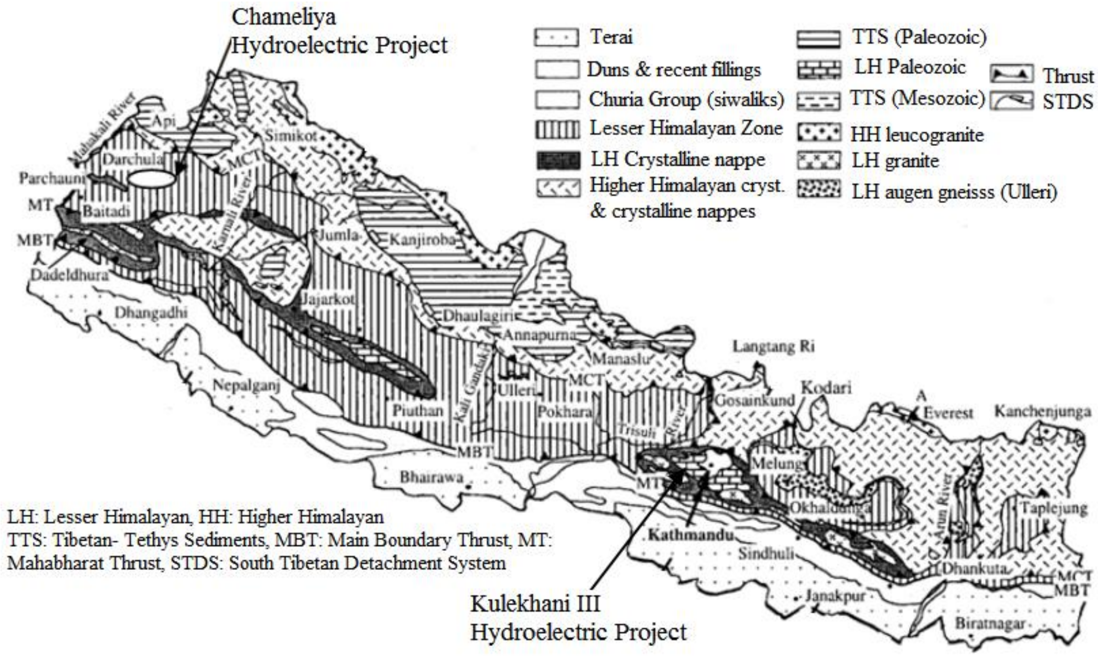

Figure 4-1 Project locations and geological map of Nepal. (the project location added on the geological map after Upreti, 1999)

4.2 Kulekhani III Hydropower Tunnel

4.2.1 Introduction

Kulekhani-III (KL-III) hydropower project is the cascade scheme of Kulekhani storage project with an installed capacity of 14 MW. The project is designed to utilize a net head of 103.17 m and a design discharge of 16 m^3/s to generate peak power of 14 MW. The project lies in Makawanpur district, Narayani zone of central development region in Rapti river basin. The power station of the project is uses the regulated flow of Kulekhani reservoir via tailrace of Kulekhani -III hydropower project and along with water from

Khani Khola. The length and diameter of headrace tunnel is 4221.63 m and 3.5 m respectively with a horseshoe shaped.

4.2.2 Geology of Project Area

The project area lies in the southernmost part of Kathmandu synclinorium characterized by meta-sedimentary rocks and crystalline rocks of Nuwakot complex and Kathmandu complex. The area comprises of crystalline rocks as garnet-mica schists (Kalitar formation), Marble (Bhainse Dobhan marble) and meta- sedimentary rocks such as schists of Precambrian age and quartzite, phyllite (Robang formation), siliceous dolomite (Malekhu formation) and slaty phyllite (Benighat slates) of Paleozoic age. The general trend of rocks is almost east to west and dips steeply towards north. The headrace tunnel passes across marble, schists, quartzite phyllite, siliceous dolomite and slaty phyllite. The tunnel passes across sheared zones and thrusts. Mahabharat thrust is the main structure at 1450 m chainage. Seismic refraction survey shows about 12-25 m wide weak zones (velocity 1600m /s) along the thrust (NEA, 1997).

NEA, 2003 conducted the in situ rock test for Kulekhani hydropower project. The tests were performed in the exploratory adit in order to obtained rock mechanics data for design of underground tunnel and cavern. The exploratory adit was planned to drive to check actual condition of siliceous dolomite at excavation face. As a result of observation of the adit, rock conditions in the section around 70 m to 90 m from the adit portal is poor to relatively poor, however moderately fair rock condition is confirmed in the rest of the section (NEA, 2003). Plate load and block shear test were performed as shown in Figure 4-2. Plate load testing was performed for determining moduli of the deformation and the elasticity (Young's modulus) and block shear test was performed to measure the peak and residual direct shear strength as a function of stress to the sheared plane. The normal stress had been varied as 5 kg/cm^2, 7.5 kg/cm^2 and 10 kg/cm^2.

Plate loading test was carried out at three spots of the branch Adit-tunnel around 10 m from the excavation face as shown in Figure 4-2. Both the modulus of elasticity and the modulus of deformation can be calculated with the same formula as

$$\mathrm{E\ or\ D} = (1-\mu^2)\frac{\mathrm{dF}}{\mathrm{dS}}0.5\mathrm{a} \tag{4.1}$$

Where, E is the modulus of elasticity (kgf/cm^2), D is the modulus of deformation (kgf/cm^2), a is the radius of steel plate in cm, μ is the Poisson's ratio (0.2 for hard rock and 0.25 to 0.3 for soft rock), dF is the increase load in section of load-displacement curve (kgf= ton/1000), dS is the increase displacement for the section of load-displacement for the same section as above in cm.

If the gradient of a tangential line of stress-displacement curve for the peak stress is placed in the place of dF/dS, the formula, equation (4. 1), will give a modulus of elasticity and if the gradient of a line enveloping the stress-displacement curve of the initial stress is used for dF/dS, it will give a deformation modulus as shown in Figure 4-3. Table 4.1gives the value of modulus of elasticity and deformability after test.

Table 4.1Plate load testing (after NEA, 2003)

Location	Modulus of Deformation (MPa)	Modulus of Elasticity (MPa)
PL1	3183.9	14650.0
PL2	9366.9	25340.5
PL3	1869.5	8392.9

The results of the plate loading test indicate hard and compact state of rock while the result of shearing test, where both (plate loading and rock shear testing) tests were performed in adjacent location, indicates the relatively soft and the poor rock condition (NEA, 2003). From the laboratory test of rock samples near the in-situ rock testing, the uniaxial compression strength of dolomite appears to be more than 50 MPa. According to the study on the relationship between the uniaxial compression strength and the shear strength of similar rock of dolomite on the basis of numerous data of rock samples obtained in Japan, the shear strength of rock is 2 to 3 MPa if the uniaxial strength of rock is more than 50 MPa. It was also recommended that the modulus of deformation lies between 2000 to 3500 MPa when the uniaxial compression strength of 50MPa based on the said study of correlation between uniaxial compression strength and the modulus of deformation. Modulus of deformation of rock at testing location is judged to be more than 3,000 MPa. Considering the result of in-situ rock tests and laboratory tests, following figures were suggested, shown in Table 4.2, for rock at the location of in-situ.

Table 4.2Physical properties of rock (after NEA, 2003)

Parameters	Values
Shear strength	2 to 3 MPa
Friction angle	45 to 50 degree
Modulus of deformation	3000 to 5000 MPa

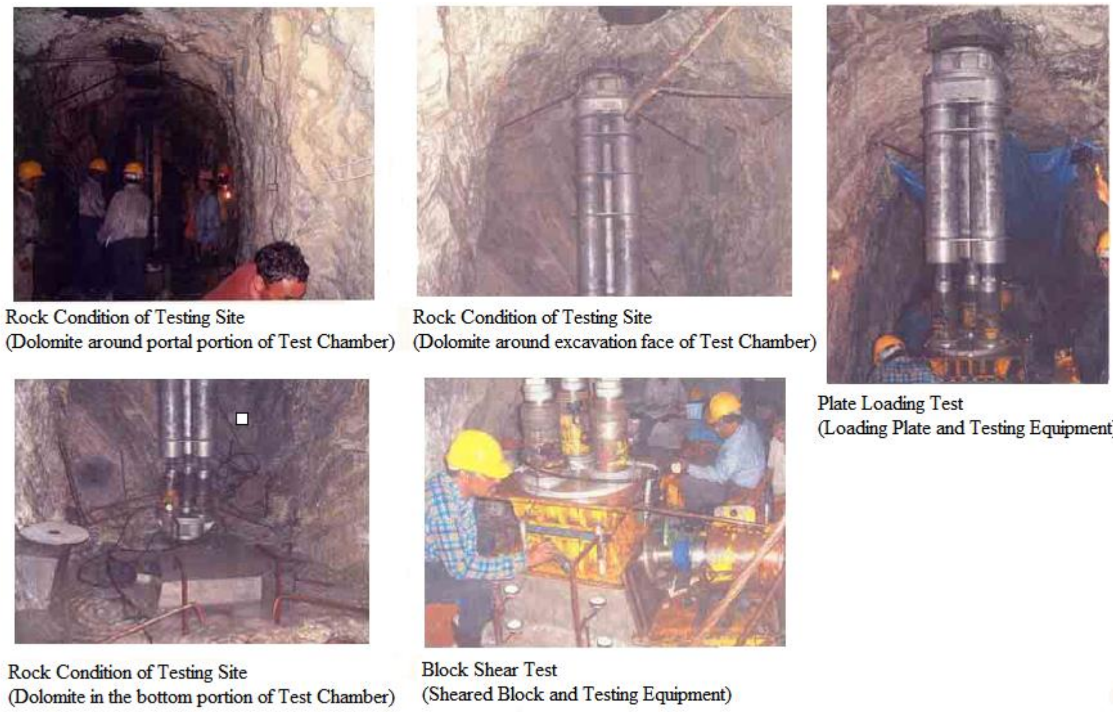

Figure 4-2 In-situ rock test (NEA, 2003)

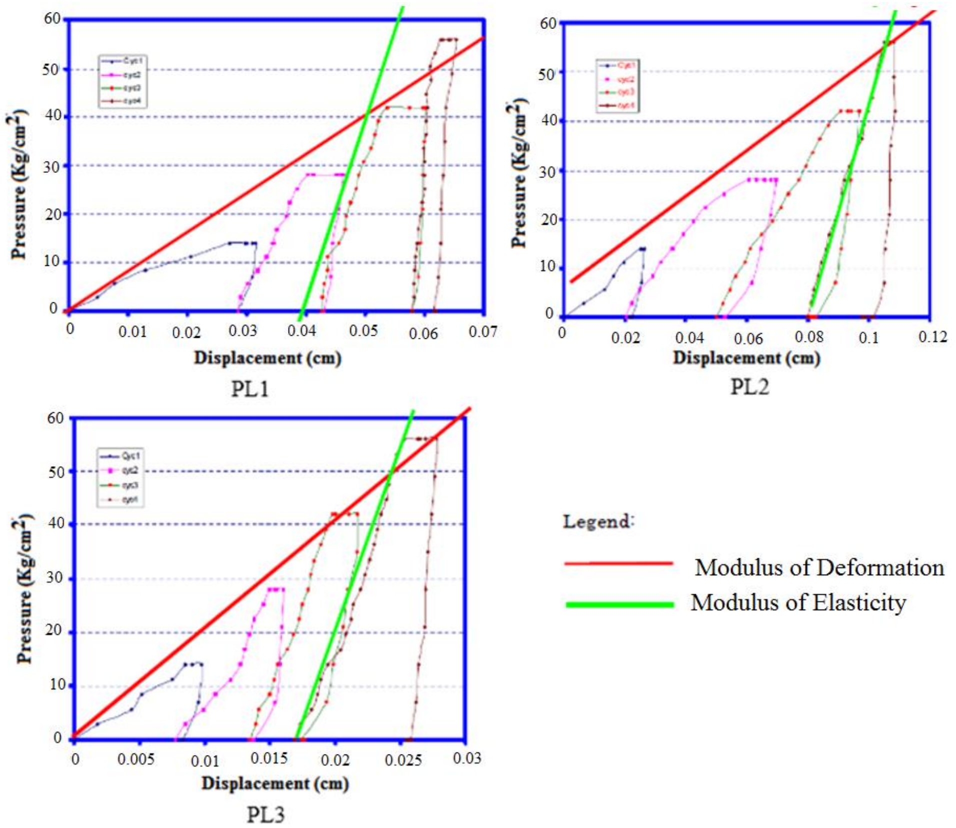

Figure 4-3 Stress-displacement test at three spots by plate loading test (NEA, 2003)

4.2.3 Design of Tunnel Support

Most of the hydropower tunnel supports are designed based on the rock mass classification in Himalayan region of Nepal. The Q- system, proposed by Barton et al. (1974), is more popular for the estimation of tunnel supports in the Himalayan region of Nepal. Based on the Q- value the rock masses are classified as poor, fair and good quality of rocks. The rock mass of this tunnel is categorizing into four classes: very poor, poor, fair and good as shown in Table 4.3. The supports are also recommended based on these rock classes as shown in Table 4.4.

Table 4.3 Rock mass quality along the headrace tunnel (after NEA, 1997)

Chainage		Main Rock Type	Overburden depth(m)	Rock mass classification	Q-number	Support category
From	To					
0+170	0+715	Marble	106.43	Good	10.63	R1
0+715	0+725	Sheared schist	185.82	Very poor	0.1	R4
0+725	0+990	Garnetiferous schist	182.52	Poor	2.7	R3
0+990	1+215	Quartzite schist	163.68	Fair	5	R2
1+215	1+430	Schistose Quartzite & dolomite	138.73	Fair	4.7	R2
1+430	1+450	Sheared schist & dolomite	140.59	Very poor	0.1	R4
1+450	2+355	Quartzite	330.0	Good	13.33	R1
2+355	3+635	Phyllite	315.27	Poor	2	R3
3+635	3+650	Sheared phyllite& dolomite	238.45	Very poor	0.1	R4
3+650	3+965	Siliceous dolomite	236.2	Fair	4.7	R2
3+965	4+337	Slaty Phyllite	173.63	Poor	2.3	R3

Table 4.4Rock mass classification and support based on Q system for Kulekhani III hydropower tunnel (after NEA, 1997)

Rock Class	Support category	Support description	Rock mass description
Very poor	R4	25mm dia. 2.5 m rock bolts in distribution 1.0×1.5 m^2. 100 mm SFRS in walls and crown , 200 mm thick concrete lining is applied with steel ribs ISMB 175	10 m wide shear zone in between the good quality of marble and poor quality of schists from 0+715 to 0+725 and another 20 m thick very poor quality sheared schistose dolomite in encountered, the rock was sheared due to Mahabharat Thrust(MT) , from chainage 1+430 to 1+450.
Poor	R3	25mm dia. 2.5 m rockbolts in distribution 1.5×1.5 m^2. 100 mm SFRS in walls and crown , 200 mm thick concrete lining is applied without steel ribs.	Poor quality of granetiferrous schist from chainage 0+725 to 0+990. From 2+355 to 3+3+365, poor quality of phyllite is encountered with competent and incompetent band. The rock is folded and dissolution have occurred along the fracture zones from 2+355 to 3+365, poor quality slaty phyllite is encountered in this section.
Fair	R2	25mm dia. 2.5 m rockbolts in distribution 1.75×2.5 m^2. 50 mm SFRS in walls and crown, 200 mm thick concrete lining is applied without steel ribs.	The rock is moderately weathered having 0.5 - 10 cm wide clay filled joints along bedding plane at the beginning of tunnel from 0+000 to 0+170 . The light color quartzite is thinly bedded and interbedded with dark greenish grey schists from 0+990 to 1+430. The light grey quartzite and dolomite interbedded with micaceous schist and thickly bedded from 3+650 to 3+965.
Good	R1	25mm dia. 2.5 m rockbolts in distribution 2.0×2.5 m^2. 50 mm SFRS in walls and crown, 200 mm thick concrete lining is applied without steel ribs.	From 0+170 to 0+715 good quality of marble exists and good quality light grey quartzite with intercalation of thin greenish grey phyllite is encountered from 1+450 to 2+355 .

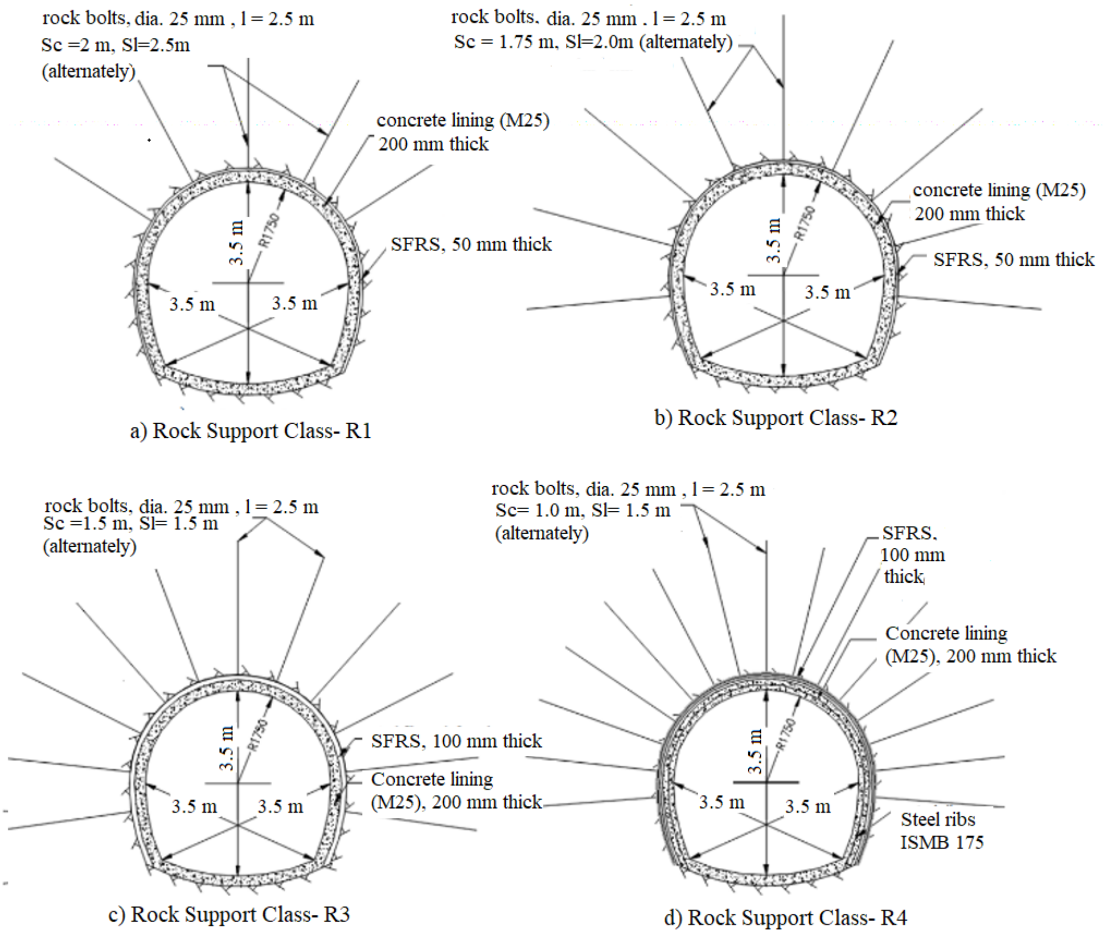

Figure 4-4 Design tunnel support of Kulekhani III hydropower tunnel (NEA,1997)

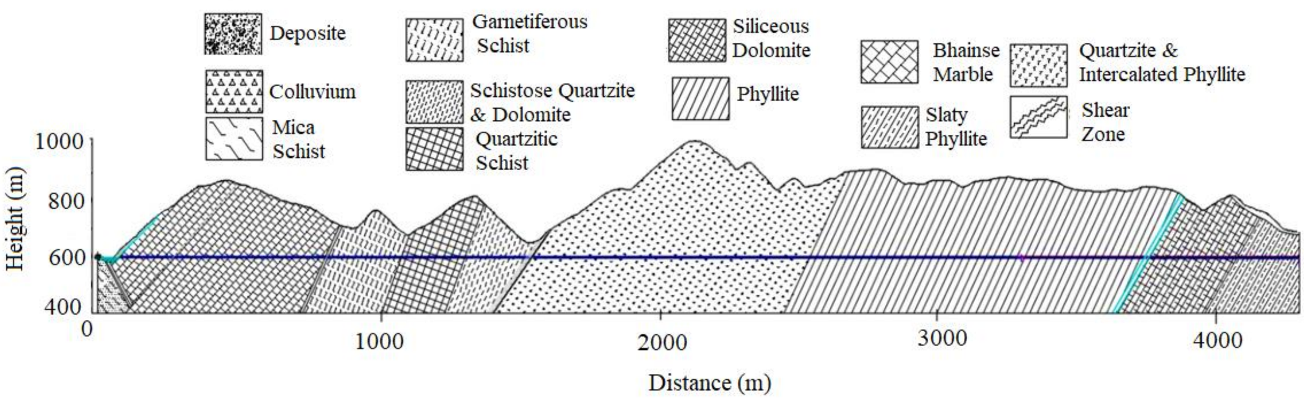

Figure 4-5 Longitudinal geological map of Kulekhani III hydropower tunnel along the alignment (Source: Kulekhani III hydropower project)

4.3 Chameliya Hydropower Tunnel

4.3.1 Introduction

Chameliya hydropower tunnel is located in Shikhar of Darchula district, far-western region of Nepal. The project area lies in Lesser Himalayas zone, in the catchment of the Chameliya River. The installed capacity of the project is 30 megawatt (MW). The design discharge and gross head of the project are $36m^3/s$ and 103.7 m respectively. The headrace tunnel of Chameliya Hydroelectric project is taken as the second case study. The total length of headrace tunnel is 4067 m and the diameter of the horseshoe section is 5.2 m.

4.3.2 Geology of Project Area

The project lies in the western part of Lesser Himalayan region of Nepal. The main rock types along the alignment of headrace tunnel are dolomite, sandstone, slate, dolomite intercalated with slate, talcosis phyllite and dolomite interbedded with phyllite (Basnet, 2013). The rocks are highly jointed, weathered with numbers of shear bands and crushed zone, Figure 4-6. Massive fractured and jointed dolomite is present up to adit-1 with three random joint sets with multiple shear bands and crushed rock material. From chainage 1+000 m to 1+600 m, slightly weathered and fairly jointed rock mass is present. The rock mass is classified as poor based on the rock mass quality number. The Q- values lie in the range of 1 to 2. No shear bands and crushed zones are encountered in this region during the tunneling and no severe problems were encountered. Moderately weathered and highly jointed dolomite with crushed zone is observed from chainage 1+800 m to adit-1, Figure 4-6. The rock mass is classified as very poor with Q-value of less than 1, multiple shear bands and weakness zones makes rock mass very poor.

The maximum rock cover above the headrace tunnel is nearly 470 m between the adit-1 and 2, and nearly 275 m between adit -2 and 3, Figure 4-6. The rock mass is classified as poor quality from chainage 0+000 m to 3+000 m, and main rock type is dolomite with slate.

Similarly, the rock mass from chainage from 3+000 m to 4+000 m is classified into extremely poor rock mass. The Q-value is less than 0.01, as presented in Table 4.7. The tunnel length of almost 800 m length between adit-2 and 3, Figure 4-6, severely squeezed. The convergence of tunnel was measured in 20 tunnel sections, presented in Table 4.7.

The maximum convergence was 2.39 m at chainage of 3+398 m and minimum of 0.062 m at change 3+795 m, with corresponding overburden 275 m and 222 m respectively.

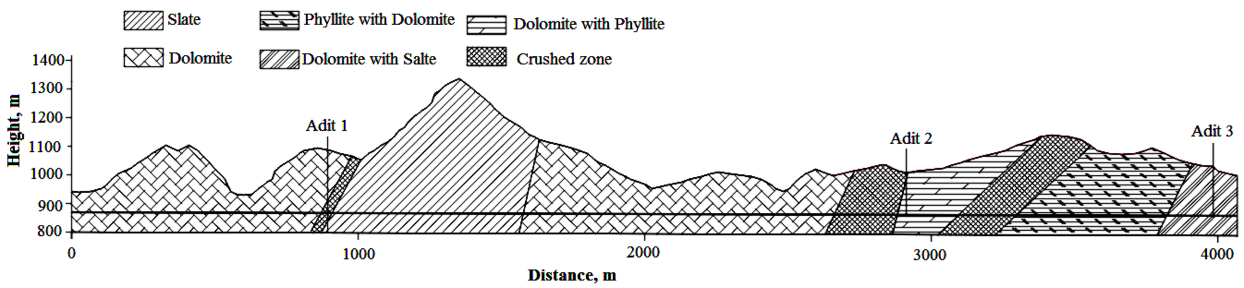

Figure 4-6Longitudinal geological map of Chameliya hydropower tunnel along the alignment (Source: Chameliya hydropower project)

The Q- value was calculated based on the face mapping of the tunnel face as shown in Figure 4-7. Based on the Q –value tunnel supports were recommended during the construction and installed. But the installed support was not sufficient to control the excessive deformation of the tunnel.

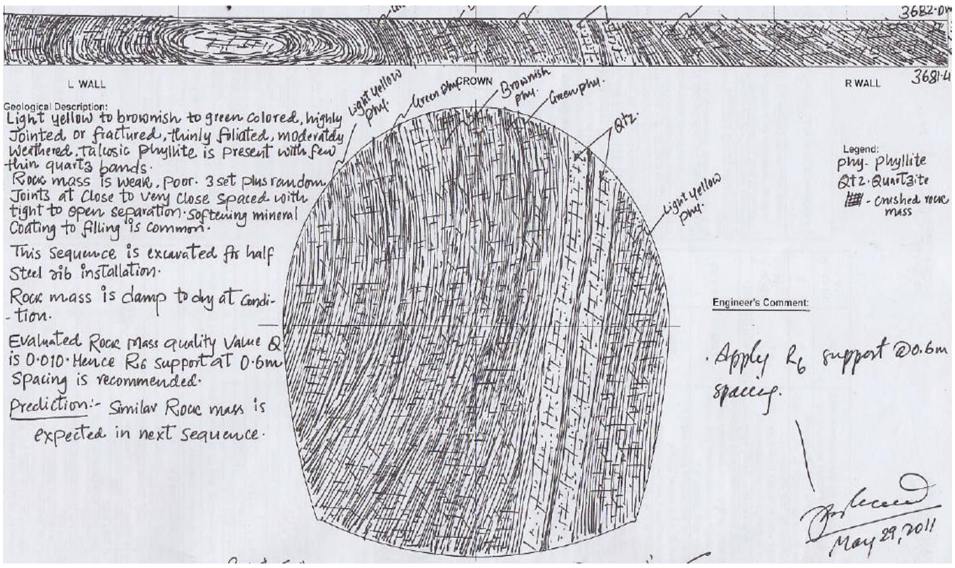

Figure 4-7 Face map of tunnel section with comments and recommendations at chainage 3+681 (Source: Chameliya Hydroelectric Project)

4.3.3 Design of Tunnel Support

Based on the Q- value different support system was designed by the rock mass classification approach proposed by Barton et al. (1974). The details of rock mass classification approaches are discussed in Chapter 2. The details of support systems are given in Table 4.5.

Table 4.5 Rock mass classification and support pattern for Chameliya hydropower tunnel based on the Q- system (Source: Chameliya Hydropower Project)

Rock Class	Q-Value	Support category		Rock Support details
Strong	10<Q	R1	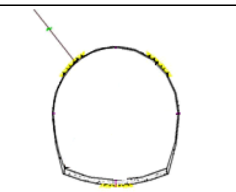	25mm dia. 3m rockbolts in distribution 2.0×2.5 m^2. 50 mm SFRS in walls and crown , 200 mm thick concrete lining is applied in invert without steel support.
Very Good	4<Q<10	R2	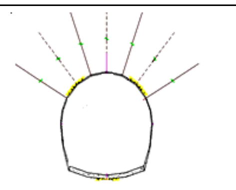	25mm dia. 3m rockbolts in distribution 1.5×1.5 m^2. 50 mm SFRS in wall and crown, 200 mm thick concrete lining is applied in invert without steel support.
Good	1<Q<4	R3	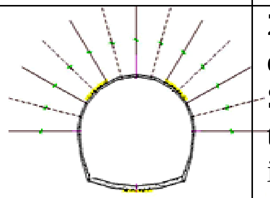	25mm dia. 3m rockbolts in distribution 1.2×1.2 m^2. 90 mm SFRS in wall and crown, 200 mm thick concrete lining is applied in invert without steel support
Fair	0.1<Q< 1	R4	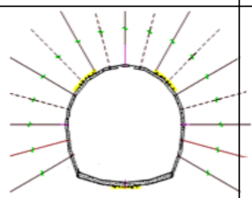	25mm dia. 3m rockbolts in distribution 1.2×1.2 m^2, upper 240^0. 120 mm SFRS in wall and crown, 200 mm thick concrete lining is applied in invert without steel support
Poor	Q<1	R5	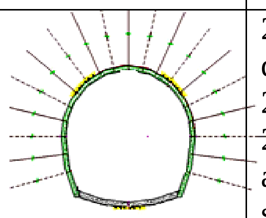	25mm dia. 3m rockbolts in distribution 1.0×1.0 m^2, upper 240^0. 200 mm SFRS in wall and crown, 200 mm thick concrete lining is applied in invert without steel support ,4 bar lattice girder bar size 18, 26 mm is provided at 1.0 m c/c.
Very poor	Q<0.1	R6	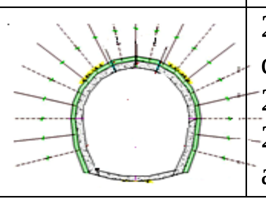	25mm dia. 3m rockbolts in distribution 1.0×1.0 m^2, upper 240^0. 200 mm SFRS in wall and crown, 200 mm thick concrete lining is applied in invert without steel

Table 4.6Details of selected section between chainage 0+180 to 3+103, (Basnet, 2013)

SN	Chainage	Rock Type	Overburden depth, H (m)	Q- value	Support category
1	0+180	Dolomite, Joint, Shear band	140.2	0.25	R3
2	0+310	Dolomite, Joint, Shear band	220.7	0.08	R4
3	0+410	Dolomite, shear band	232.5	1.12	R2
4	1+340	Dolomite with slate	464.0	0.5	R3
5	2+235	Weathered crushed dolomite	140.0	0.01	R5
6	3+103	Dolomite	181.2	1.25	R2

Table 4.7Details of squeezed section between chainage 3+172 to 3+820, (Basnet, 2013)

SN	Chainage	Rock Type	Overburden depth, H (m)	Q- value	Support category	Measured Convergence, (m)
1	3+172	Highly fractured and heavily jointed Dolomite	199.7	0.02	R5	0.238
2	3+190	Dolomite, Fractured, Shear band	203.9	0.031	R5	1.326
3	3+253		220.1	0.01		0.104
4	3+275		230.7			0.822
5	3+296	thinly foliated phyllite within very thin band of dolomite	239.5	0.01	R6	0.650
6	3+305		243.2			1.117
7	3+314	Very weak thinly foliated Phyllite with some bands of dolomite	246.3			0.198
8	3+398		274.4			2.319
9	3+404	Very thinly foliated, highly jointed or fractured and crushed Talcosic Phyllite with few dolomite and several shear/talc bands, few bands of dolomite	275.2	0.008	R6	2.142
10	3+420		277.1			1.570
11	3+439		275.5			1.752
12	3+454		274.4			1.420
13	3+499		268.0			0.801
14	3+543		249.8			2.090
15	3+681		210.8			0.952
16	3+709		212.5			2.038
17	3+733	Highly jointed or fractured, thinly foliated talcosic phyllite	219.1	0.01	R6	0.630
18	3+764	Jointed or fractured, thinly foliated Phyllite. At right wall dolomite and phyllite present	230.0	0.015	R5	0.510
19	3+795		222.6			0.062
20	3+820		211.4			0.941

4.4 Squeezing assessment

- Both Singh et al. (1992) and Goel et al. (1994) empirical approaches are used for accessing the squeezing problems of tunnels. Both uses the Barton's rock mass quality.
- Goel et al. (1994) includes five parameters of rock mass quality proposed by the Barton, and consider SRF as 1 and define the rock mass number, N.
- Semi- analytical approach proposed by the Hoek & Marinos's (2000) and analytical solution by Carranza- Torres & Fairhurst (2000) based on the Hoek-Brown criteria are more convenient to use for highly jointed rock mass of Himalayan region (Shrestha, 2005).

4.4.1 Squeezing Assessment by Empirical Approach

4.4.1.1 Singh et al. (1992) Approach

Based on the rock mass quality defined by the Barton et al. (1974) and the height of overburden Singh et al. (1992) defined a demarcation line which defines weather the tunnel section will undergo squeezing or not. It gives the empirical prediction of squeezing conditions of tunnel. In Figure 4-8, the rock mass quality and tunnel depths of both Kulekhani III and Chameliya hydropower tunnels are plotted.

In case of Chameliya tunnel, the tunnel section are more susceptible to squeezing as its Q- value is less than 0.01, extremely poor rock mass, with an overburden between 200 and 300 m , from chainage 3172- 3820 m, as seen in Figure 4-8. During the construction, the tunnel had faced squeezing problems. If the overburden is more than 400 m, and Q-value between 0.1 and 1, poor rock mass, there is also highly susceptible to squeezing, from chainage 180- 3103 m, as seen in Figure 4-8. As the Q-value of rock mass is greater than 1, the risk of squeezing is reduced.

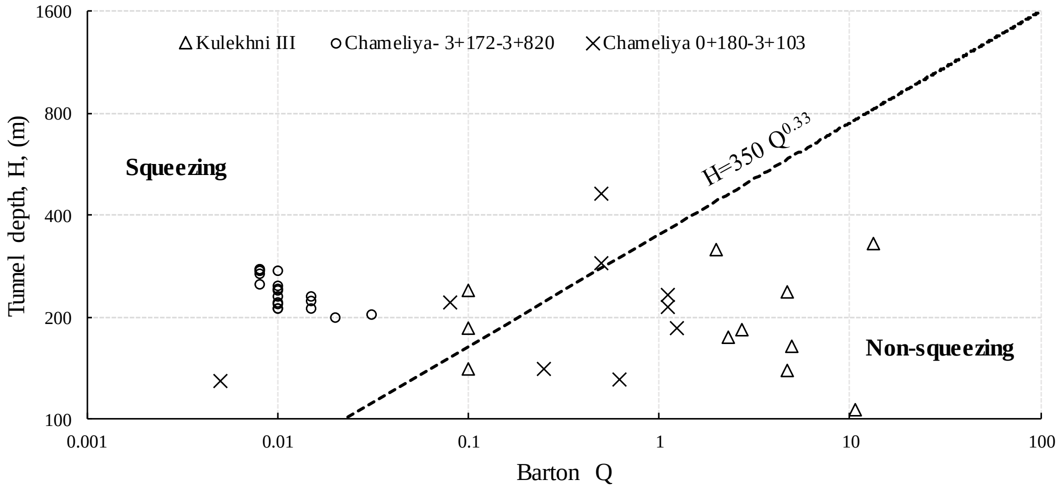

Figure 4-8 Variation of rock mass quality with tunnel depth of Kulekhani III and Chameliya hydropower tunnel by using the Singh et al., 1992 approach to predict the squeezing condition

Therefore, the squeezing of tunnel highly dependent to the rock mass quality rather than the rock cover. It is very useful to determine whether the tunnel will suffer for squeezing or not, the empirical relation given by the Singh et al (1992) is very useful for early stage of tunnel analysis in the Nepal Himalaya.

Table 4.8 Singh et al. (1992) for squeezing assessment of Kulekhani III tunnel

Chainage	H (m)	Q- value	$H=350Q^{1/3}$	Remarks
0+715	106.43	10.63	769.57	No squeezing
0+725	185.82	0.1	162.46	squeezing
0+990	182.52	2.7	487.37	No squeezing
1+215	163.68	5	598.49	No squeezing
1+430	138.73	4.7	586.27	No squeezing
1+450	140.59	0.1	162.46	No squeezing
2+355	330.00	13.33	829.87	No squeezing
3+635	315.27	2	440.97	No squeezing
3+650	238.45	0.1	162.46	squeezing
3+965	236.2	4.7	586.27	No squeezing
4+337	173.63	2.3	462	No squeezing

4.4.1.2 Goel et al. (1994) Approach

Goel et al. (1995) defined the rock mass number, denoted by N, as stress-free rock mass quality Q. Stress effect has been considered indirectly in the form of overburden height H. Thus N can be defined as with stress reduction factor (SRF) is equal to 1 of Q system of Barton et al. (1974). Rock mass number, N, is needed because of the problem and uncertainties in obtaining the correct rating of Barton's SRF parameter

Considering the overburden depth H, the tunnel span or diameter B, and the rock mass number N from 99 tunnel sections, Goel et al. (1995) plotted the available data on log-log diagram, as shown in Figure 2-7, between N and $HB^{0.1}$. Out of 99 tunnel section data, 39 data were taken from Barton's case histories and 60 from projects in India. Out of those 60 data 38 data were from 5 projects in Himalayan region.

Table 4.9 Singh et al. (1992) for squeezing assessment of Chameliya tunnel

Upstream of adit-1				between adit- 2 and 3			
chainage	Tunnel depth (m)	Q value	$H=350Q^{1/3}$ (m)	chainage	Tunnel depth (m)	Q value	$H=350Q^{1/3}$ (m)
0+180	140.2	0.25	220.49	3+172	199.7	0.02	95
0+310	220.7	0.08	150.81	3+190	203.9	0.031	109.95
0+410	232.5	1.12	363.47	3+253	220.1	0.01	75.41
0+600	58.5	1.12	363.47	3+275	230.7	0.01	75.41
0+910	213.1	1.12	363.47	3+296	239.5	0.01	75.41
1+340	464.0	0.5	277.8	3+305	243.2	0.01	75.41
1+577	289.4	0.5	277.8	3+314	246.3	0.01	75.41
2+020	90.4	0.5	277.8	3+398	274.4	0.01	75.41
2+355	131.1	0.62	298.45	3+404	275.2	0.008	70
2+368	129.4	0.005	59.85	3+420	277.1	0.008	70
3+103	185.0	1.25	377.03	3+439	275.5	0.008	70
				3+454	274.4	0.008	70
				3+499	268.0	0.008	70
				3+543	249.8	0.008	70
				3+681	210.8	0.01	75.41
				3+709	212.5	0.01	75.41
				3+733	219.1	0.01	75.41
				3+764	230.0	0.015	86.32
				3+795	222.6	0.015	86.32
				3+820	211.4	0.015	86.32

All the 27 squeezing tunnel sections were observed in those 5 projects in Himalayan region. Other 72 data sets were from non-squeezing sections. As shown in the same figure, a line AB distinguishes the squeezing and non-squeezing cases. The equation of that line is $H = 275\ N^{0.33}B^{-0.1,}$ where H is in m. The data points lying above the time represents squeezing conditions, whereas those below this line represent non squeezing condition.

By plotting rock mass number with the product of depth and width of tunnel, as shown in Figure 4 11, it is gives the idea of whether the tunnel will go squeezing or not. They defined the degree of squeezing as defined in Table 2.18. The Kulekhani III tunnel will have undergo very mild to mild squeezing when it passes through the sheared zones and other sections of tunnel are quite safe from rock squeezing. In case of the Chameliya tunnel, the tunnel section upto chainage 3+000 m, the tunnel undergoes mild to moderate squeezing, like Chainage 1+340 m, because it has high overburden compare to other sections. But the tunnel section in between adit-2 and 3, it undergoes high squeezing, which was also happened during the tunneling. The rock mass number is also good for predicting the degree of rock squeezing behavior during tunneling in Himalayan region of Nepal.

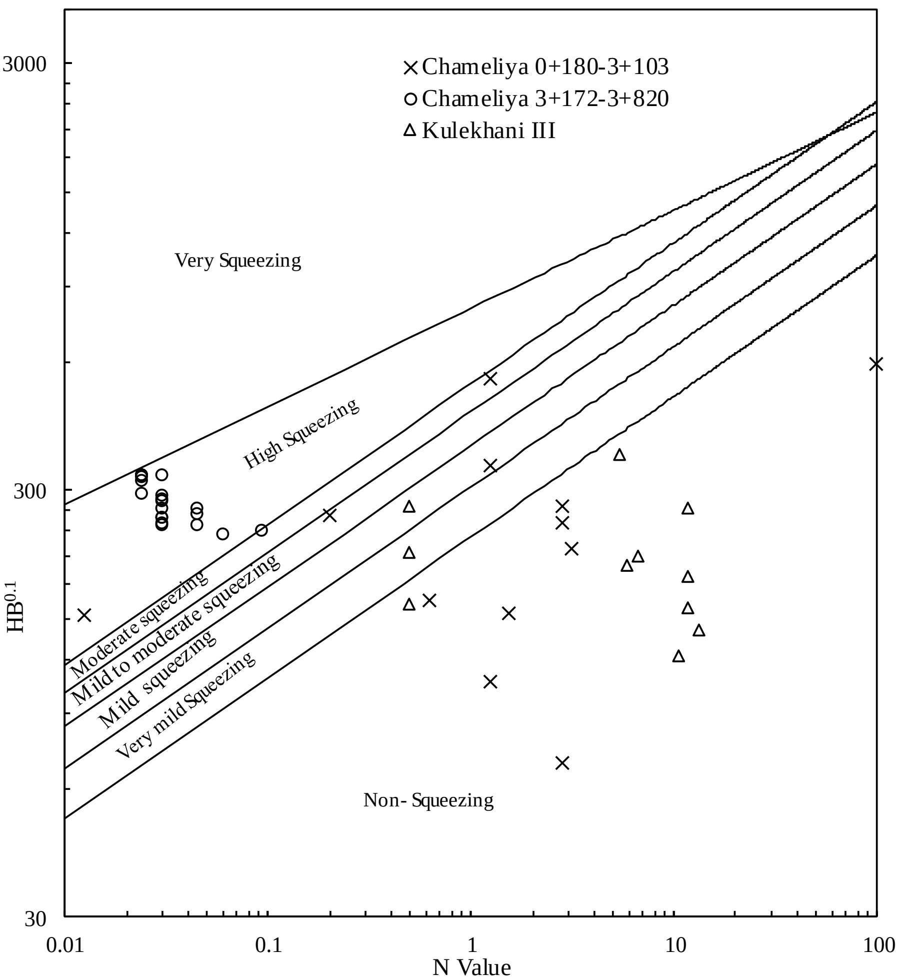

Figure 4-9 Prediction of squeezing by Goel et al. (1994) by using rock mass number

Table 4.10 Goel et al. (1994) for squeezing assessment of Kulekhani III tunnel

Chainage	tunnel depth, H (m)	tunnel width, B (m)	N(SRF=1)	$HB^{0.1}$	$H_{lim}=275N^{0.33}B^{-0.1}$
0+170	106.43	4	10.63	122.26	522.26
0+715	185.82	4	0.5	213.45	190.45
0+725	182.52	4	6.67	209.66	447.8
0+990	163.68	4	11.67	188.02	538.59
1+215	138.73	4	11.67	159.36	538.59
1+430	140.59	4	0.5	161.5	190.45
1+450	122.6	4	13.33	140.83	562.76
2+355	315.27	4	5.42	362.15	418.16
3+635	238.45	4	0.5	273.91	190.45
3+650	236.2	4	11.67	271.32	538.59
3+965	173.63	4	5.83	199.45	428.35

Table 4.11Goel et al. (1994) for squeezing assessment of Chameliya tunnel

Upstream of adit-1					
Chainage	tunnel depth, H (m)	tunnel width, B (m)	N(SRF=1)	$HB^{0.1}$	$H_{lim}=275N^{0.33}B^{-0.1}$
0+180	140.2	5.2	0.625	165.32	199.7
0+310	220.7	5.2	0.2	260.31	137.11
0+410	232.5	5.2	2.8	274.13	327.56
0+600	58.5	5.2	2.8	68.95	327.56
0+910	213.1	5.2	2.8	251.26	327.56
1+340	464.0	5.2	1.25	547.21	251.02
1+577	289.4	5.2	1.25	341.25	251.02
2+020	90.4	5.2	1.25	106.64	251.02
2+355	131.1	5.2	1.55	154.64	269.49
2+368	129.4	5.2	0.0125	152.57	54.92
3+103	185.0	5.2	3.125	218.16	339.65
Between adit-2 and 3					
3+172	199.7	5.2	0.06	235.49	92.16
3+190	203.9	5.2	0.093	240.43	106.5
3+253	220.1	5.2	0.03	259.5	73.31
3+275	230.7	5.2	0.03	272.04	73.31
3+296	239.5	5.2	0.03	282.43	73.31
3+305	243.2	5.2	0.03	286.79	73.31
3+314	246.3	5.2	0.03	290.42	73.31
3+398	274.4	5.2	0.03	323.61	73.31
3+404	275.2	5.2	0.024	324.47	68.11
3+420	277.1	5.2	0.024	326.73	68.11
3+439	275.5	5.2	0.024	324.91	68.11
3+454	274.4	5.2	0.024	323.52	68.11
3+499	268.0	5.2	0.024	316.01	68.11
3+543	249.8	5.2	0.024	294.58	68.11
3+681	210.8	5.2	0.03	248.62	73.31
3+709	212.5	5.2	0.03	250.56	73.31
3+733	219.1	5.2	0.03	258.31	73.31
3+764	230.0	5.2	0.045	271.26	83.81
3+795	222.6	5.2	0.045	262.48	83.81
3+820	211.4	5.2	0.045	249.28	83.81

4.4.1 Semi-analytical Method

Hoek (1999), published details of an analysis that showed the ratio of the uniaxial compressive strength of the rock mass to the in-situ stress can be used as an indicator of potential tunnel squeezing problems. Hoek & Marinos (2000) proposed an empirical equation for estimating the uniaxial strength of rock mass strength based on the results of numerous tunnels excavation in weak rocks.

Kulekhani III hydropower tunnel

Five tunnel sub-section are chosen for the squeezing assessment of Kulekhani III hydropower tunnel as shown in Figure 4-5. The rock mass properties and other factors are shown in Table 4.12

From chainage 0+715 m to 0+725 m, 10 m shear zone of very poor quality sheared schist has followed good quality of marble. The average overburden is 185 m in this subsection. From chainage 1+450 m to 2+355m good quality of quartzite, the average overburden is 330 m. After good quality of quartzite, poor quality of phyllite is occurred from chainage 2+355 m to 3+635 m with average overburden is 315 m. The siliceous dolomite is occurred from chainage 3+650 m to 3+965 m with average overburden of 236 m.

Table 4.12 Estimated rock mass properties and factors for analysis (NEA, 1997)

Tunnel section	A	B	C	D	E
Chainage	0+715 - 0+725	1+450 - 2+355	2+355 - 3+635	3+650-3+965	3+635-3+650
rock type	Sheared Schist	Quartzite	Phyllite	Siliceous dolomite	Shear zone
support class	R4	R1	R3	R2	R4
H (m)	185.82	330.0	315	236	238
Density t/m^3	2.7	2.7	2.7	2.7	2.7
ν	0.2	0.2	0.2	0.2	0.2
Q-number	0.1	13.33	2.0	4.7	0.1
RMR_{89}	35	67	55	60	35
Average GSI	30	62	50	55	18.4
σ_{ci} (MPa)	30	200	18.4	45.6	30
σ_0 (Mpa)	5.02	8.91	6.75	6.37	6.42
E_{ci} (MPa)	12000	35000	9200	15000	9200
mi	12	20	7	9	7
σ_{cm} (MPa)	0.516	15.68	3.011	8.044	-
E_{rm} (MPa)	2075.27	3637.9	1351.9	3033	805

Note: H, overburden depth; ν, Poisson’s’ ratio; RMR, rock mass rating; GSI, geological strength index; σ_{ci}, intact strength of rock; σ_0, insitu stress; E_{ci}, intact modulus of rock ; σ_{cm}, compressive strength of rock mass ;E_{rm}, modulus of rock mass

As per the Hoek & Marinos (2000), the rock mass strength is given by the equation (4. 2) based on the GSI and m_i.

$$\sigma_{cm} = (0.0034m_i^{0.8})\sigma_{ci}(1.029 + 0.025e^{-0.2m_i})^{GSI} \tag{4.2}$$

$$\frac{R_p}{r} = 100(1.25 - 0.625\frac{p_i}{\sigma_0})(\frac{\sigma_{cm}}{\sigma_0})^{(\frac{p_i}{\sigma_0}-0.57)} \tag{4.3}$$

The radius of plastic zone and deformation of the tunnel are given by the equations (4.3) and(4.4) respectively. The internal pressure is used to simulate the effects of supports in the analysis.

$$\epsilon = \frac{u_r}{r} = 100(0.02 - 0.025\frac{p_i}{\sigma_0})(\frac{p_i}{\sigma_0})^{(2.4\frac{p_i}{\sigma_0}-2)} \tag{4.4}$$

where R_p is radius of plastic zone in m, r is the radius of tunnel in m, $u_r$is the tunnel deformation in m, p_i is the internal support pressure in MPa, σ_o is the in-situ stress in MPa and σ_{cm} is the rock mass compressive strength in MPa.

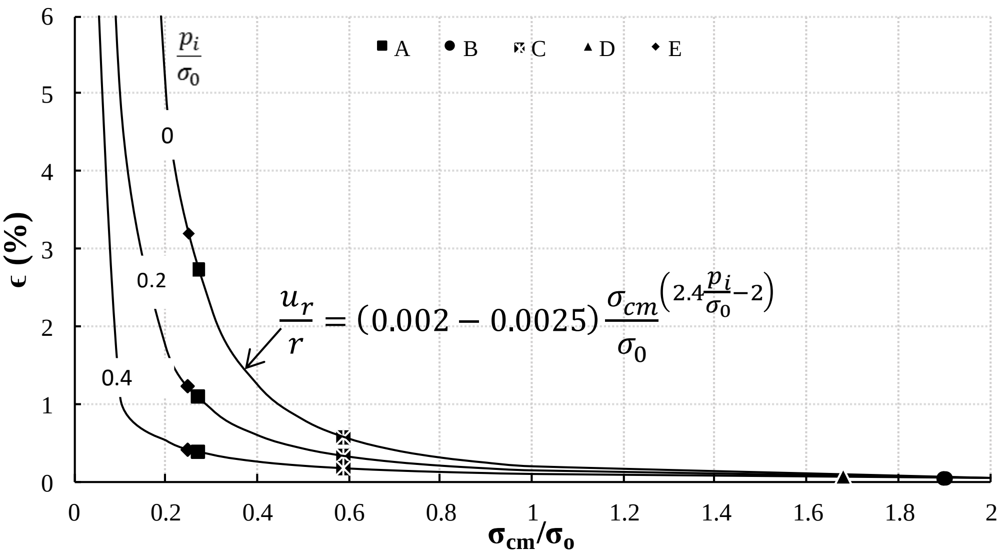

Figure 4-10 Percentage of tunnel strain versus the ratio of rock mass strength to in-situ stress for varying support pressure, p_i , Hoek & Marinos (2000) approach

In an unsupported tunnel, that is, internal pressure p_i is zero, and the rock mass strength is below 30% of in-situ stress the sub-section A and E, shear zone, the tunnel stain is near and more than 3% compare to the other sections. If the rock mass strength is more than 50% of the in-situ stress, then the tunnel strain is less than 1%, shown in Figure 4-10.

The very poor rock mass, GSI is less than 30, of shear zone of tunnel section A and E of Kulekhani III tunnel, the tunnel strain is more than 3%, when the rock mass strength is less than 30 % of the in-situ stress. If the internal pressure is maintaining at 20 % of the in-situ stress, the tunnel strain is reduced to 1% from the 3% and if the internal pressure is increased to 40% of the in-situ stress, then the tunnel strain is reduced to less than 1%. The internal pressure is used to simulate the effects of support. Therefore, immediate installation of support would interact the surrounding rock mass to reduce the tunnel squeezing effectively. For the tunnel section B, C and D, shown in Figure 4-5, the GSI is more than 30 and considered as good quality of rock mass, the tunnel strain is less than 1%. The rock mass strength is more than 50 % of the in-situ stress. There are no stability problems and very simple tunnel supports are sufficient.

Chameliya hydropower tunnel

During the construction of the headrace tunnel, there is very severe squeezing between adit-2 and adit-3, chainage 3+172 m to 3+820 m, nearly 800 m length of tunnel. The main rock type is talcosic phyllite.

In Chameliya tunnel, from chainage 3+172 m to 3+820 m, tunnel undergoes high squeezing with excessive deformation. These deformations are plotted in the Figure 4-11; it shows that the tunnel strain is more than 40 %. It is found that the rock mass strength is less than 10% of the in-situ stress. In such case, if the support pressure is 20% of in-situ stress, the support pressure is not sufficient to control deformation, if support pressure is 40 % of in-situ stress, the tunnel strain is reduced to 5 %. In such case face stability problems likely to occur. The face would be stabilized by forepoling and face reinforcement during tunneling.

Therefore, in such extremely poor rock mass, if the rock mass strength is less than 10% of the in-situ stress, very squeezing and face stability problems is occurred. The face reinforcement, forepoling and shotcrete embedded with steel sets would be good options for the support design. Up to chainage 3+172 m, there is no such significant squeezing problems during tunneling and the main rock type is jointed dolomite with slate, with average GSI is 40, Figure 4-12.As the rock mass strength is less than 40% of the in-situ stress, there are significant deformations of tunnel and controlled by installation by adequate support, Figure 4-11. This shows clear influence of support pressure on the tunnel deformation. The main purpose of the tunnel support is to maintain confinement for the rock mass to help the rock support itself.

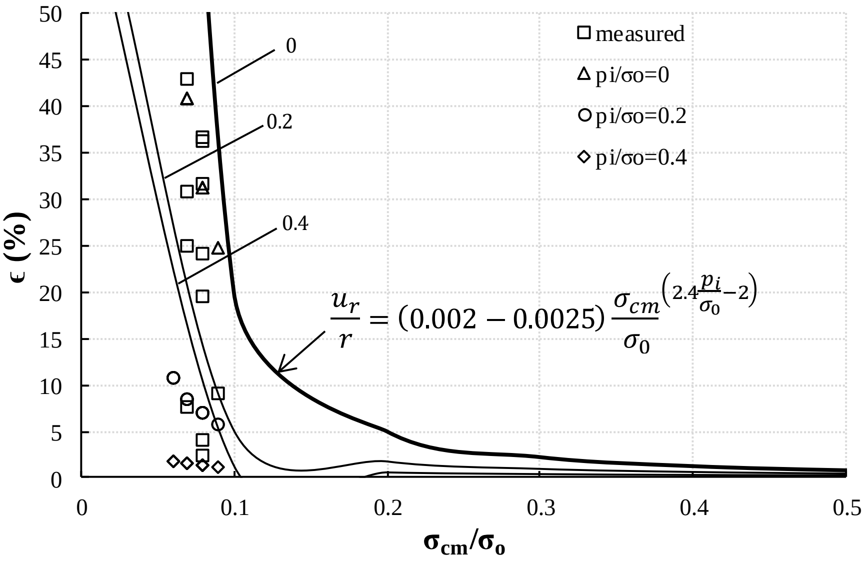

Figure 4-11 Percentage of tunnel strain versus the ratio of rock mass strength to in-situ stress for varying support pressure, p_i, (3+172 to 3+820 of Chameliya tunnel, Squeezed section), Hoek & Marinos (2000) approach

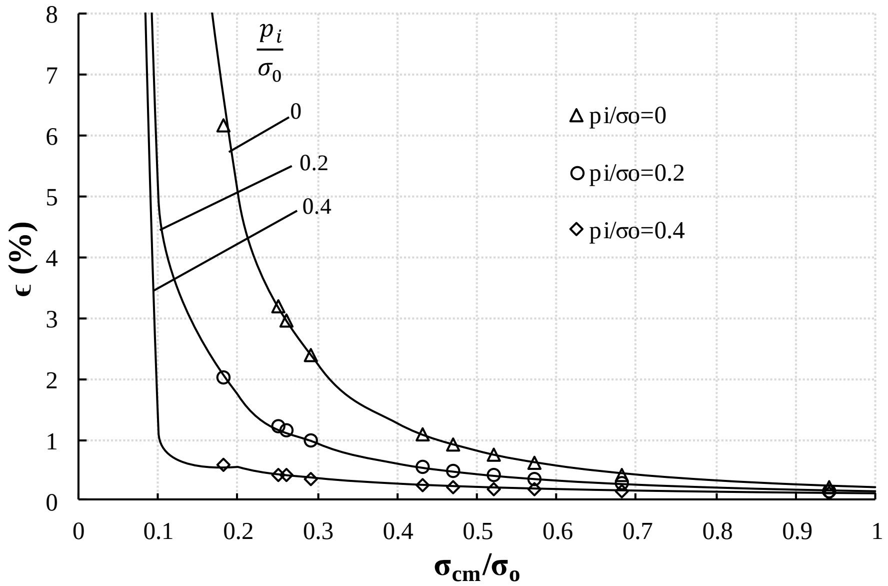

Figure 4-12 Percentage of tunnel strain versus the ratio of rock mass strength to in-situ stress for varying support pressure, p_i, (0+180 to 3+120 of Chameliya tunnel), Hoek & Marinos (2000) approach

4.4.2 Analytical Methods: Convergence Confinement Method (CCM)

Support capacity curve and ground reaction curve of Kulekhani III tunnel

The headrace tunnel passes through good to fair quality of rock masses like marble, schist, slate, phyllite and quartzite, shown in Figure 4-5, including the shear zones due to existing Mahabarat thrust, where the rock mass might be fractured and altered to clay in some extent (NEA, 2003). The rock mass properties of analyzed section are shown in Table 4.13.

- At chainage 2+355 m, 3+635 m and 3+965m rock mass characterized by quartzite, phyllite and dolomite respectively, the internal pressure is drastically reduced to zero with very small radial deformation, shown in Figure 4-13. The GSI of rock masses of these sections are more than 50 and considered as fair to good quality of rock mass (Marinos et al., 2005). Similarly, at chainage 0+725m and 3+650 m characterized by shear zones composed of schists and phyllite respectively, the internal pressure is reduced to zero with high radial deformation compare to the other sections, as shown in Figure 4-13.
- The longitudinal displacement profiles of different tunnel section are shown in Figure 4.16. The GSI of rock mass greater than 50, the maximum radial displacement of tunnel occurs when the excavation face is 2 times the tunnel diameter, at 8 m behind the tunnel face, as shown in Figure 4-14.
- Similarly, for the very weak rock mass, GSI is less than 30, shear zones, at chainage 0+725 m and 3+650 m, the maximum radial displacement occurs behind the 2 times the tunnel diameter from tunnel face, Figure 4-14. The radial deformation at 3+ 650 m has more than that of 0+725 m, because the 3+650 m section has high overburden pressure, Table 4.13.

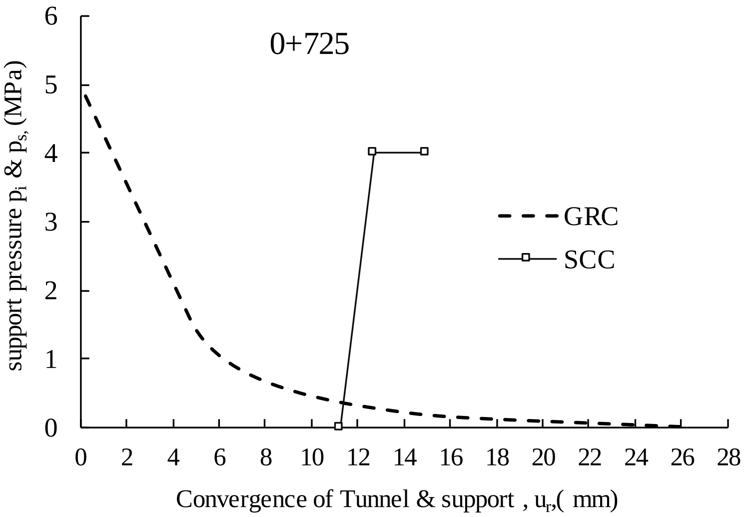
0+725
support pressure p_i & $p_{s,}$ (MPa)
Convergence of Tunnel & support , u_r,(mm)
GRC
SCC
0
1
2
3
4
5
6
0 2 4 6 8 10 12 14 16 18 20 22 24 26 28

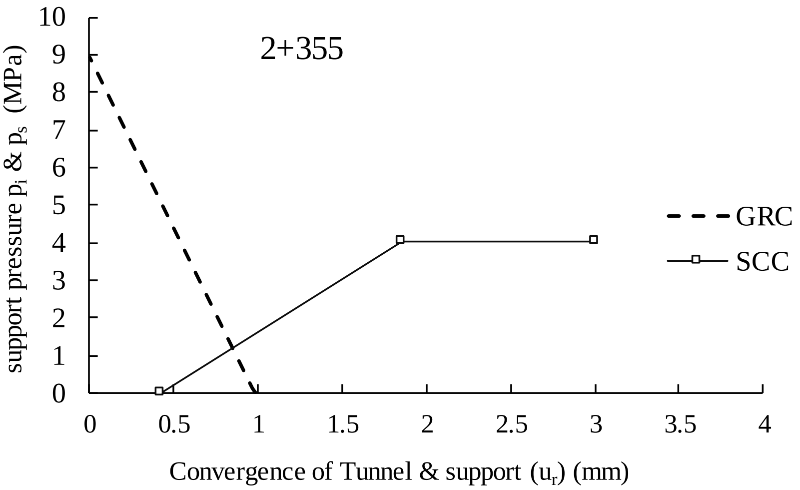
2+355
support pressure p_i & p_s (MPa)
Convergence of Tunnel & support (u_r) (mm)
GRC
SCC
0
1
2
3
4
5
6
7
8
9
10
0 0.5 1 1.5 2 2.5 3 3.5 4

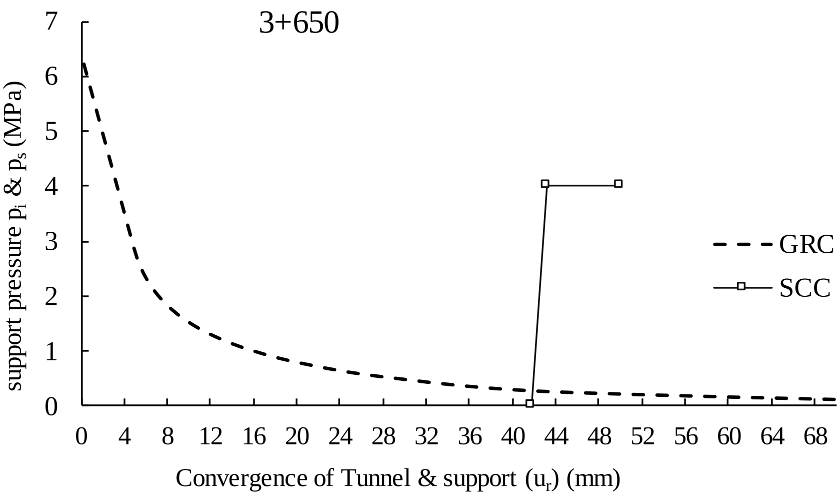
3+650
support pressure p_i & p_s (MPa)
Convergence of Tunnel & support (u_r) (mm)
GRC
SCC
0
1
2
3
4
5
6
7
0 4 8 12 16 20 24 28 32 36 40 44 48 52 56 60 64 68

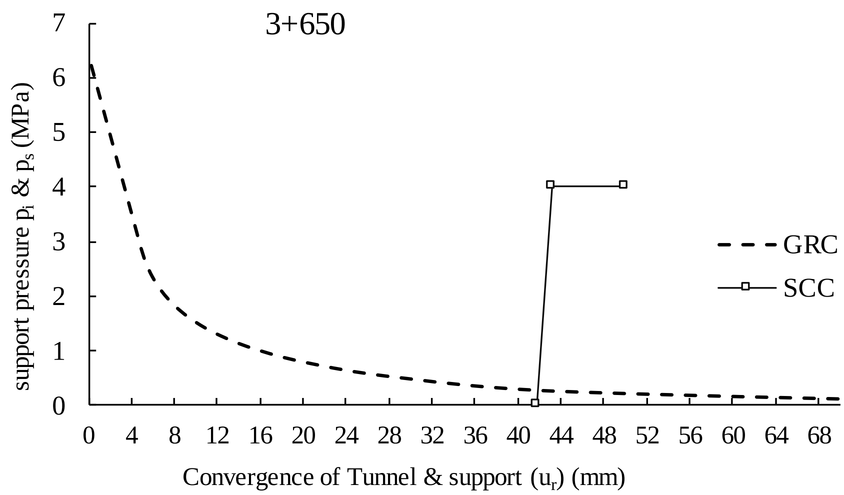

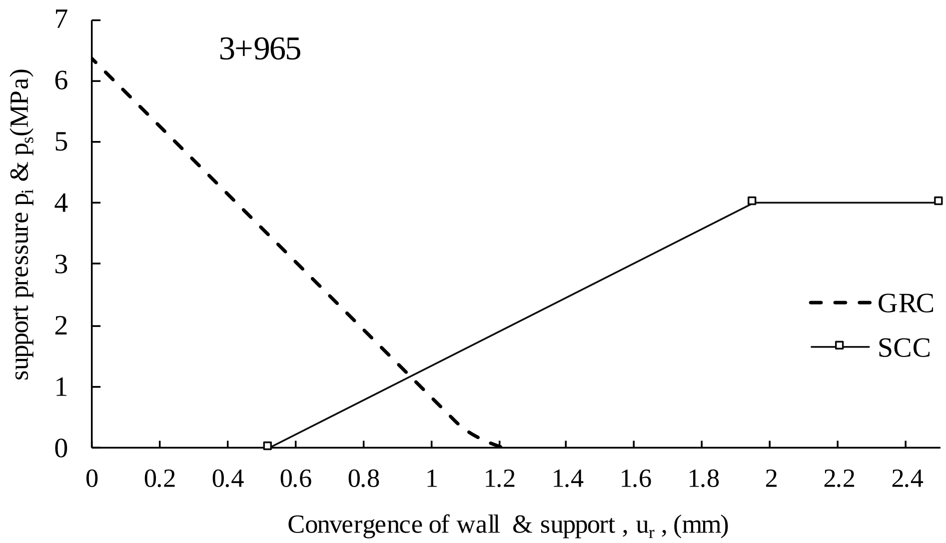

Figure 4-13 Ground reaction curves and support capacity curves of different tunnel section of Kulekhani III tunnel, by using CCM approach

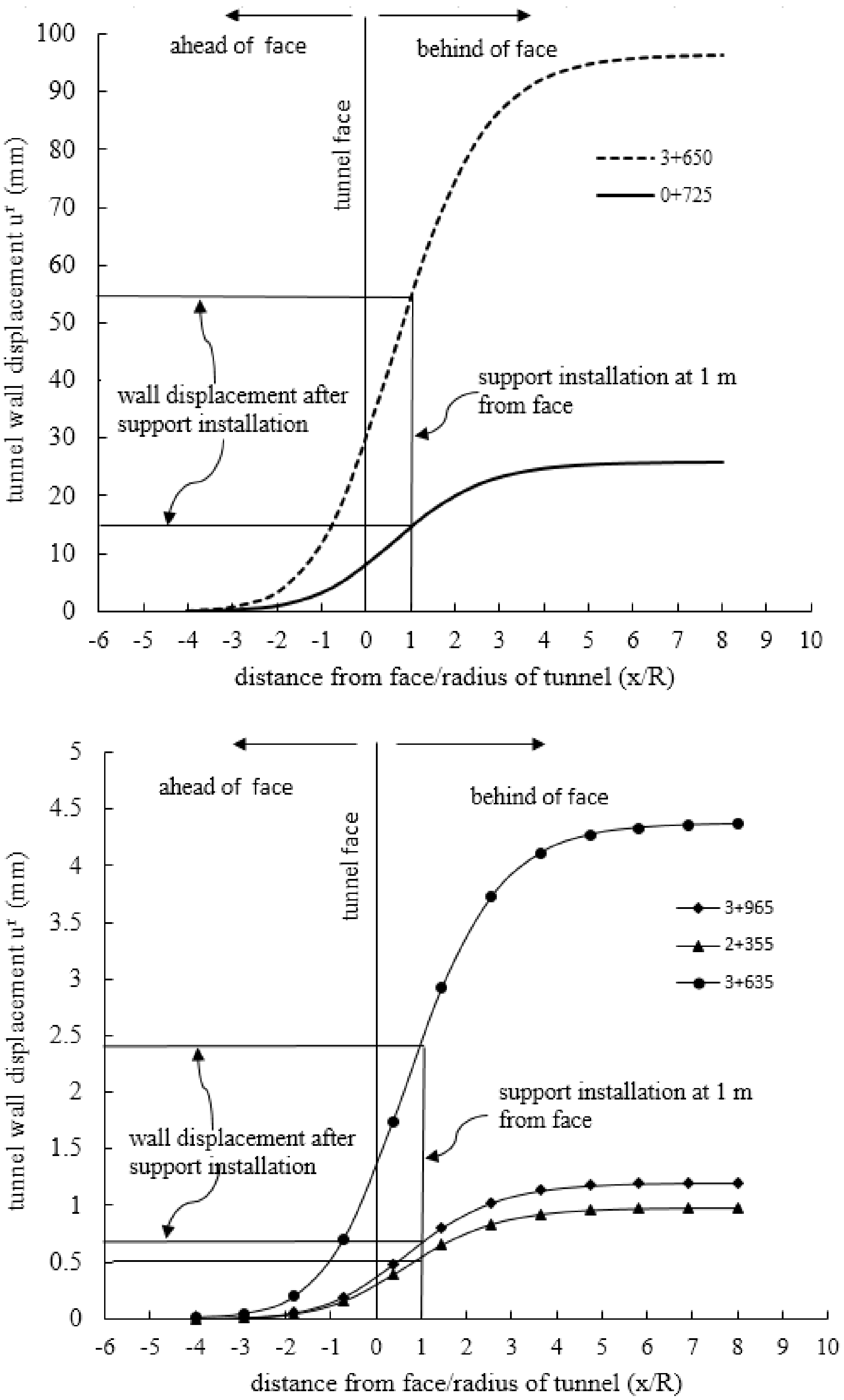

Figure 4-14 Longitudinal displacement profiles of different tunnel section of Kulekhani III hydropower tunnel, by using CCM approach

Therefore, in such weak rocks, the overburden pressure has played a significant role to increase the radial deformation of tunnel in Lesser Himalayan region of Nepal.

The support capacity curve gives the interaction between the rock mass and support system after the installation of support. During the advance of the tunnel, the rock mass and the support system deform together, and the support system takes part of the load that the tunnel face had been carrying previously before installing the support system. When the tunnel face moves ahead, the rock mas and the support system reach equilibrium and the support system takes the final load or design load,p_s^d and the rock mass and support system are deformed together, u_r^D. The detail of convergence confinement method is presented in 2.5.1 of chapter 2 with nomenclature. The results from CCM for all sections are presented in Table 4.13.

Table 4.13 Tunnel section for CCM analysis of Kulekhani III tunnel

Parameters	A	B	C	D	E
Chainage	0+715 -0+725	1+450 - 2+355	2+355 - 3+635	3+650-3+965	3+635-3+650
u_r^D (mm)	12	0.8	2.2	0.9	42
Tunnel strain (%)	0.6	0.04	0.11	0.05	2.1
u_r^o (mm)	11	0.427	1.89	0.52	42
p_s^{max} (MPa)	4.08	4.08	4.08	4.08	4.08
p_s^d (MPa)	0.4	1.5	1	1.1	0.3
FoS	10	2.67	4	3.64	13
u_r^M(mm)	26	1	4.5	2	96

Note: u_r^D, deformation of support and rock mass converged together after face effect disappeared;u_r^o, deformation of section behind the face;p_s^{max}, maximum pressure that the support can accept before collapse;p_s^d, final load or design load taken support; FoS, factor of safety; u_r^M, maximum radial tunnel deformation when internal pressure is zero.

The support takes less load than its maximum capacity. Therefore, the provided combination of supports is sufficient in all sections, Table 4.13. At chainage 3+650 m, shear zone, the maximum radial deformation is 96 mm when internal pressure is zero. The value of support pressure,p_s^d, is 0.3 MPa and the support and rock mass deform by 42 mm, u_r^D, Table 4.13. The maximum tunnel closure is 2.1 %, which is more than 1% so the support should be revised in this section during the tunneling.

When the tunnel passes through quartzite, at chainage 2+355m, the tunnel strain is 0.04 %, less than 1%, indicates the reduced probability of squeezing. The support and rock mass deformed by 0.8 mm when the tunnel face is far away. The support pressure taken by the supports is 1.5 MPa, which is less than its allowable support pressure.The maximum allowable of pressure,p_s^{max}, taken by the support is 4.08 MPa, Table 4.13.

Ground reaction curve and support capacity curve of Chameliya tunnel

Table 4.14 Details of tunnel sections for CCM analysis

Chainage	0+410	1+340	3+681	3+764
Main rock type	Dolomite Phyllite	Slate	Talcosic Phyllite	Talcosic Phyllite
support class	R2	R3	R6	R6
Overburden (m)	232	464	210	230
Density t/m^3	2.7	2.7	2.7	2.7
ν	0.2	0.2	0.3	0.3
Q-number	1.12	0.5	0.01	0.015
Average GSI	45	40	20	20
σ_{ci} (MPa)	31	31	15	15
σ_0 (Mpa)	6.24	12.5	5.67	6.21
mi	9	9	7	7

The headrace tunnel of Chameliya hydropower passes through the highly jointed, weathered Dolomite with slate and extremely poor talcosic phyllite, Figure 4-6. During the tunneling multiple shear bands and crushed zones were observed. In this study four tunnel sections are considered at different chainages 0+410 m ,1+340 m, 3+681 m and 3+764 m.

- The rock mass quality of 0+410 m and 1+340 m are very poor and poor respectively and the average overburden at chainage1+340 m is 470 m.
- The rock mass of the remaining two sections at chainages 3+681m and 3+764 m are classified as extremely poor rock masses as their Q value is less than 0.01. During the tunneling these sections undergo heavy squeezing.
- The internal pressure at chainage 0+410 m is drastically reduced to zero from the in-situ stress as the radial displacement is increased from zero to 15 mm. But in case of the chainage 1+340 m, the internal pressure is becoming zero when there is high deformation in the tunnel. Therefore, the internal pressure is slowly reduced by large deformation of tunnel even though the rock mass has good quality and immediate installation of support is not good in such situation, Figure 4-15.

- In case of 3+681m and 3+764 m, extremely poor rock mass, GSI is less than 30, the internal pressure drastically dropped at the first, excavation phases, and then slowly decreases to zero as the tunnel goes high deformation, more than 1400 mm, as shown in Figure 4-15. In such conditions the face reinforcement should be done before excavation of tunnel.
- An over-excavation of tunnel section, like at chainage 3+681 m and 3+764 m of Chameliya tunnel section, would be good option to relax the internal pressure in such very weak rock mass with high overburden pressure where large radial deformations are likely to occur. If the support is installed immediately after excavation, the support would have deformed slowly and fail.
- The longitudinal displacement profile of different sections of Chameliya hydropower tunnel is shown in Figure 4-16. For extremely poor rock mass, the maximum longitudinal displacements are nearly 1400 mm and 2000 mm for an unsupported tunnel.

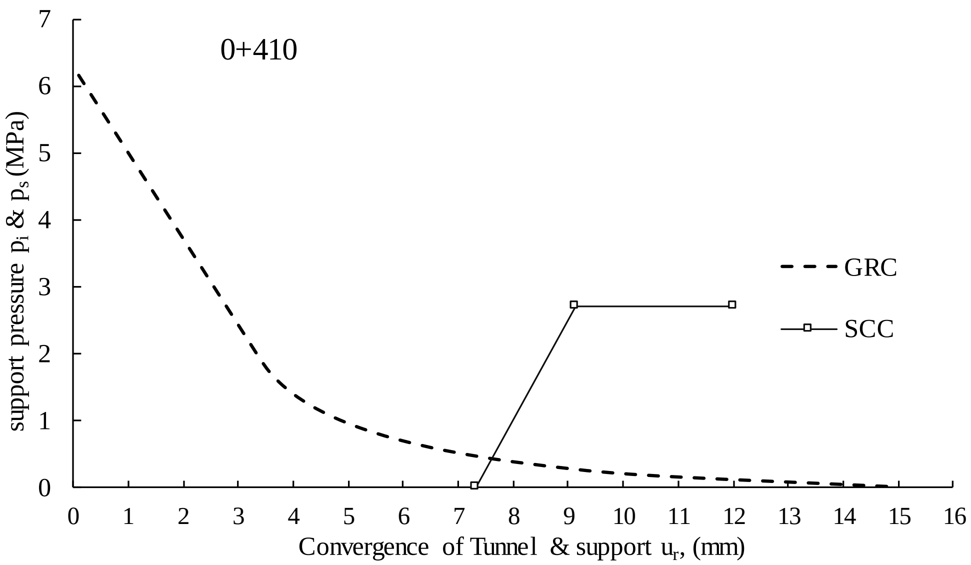

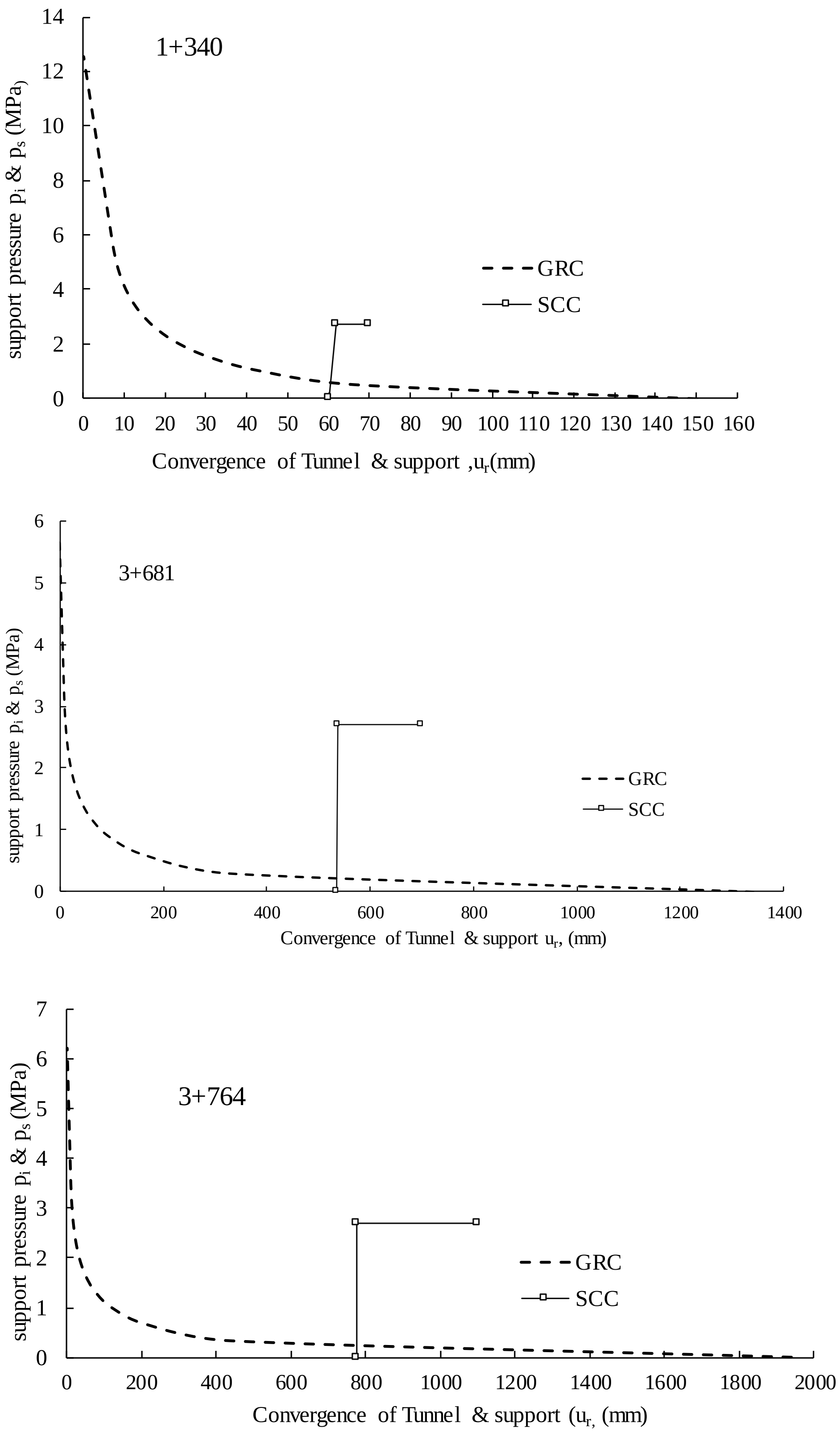

Figure 4-15Ground reaction curves and support characteristics curves at different chainages of Chameliya hydropower tunnel, by using CCM approach

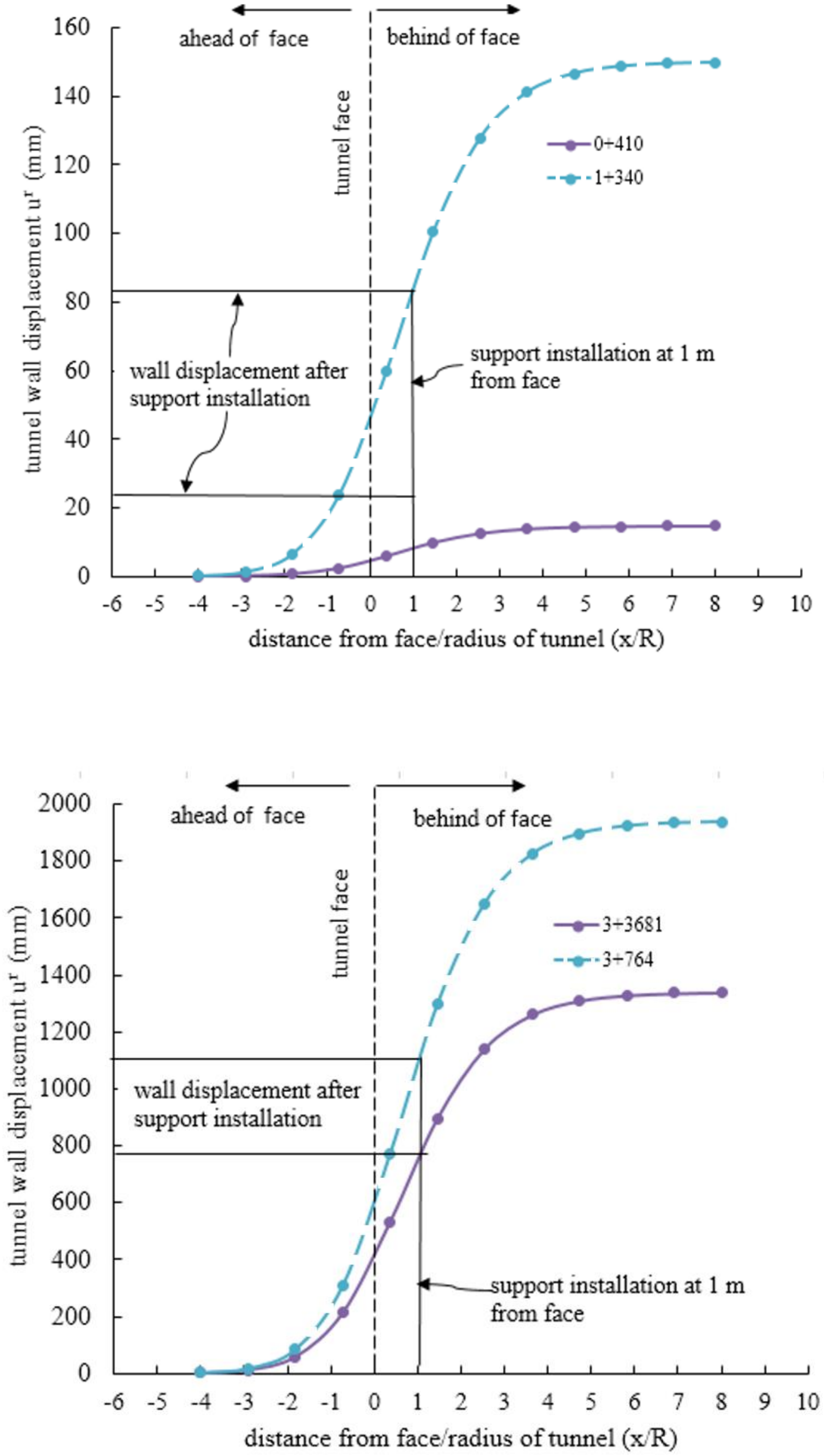

Figure 4-16Longitudinal displacement profile of Chameliya hydropower tunnel, by using CCM approach

Table 4.15Tunnel section for CCM analysis of Chameliya tunnel

Chainage	0+410	1+340	3+681	3+764
u_r^D (mm)	7.5	62	667	800
Tunnel strain (%)	0.28	2.3	24.7	29.63
u_r^o (mm)	7.33	60	536	775
p_s^{max} (MPa)	2.7	2.7	2.7	2.7
p_s^d (MPa)	0.4	0.5	0.4	0.4
FoS	6.74	5.39	6.74	6.71
u_r^M(mm)	14.75	150	1338	1963

Note: u_r^D, deformation of support and rock mass converged together after face effect disappeared;u_r^o, deformation of section behind the face;p_s^{max}, maximum pressure that the support can accept before collapse;p_s^d, final load or design load taken support; FoS, factor of safety; u_r^M, maximum radial tunnel deformation when internal pressure is zero.

Four tunnel sections of Chameliya are analyzed by CCM and results are shown in Table 4.15. Tunnel section at chainage 0+410 m, the main rock type is dolotmite and GSI is 45, Table 4.15, and overburden is 232 m, tunnel closure is 0.28% less than 1%. There would be less chance of rock squeezing problem. The design load on support is 0.4 MPa, while the maximum pressure provided by the support is 2.7 MPa, Table 4.15. Similarly, at change 1+340m , the main rock type is slate with GSI 40 and overburden is nearly 470m. The tunnel closure is 2.3 % more than 1% and high probability of rock squeezing but the design load on the support is below the maximum pressure provided by the support. The excessive deformation due to the high overburden.

But the tunnel sections 3+681 m and 3+764m are composed of talcosic phyllite, extremely poor rocks and high overburden, average tunnel depth is 275 m. The maximum tunnel closure is 30%, very high squeezing. The load on the support is 0.4 MPa which is less than the maximum support pressure provided by the support system. In these sections, the maximum radial deformation is more than 1500 mm, Figure 4-16, behind the tunnel face. Therefore, in such geological section, face reinforcement should be carried during the tunnel excavation and controlled blasting should be adopted so that the surrounding rock mass would not be disturbed.

4.5 Conclusions

In this chapter two hydropower tunnels are discussed in detail. The Kulekhani III hydropower tunnel passes through marble, quartzite, phyllite and silicious dolomite with shear schists and phyllite. The rock mass quality is varying from poor to good, GSI varying from 30 to 62, with shear zones. The Chameliya headrace tunnel passes through poor to extremely poor rock mass conditions. Highly jointed and weathered dolomite and talcosic phyllite are the main rock types and have a number of multiple shear bands and crushed zones encountered during the tunneling.

These two hydropower tunnels are analyzed in terms of assessment of squeezing by empirical, semi-analytical and analytical methods. Empirical methods given by Singh et al. (1992) and Goel et al. (1994) are useful to access tunnel squeezing in such geological conditions of Nepal. The latter gives the degree of squeezing which is very important for designing the support.

Semi-analytical methods given by Hoek & Marinos (2000) is an also good tool for predicting the potential of squeezing and tunnel support design based on the tunnel strain.

Analytical methods proposed by Carranza-Torres and Fairhurst (2000), based on the Hoek- Brown failure criteria is very useful to design the tunnel support in such weak geology having overburden pressure. It gives a clear idea on the ground response and support interaction with surrounding rock mass during tunneling.

5 NUMERICAL MODELLING

5.1 General

In the Himalayan region of Nepal, the estimation of rock support pressure and selection of tunnel supports are carried out by empirical approaches based on the rock mass classification. Among them, the Q-system of rock mass classification proposed by Barton *et al.* (1974) is mostly used in the Himalayan region to design the tunnel support. Due to the high overburden pressure and weak rock quality, there is excessive deformation in the hydropower tunnels during and after construction. The Q–system rock mass classification approach is not able to predict the deformation of tunnels and the designed support system is not able to control deformation in tunnels in weak rock mass conditions. Tunnel excavation is a three-dimensional problem and to study stress and deformation around the tunnel face 3D modeling is necessary. However, the two-dimensional modeling approach is still the most common tool in the current practice of tunnel projects' design calculations due to its reduced calculation time and relative simplicity (Janin *et al.*, 2015).

Many researchers compared the 2D and 3D numerical modeling approach and their uses. Eberhardt (2001) demonstrated that three-dimensional numerical analysis allows a more detailed examination of stress concentration around the ends and edges of an excavation. In the case of an advancing tunnel face, three-dimensional stress effects play an important role, especially with respect to induced stress concentration and rock strength degradation. Dhawan *et al.* (2002) performed 2D and 3D elastic -plastic analyses for four underground openings and compared the results with *in situ* measurements. They found that 2D analysis underestimates the deformation, while, on the other hand, 3D analysis results are compared with *in situ* measurements.

Janin *et al.* (2015) investigated and compared the ability of the 2D and 3D numerical approaches to reproduce the real behavior of tunnels, based on *in situ* measurements. The 3D calculation correctly simulates the in-situ data, confirming that this tool can represent the complexity of a tunnel excavation process. 2D calculations were also performed, and stress release coefficients were determined by fitting the 2D results to the 3D results. This solution produced numerical results that reproduced the in-situ ground deformations globally; however, the 2D approach is shown to be unable to represent the real phenomenon of tunnel excavation in all its complexity. 2D simulation cannot represent the complex three-dimensional phenomenon of support loading, particularly near the tunnel face.

In this chapter two hydropower tunnels from Lesser Himalayan region, Kulekhani III and Chameliya hydropower tunnel, have been taken as 3D numerical modeling for case studies. Both tunnels pass through very weak to extremely poor rock mass with high rock cover. The details of the case studies are discussed in Chapter 4 with analytical studies.

5.2 Modeling and Analysis

The numerical analysis has been performed using RS3, 3D finite element programs for soil and rock applications developed by Rocscience. RS3 is used for 3-dimensional analysis of underground excavation, tunnel support design and other geotechnical works. It uses a series of extruded 2-dimensional slices to create a 3D model. It offers a fastest and simplest way to model multistage excavation and support installation. It offers a wide variety of support elements for support design including bolts, liners, beams and piles. Different types of loading can be modelled, restraints and boundary conditions can be easily applied, and meshing is automatic with 4-noded or 10-noded tetrahedral elements. Several options are available to view and display the results in 2D and 3D. Both, Mohr-Coulomb and generalized Hoek-Brown failure criteria are available for material modelling (Rocscience, 2016). There are also some other models available.

5.2.1 Stress Regime in Nepal Himalayan

Stress regime is one of the major factors in the design of underground structures in the Himalayan region of Nepal. The excessive deformation and support failure around the tunnel are common in this region due to high rock stress. During the tunneling, the rock depth varies from few hundred to 1000 m in rock mass stress which results high vertical stress caused by the overburden.

The vertical stress is linearly increases with the depth of the rock and is given by

$$\sigma_v = \gamma z \tag{5.1}$$

Where σ_v is the vertical stress in MPa, γ is the unit weight of rock –typically 0.027 MN/m^3, and z is the depth of rock in m.

According to Humagain (2000), there is very few in-situ stress measurement in the Lesser Himalayan region in Nepal. In the western Nepal, in situ stress measurements using overcoring and flat jack method were executed in the site of the powerhouse cavern of the Karnali –Chisapani Hydropower Project. The maximum stress σ_1 trends 353^0 i.e. N07W/S07E plunging 64^0 and minimum σ_3 S72E/N72W plunging 07^0 and intermediate σ_2 S10W/ N10E plunging at 25^0. Similarly, the in-situ stress measurement reported from powerhouse cavern site of the Arun Hydropower project in the eastern Nepal, the maximum stress direction σ_1 N25W/S25E plunging 04^0 and minimum σ_3 N30E/S30E plunging 86^0 and intermediate σ_2 N66E/ S66E plunging at 02^0. Further, World Stress Map, shows that the direction of tectonic stress in the mid-eastern Lesser Himalayan region is oriented horizontally with Northeast-Southeast as seen in Figure 5-1.

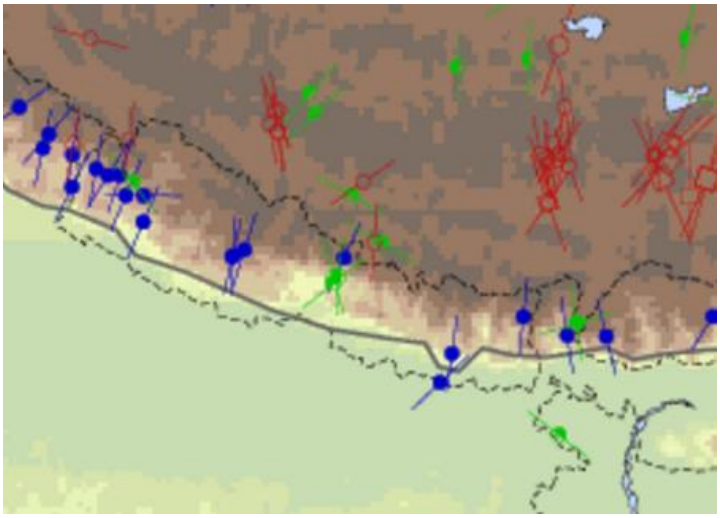

Figure 5-1 Stress map of the Nepal Himalaya (World stress map, 2008)

The ongoing tectonic deformation and active reverse faulting mechanism have considerable influences on the magnitude of major tectonic principal stresses in the Himalayan. The major stress in the Himalayan is oriented horizontally with Northeast-Southwest trend (Panthi, 2006). Rock stress measurements carried out at Kaligandaki Hydropower project showed that the tectonic stress component is approximately 3 MPa.

As compare to the vertical stress, the horizontal stress is very low due to low Poisson's ratio of weak rock mass (Shrestha & Panthi, 2014). In this region, the total horizontal stress contributes to the tectonic stress and horizontal component of vertical stress. This, according to Shrestha & Panthi (2014), can be expressed as follows:

$$\sigma_{h(total)} = \sigma_v \frac{\upsilon}{1-\upsilon} + \sigma_t \tag{5.2}$$

where, $\sigma_{h(total)}$ is the total horizontal stress including tectonic stress in MPa, σ_v is the vertical stress in MPa, υ is the Poisson's ratio, σ_t is the tectonic stress in MPa.

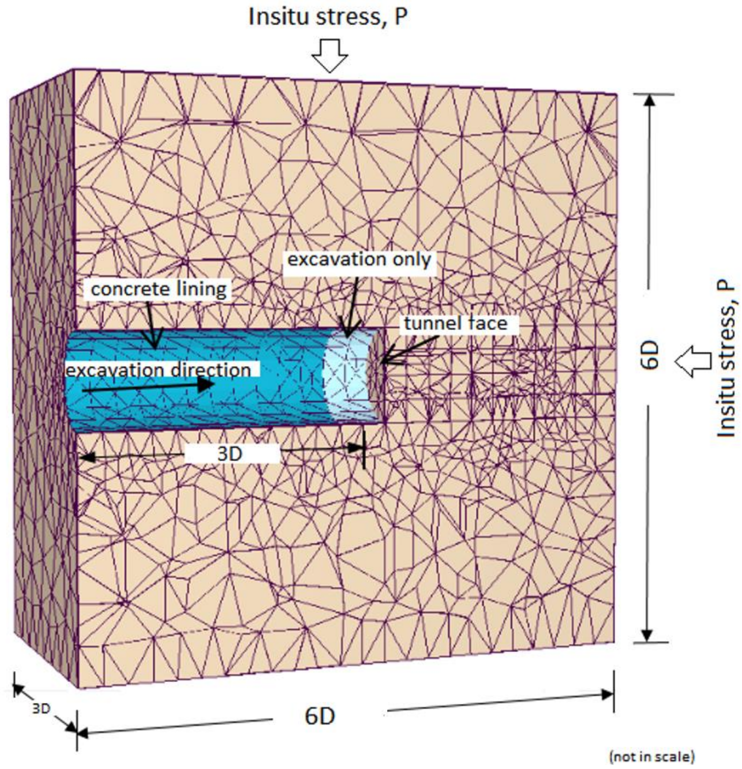

Figure 5-2 3D model for circular tunnel analysis

In Lesser Himalayan region, the tectonic stress is estimated as 3 MPa (Shrestha & Panthi, 2014). Therefore, the hydrostatic state of stress field is considered for analysis, for deep tunnel (Sari & Pasamehmetoglu, 2004) in which it is assumed for analysis in which vertical and horizontal stresses are equal. The rock mass is modelled by both elastic perfectly plastic and strain softening failure criteria based on the GSI value as discussed in chapter 3. The dimension of 3D model is illustrated in Figure 5-2.

The length, depth and width of the model is taken as six times the diameter of the tunnel for the 3D modelling. In 3D analysis, stage wise excavation has been simulated by removing the elements in sequence, in steps of 1 m in the longitudinal direction. Then support is installed 2.0 m behind from the tunnel face sequentially, as illustrated in Figure 5.3(a), and also shown in the 3D model. The stresses and deformations are observed at the crown, wall and invert of the tunnel in two conditions: first, when the support is 1 m behind the observed section, at section A-A', which is 1 m behind the tunnel face; and second, when the support is installed at excavation face, that is, section B-B', as shown in Figure 5.3.

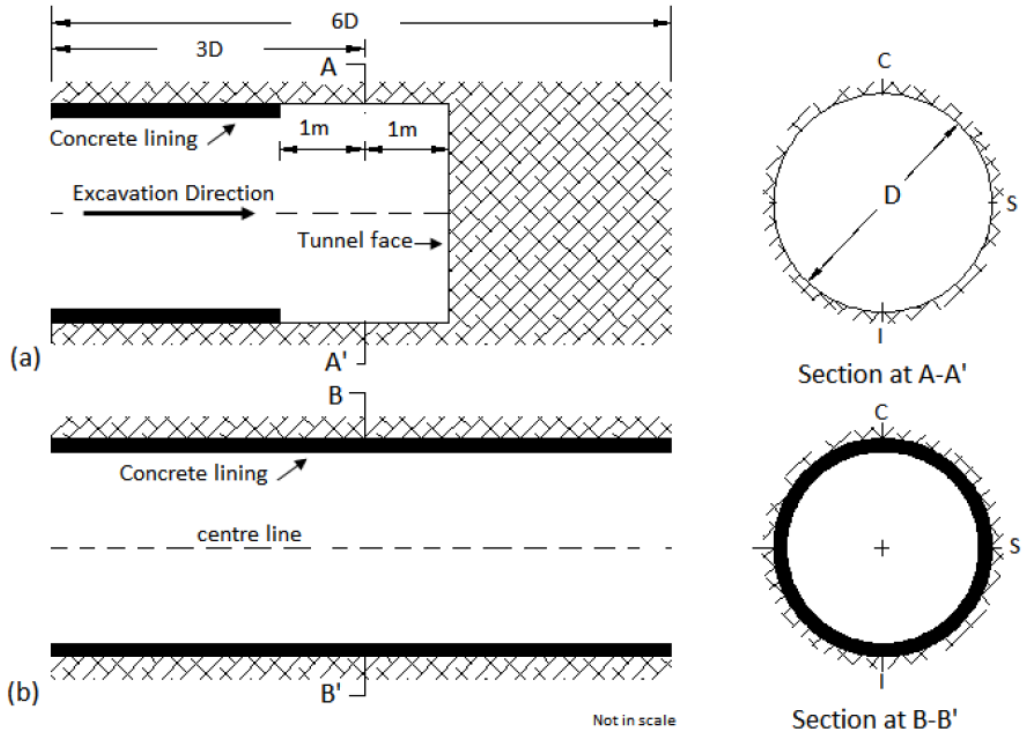

Figure 5-3 Illustration of stage wise tunnel excavation and support installation in 3D model of actual tunneling method (a) support installed 1m behind observed section (b) with support

5.3 Selection of Case Studies

In this study two hydropower tunnels, Kulekhani-III hydropower project and Chameliya hydropower project, are taken as case studies. Both projects are located in the Lesser

Himalayan region of Nepal, area characterized by meta-sedimentary rocks. The details of case studies are discussed in Chapter 4.

Case I- Kulekhani III Hydropower Tunnel

The length of headrace tunnel and diameter of Kulekhani-III hydropower project tunnel are 4221.63 m and 4.0 m respectively. The tunnel passes across marble, schists, quartzite phyllite, siliceous dolomite and slaty phyllite as shown in Figure 4-5. The rock mass classification along the headrace tunnel and support category is given in Table 4.3 in Chapter 4. Four tunnel sections are modelled and analyzed in detail. The tunnel sections are selected based on the rock mass quality and rock overburden. Detailed laboratory studies were carried out from drilling core sample from slaty phyllite. The tests were performed in the exploratory adit in order to obtained rock mechanics data for design of underground tunnel and cavern. The test results are shown in Table 5.1.The estimated rock mass properties of selected tunnel sections are given in Table 5.2.

Table 5.1 Laboratory test results of Kulekhani III headrace tunnel's rock types (NEA 2003)

Rock unit	Unit weight (kN/m^3)	Uniaxial compressive strength (MPa)	Tensile strength (MPa)	Modulus of elasticity (GPa)	Poisson's ratio	Internal friction angle (ϕ^0)
Marble	2.72	100	7.04	20	0.2	32
Garnetiferous Schist	2.78	35	-	9	0.22	23
Quartzitic Schist	2.78	40	-	20	0.22	25
Quartzite	2.83	200	-	35	0.2	35
Phyllite	2.83	18.4	7.09	6	0.2	26
Siliceous Dolomite	2.78	45.6	9.83	15	0.2	28
Slaty Phyllite	2.61	34.5	-	8	0.22	25

Case II- Chameliya Hydropower Tunnel

Chameliya Hydroelectric Project (CHP) is an under construction national priority project of Nepal. The main rock types within the project area are dolomite, sandstone, slate, dolomite intercalated with slate, talcosis dolomite and dolomite interbedded with phyllite (Basnet, 2013). The longitudinal geological profile of headrace tunnel is shown in Figure 4-6. The maximum rock cover above the headrace tunnel is nearly 470 m in between the adit-1 and adit-2. The rock cover between Adit -2 and Adit -3 is nearly 275 m and rock mass is poor compared to rest of the tunnel alignment. Due to the high overburden and weak rock mass the headrace tunnel in between these sections has excessive deformation during the tunnel excavation, Figure 4-6. It had been found that nearly 800 m, from chainage 3+102 m to 3+922 m, of tunnel is severely squeezed. The main rock type around the tunnel consists of kaoline and phyllite, Figure 4-6. Three tunnel sections are selected for the analysis based on the rock mass quality and overburden pressure. The rock mass properties of the selected tunnel sections are given in Table 5.3.

5.4 Estimation of Rock Mass Properties

For the estimation of the rock mass properties of headrace tunnel of Chameliya Hydroelectric project an empirical relation is used. Generalized Hoek and Brown failure criteria (2002) has been used for estimation of rock mass properties. Rock mass strength is estimated by equation 5.1 as suggested by the Hoek et al. (2002).

$$\sigma_{cm} = \sigma_{ci} \frac{(m_b + 4s - a(m_b - 8s))\left(\frac{m_b}{4} + s\right)^{a-1}}{2(1+a)(2+a)} \tag{5.3}$$

where σ_{cm} is the unconfined compressive strength of rock mass in MPa, σ_{ci} is the uniaxial compressive strength of intact rock in MPa, m_b, s, and a are the material constant defined in Hoek-Brown failure criteria (2002).

The rock mass modulus is given by equation 5.2

$$E_m\ (GPa) = \left(1 - \frac{D}{2}\right)\sqrt{\frac{\sigma_{ci}}{100}} * 10^{\left(\frac{GSI-10}{40}\right)} \tag{5.4}$$

where GSI is the geological strength index, D is a factor which depends upon the degree of disturbance to which the rock mass has been subjected by blast damage and stress relaxation. The GSI is determined from the Q- value. Rock Mass Rating (RMR) and GSI value can be estimated using equations 5.3 and 5.4 proposed by Barton (1995) and Hoek & Diederichs (2006) respectively. The equations are as follows:

$$RMR = 15 * \log Q + 50 \tag{5.5}$$

$$GSI = RMR - 5 \tag{5.6}$$

Table 5.2 Estimated rock mass properties for Case I: Kulekhani III tunnel (after NEA 1997)

Chainage	2+355	3+635	3+650	3+965
Rock type	Quartzite	Phyllite	Shear zone	Siliceous dolomite
σci (MPa)	200	18.4	18.4	45.6
E_{ci} (MPa)	35000	9200	9200	15000
H (m)	330.0	315	238	236
mi	20	7	7	9
GSI	62	50	30	55
m_b	3.27	0.647	0.575	1.056
s	0.0063	0.00127	0.00042	0.00247
a	0.502	0.505	0.5223	0.504
E_{rm} (MPa)	3637.9	1351.9	805	3033

Note: GSI, Geological Strength Index; σ_{ci}, intact strength of rock; E_{ci}, intact modulus of rock ; σ_{cm}, compressive strength of rock mass ;E_{rm}, modulus of rock mass; m_b, s, a, Hoek Brown rock parameter

Table 5.3 Estimated rock mass properties for Case II: Chameliya tunnel

Chainage	0+410	1+340	3+681
Rock type	Dolomite Phyllite	Slate	Talcosic Phyllite
σci (MPa)	31	31	15
E_{ci} (MPa)	15500	15000	8250
H (m)	232	464	275
mi	9	9	7
GSI	45	40	20
m_b	0.656	0.517	0.402
s	0.000635	0.000335	0.000138
a	0.508	0.511	0.543
E_{rm} (MPa)	1641.2	1191.9	504.4

Note: H, overburden depth; v, Poisson's' ratio; RMR, rock mass rating; GSI, geological strength index; σ_{ci}, intact strength of rock; σ_0, insitu stress; E_{ci}, intact modulus of rock ; σ_{cm}, compressive strength of rock mass ;E_{rm}, modulus of rock mass

5.5 Results and Discussion

A detailed 2D numerical modeling of weak rock mass with high overburden pressure has been discussed in the Chapter 3. The rock mass is classified based on the GSI system proposed by Hoek et al. The appropriate numerical modeling of different types of Himalayan rocks are proposed in Chapter 3 and it is used to model the different tunnel sections of the case studies.

For an underground excavation and construction into deeper and more complex geological environment understanding the three-dimensional redistribution of excavation- induced stresses becomes more essential for the stability of excavation. a detailed three-dimensional finite-element study, which explores near-field stress paths during the progressive advancement of a tunnel face (Eberhardt, 2001). The effect of tunnel face advancement is well described by the 3D analysis, as compare to the 2D and closed form solution. The correct rock mass response can be captured only if the stress path is correctly represented. The induced stresses at the crown and walls at the observed section are presented to predict the state of stresses during the tunnel advancement in terms of tunnel stability (Khadka, 2016). The results are discussed based on the stress paths during the advancement of tunnel face and the internal forces developed in the tunnel support.

5.5.1 Stress Paths around advancing Tunnel

Stress history is one of the major factors for stability of the hydropower tunnel in such weak geological conditions. This can be well described using the 3D stress path representation (Barla, 1999). The stresses are plotted in terms of mean total normal stress (s) and shear stress (t), which are given in equations

$$S = \frac{\sigma_v + \sigma_h}{2} \tag{5.7}$$

$$t = \frac{\sigma_v - \sigma_h}{2} \tag{5.8}$$

where σ_v and σ_h are vertical and horizontal stresses, respectively. The analysis is carried out for hydrostatic stress field (K=1).

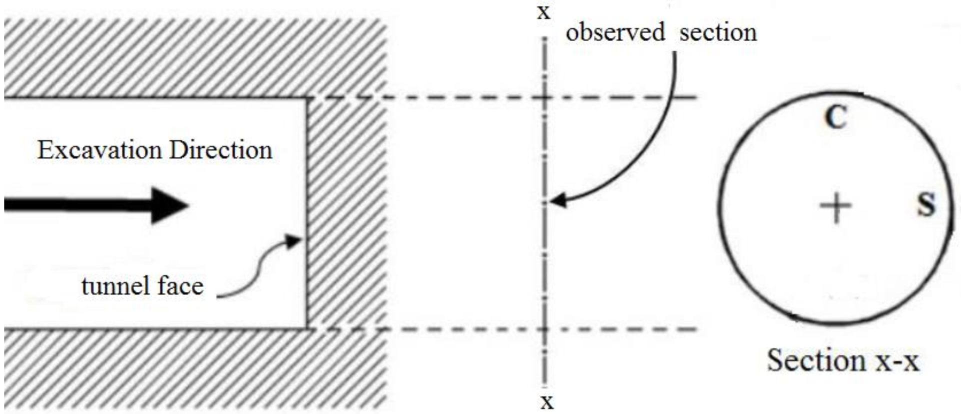

Figure 5-4 Longitudinal section of advancing tunnel and location of observed section

5.5.2 Case I- Kulekhani III hydropower tunnel

Four tunnel sections are modelled and analyzed. The headrace tunnel passes through good quality to poor rock mass quality as described in Chapter 4. Both strain-softening and elastic-plastic failure characteristics are used for modeling of different types of rock mass. The disturbance factor is taken as 0 and 0.5 for elastic –perfectly plastic model and strain-softening failure criteria, respectively considering disturbance of rock mass around the tunnel during face advancement as suggested by Hoek (2007).

In this analysis, strain-softening and elastic –perfectly plastic post failure strength parameters are used for good to poor and extremely poor rock masses respectively as shown in Table 5.4. The residual strength parameters were taken reduced, based on the rock mass quality as shown in Table 5.4, where the last columns indicate the percentage of the peak strength assumed for estimating the residual strength.

Table 5.4 Selected numerical model for analysis

Tunnel section	Rock mass	Rock type	Peak GSI	Constitutive model	Disturbance factor (D)	Remarks
2+355	Quartzite	Good	62	Strain-softening	0.5	Peak GSI is reduced by 50%
3+635	Phyllite	Poor	50	Strain-softening	0.5	Peak GSI is reduced by 70%.
3+650	Shear zone	Extremely poor	30	Elastic-plastic	0	No reduction in peak GSI
3+965	Siliceous dolomite	Fair	55	Strain-softening	0.5	Peak GSI is reduced by 60%

Table 5.5 Rock mass characterization in terms of peak and residual strength for Kulekhani III tunnel using GSI system

Rock Mass	Good		Poor		Very poor		Fair	
Chainage	2+355		3+635		3+650		3+965	
Rock type	Quartzite		Phyllite		Shear zone		Siliceous dolomite	
	Peak	Residual	Peak	Residual	Peak		Peak	Residual
GSI	62	31	50	35	30		55	33
m_b	3.27	0.748	0.647	0.317	0.575		1.056	0.370
s	0.0063	0.0001	0.00127	0.0001724	0.00042		0.00247	0.0001325
a	0.502	0.520	0.505	0.516	0.5223		0.504	0.518
E_{rm} (MPa)	3637.9	554.6	1351.9	525.7	805		3033	768

5.5.2.1 Stress path along the good quality rocks

When the excavation is far from the observed section, 6 m away from the observed section, both vertical and horizontal stresses are equal, in case of K=1. But when the excavation approaches near to the observed section the vertical stress (major stress) increases drastically while the horizontal stress (minor stress) decreases, as shown in Figure 5-5 (b). The major stress is maximum when the excavation reaches observed section at the same time the minor stress decreases drastically. When the excavation just passes through the observed section, the major stress is also decreased and remains constant when the excavation is far from the observed section.

The mean normal stress drastically decreases when the excavation face is very near to the excavation, which indicates the formation of plastic deformation around the perimeter of tunnel, as shown in Figure 5-5 (c). The major principal stress immediately starts to decrease when the face just passes through the observed section. In case of crown, the stress path follows the residual failure envelope but, in the case of the side wall, it is found that the stress path is not following the residual failure line when the excavation just passes through the observed section.

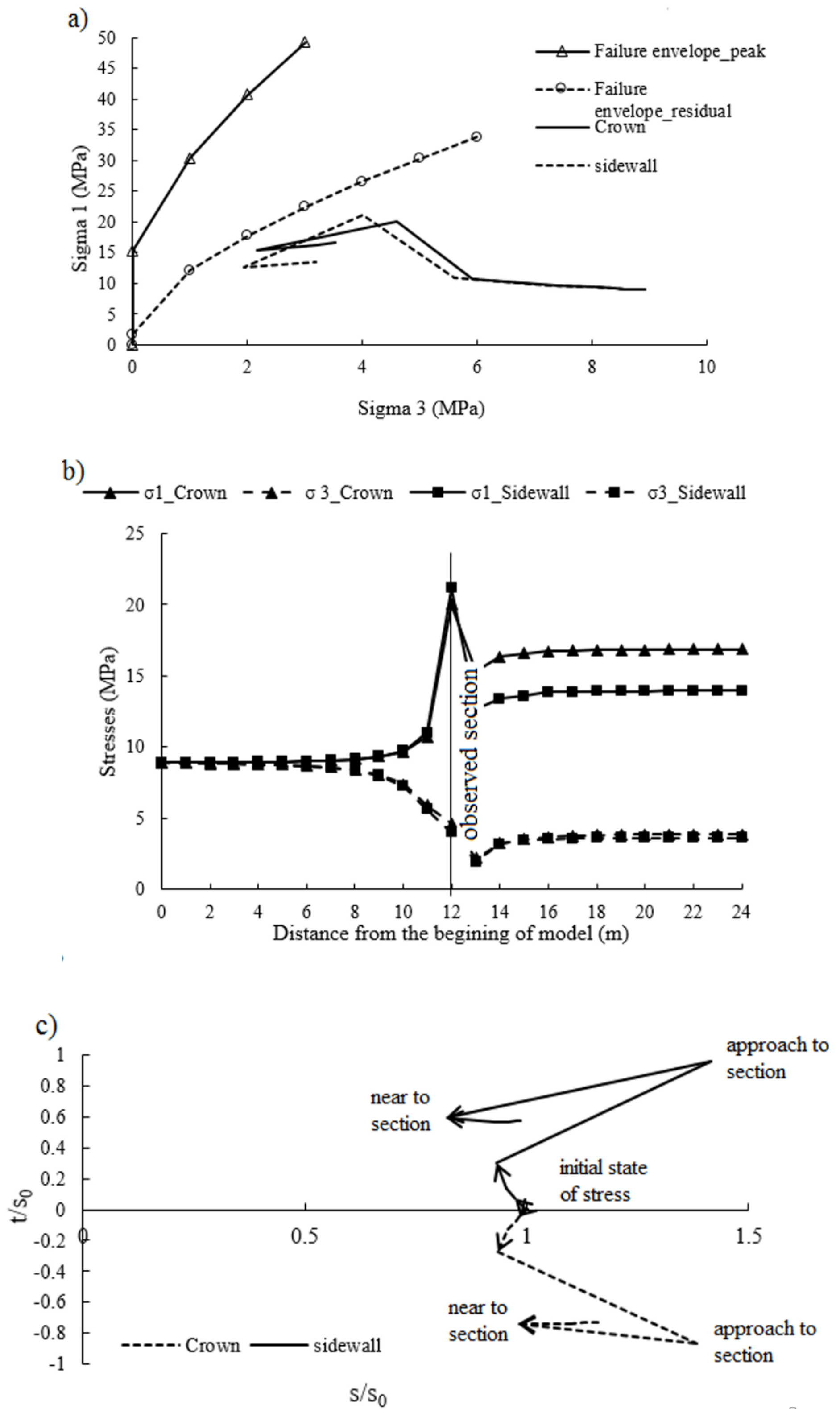

Figure 5-5 a) Relation between major and minor principal stress, b) Stresses at crown (C) and sidewall (S) considering K=1 and c) stress path during the tunnel excavation, at chainage 2+355m, Quartizite

5.5.2.2 Stress path along the poor-quality rocks

In the case of the phyllite and silicious dolomite, poor rock mass quality, the vertical stress slightly increases as the excavation reaches the observed section. When the excavation is 6 m ahead of the observed section, the vertical stress starts to increase, while the horizontal stress starts to decrease, Figure 5-6 (b). When the excavation reaches the observed section, both vertical and horizontal stresses drastically decreases and remain constant as the excavation face is far from the observed section. It is observed that the mean normal stress decreases as the excavation approximates near the observed section, and drastically decreases when it reaches the observed section, as shown in Figure 5-6 (c). The stress path is changed when the excavation face reaches near the observed section and passes through the observed section, which signifies that there is formation of plastic zone around the excavated tunnel during the face advancement of tunnel.

In the case of the silicious dolomite, fair rock mass, the trend of stress path shows that the mean normal stress is slightly decreasing as the excavation face is near to the observed section. But it drastically decreases when the excavation just passes through the observed section. It also increases slightly as the excavation face is far from the observed section

5.5.2.3 Stress path along the extremely poor-quality rocks

In the case of the shear zone, at chainage 3+650 m, extremely weak rock mass, the stress path is quite different from that of the other section having relatively stronger rock masses as shown in Figure 5-5. When the excavation proceeds towards the observed section, the vertical stress starts to increase and reaches the maximum when the excavation reaches 5-6 m ahead of the observed section. After that, it continuously decreases until the excavation face reaches the observed section and remains constant as the excavation face is far from the observed section. Similarly, the horizontal stress is continuously decreasing and reaches the minimum value as the excavation reaches the observed section and remains constant as the excavation is far from the observed section as shown in Figure 5-8 (c).

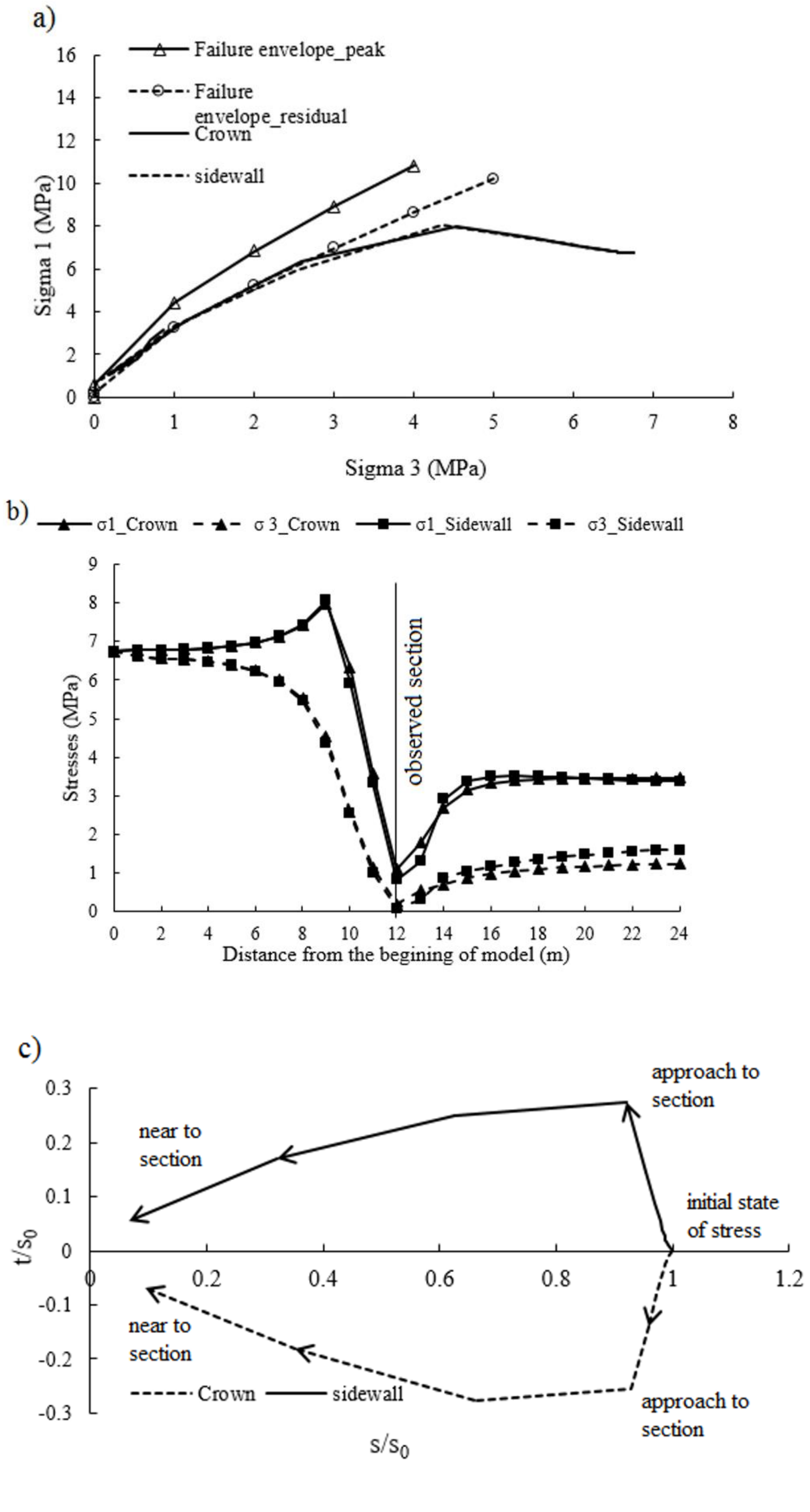

Figure 5-6 a) Relation between major and minor principal stress, b) Stresses at crown (C) and sidewall (S) considering K=1 and c) stress path during the tunnel excavation, at chainage 3+635m, Phyllite

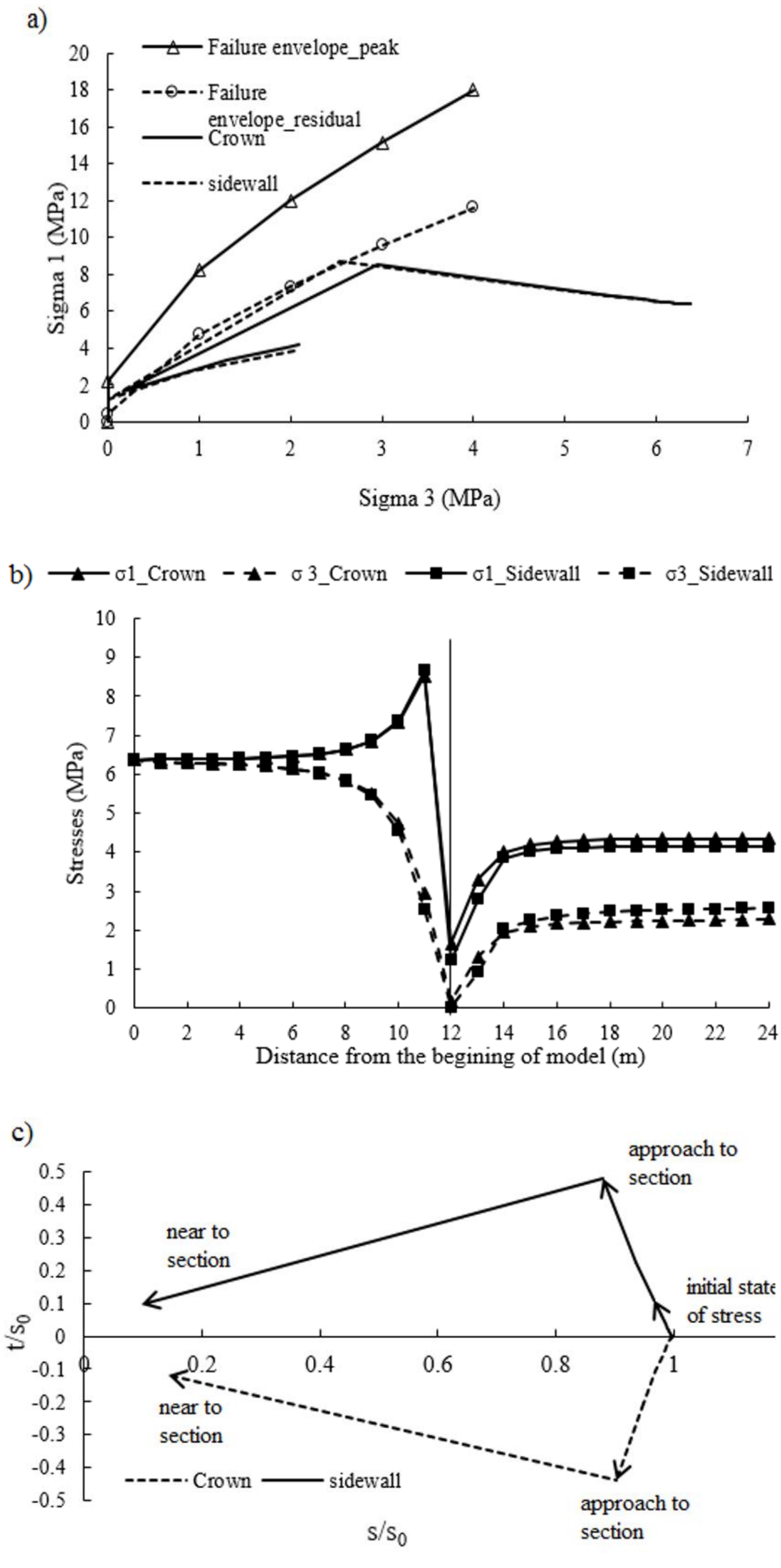

Figure 5-7 a) Relation between major and minor principal stress, b) Stresses at crown (C) and sidewall (S) considering K=1 and c) stress path during the tunnel excavation, at chainage 3+965m, Silicious dolomite

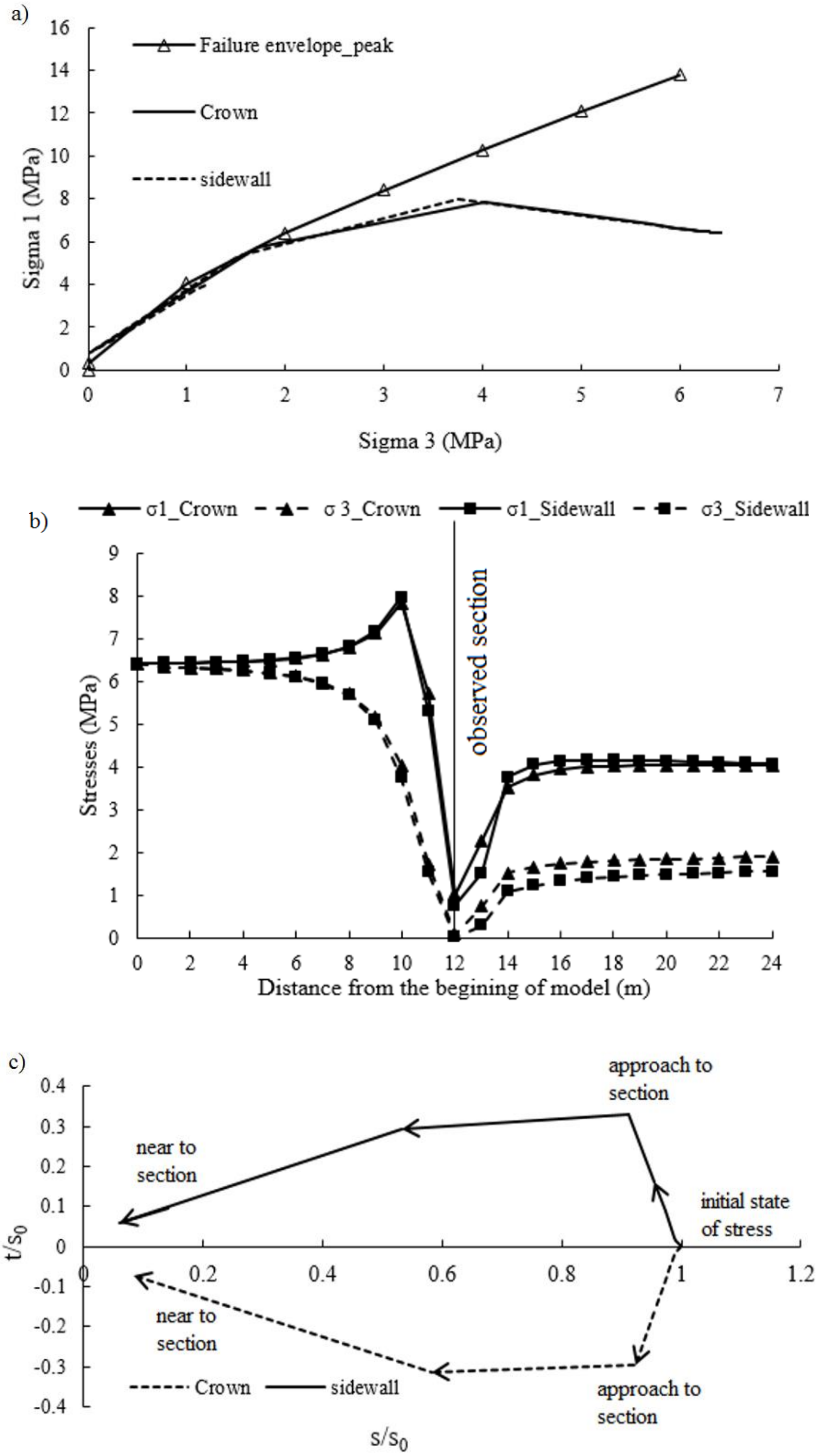

Figure 5-8 a) Relation between major and minor principal stress, b) Stresses at crown and sidewall considering K=1 and c) stress path during the tunnel excavation, at chainage 3+650m, shear zone. The rock mass is modelled as elastic perfectly plastic

There is drastically decrease of normal stress when the excavation face is still 5-6 m ahead of the observed section. This indicates that the plastic zone is already formed around the observed section of tunnel. In the case of extremely poor rock, when the excavation is far from the observed section, both major and minor principal stresses are equal. Then the minor principal stress starts to decrease and, as the excavation passes the observed section, the minor principal stress drastically decreases and follows the failure plane as shown in Figure 5-8 (c).

5.5.3 Case II- Analysis of Chameliya Hydropower Tunnel

Three tunnel sections are considered based on the rock mass quality which was analyzed by the analytical and empirical methods in Chapter 4, as shown in Table 5.6. The state of stress is discussed during the face advancement of tunnel. Strain softening, and elastic perfectly plastic failure criteria are used for very poor to poor and extremely poor rock mass respectively, as discussed in Chapter 3.

Based on the GSI values, the rock mass is characterized as poor rocks and extremely poor rocks. The rock mass at chainages 0+410 m and 1+340 m are considered as poor rock masses and at chainages 3+681 m as extremely poor rock mass. Both, strain-softening and elastic- perfectly plastic failure criteria models are used for the analysis of the Chameliya tunnel as per the rock mass condition, described in Chapter 3. The selected numerical model for the analysis is given in Table 5.6. The rock mass properties are estimated as described in section 5.3 and given in Table 5.3.

Table 5.6 Selected numerical model for analysis

Tunnel section	Rock Type	Rock mass quality	Peak GSI	Constitutive model	D	Remarks
0+410	Dolomite Phyllite	Very poor to poor	45	Strain-softening	0.5	Peak GSI is reduced by 68%.
1+340	Slate	Very poor to poor	40	Strain-softening	0.5	Peak GSI is reduced by 62%.
3+681	Talcosic Phyllite	Extremely poor	20	Elastic-plastic	0	No reduction in Peak GSI

For very poor to poor rock mass (30<GSI<50), the rock mass is analyzed by strain-softening failure criteria as per suggested by the Hoek (2007). The peak strength is reduced between 60 to 70 % as discussed in Chapter 3. For extremely poor rock mass (GSI< 30), the rock mass is analyzed by elastic perfectly plastic failure criteria. In this case only peak strength is considered for the analysis. The rock mass characterization for both cases are shown in Table 5.5.

5.5.3.1 Stress path along the poor rock mass

The major and minor principal stresses are examined during the face advancement of the tunnel, at chainage 0+410 m. Approaches the observed section, the mean normal stress increases, exceeding the strength of rock, producing plastic deformation around excavation. When the excavation face is far from the observed section, the minor principal stress gradually decreases while there is no significant change in the major principal stress. But, as when the excavation face approaches to the observed section, 2-3 m from the observed section, both principal stresses decrease gradually along the failure envelope of the rock mass, continuing to decrease as the excavation face passes through and far from the observed section.

Table 5.7 Rock mass characterization in terms of peak and residual strength for chameliya tunnel using GSI system

Rock mass	Very poor to poor				Extremely poor
Chainage	0+410		1+340		3+681
Rock Type	Dolomite phyllite		Slate		Talcosic Phyllite
	Peak	Residual	Peak	Residual	Peak
GSI	45	31	40	25	20
m_b	0.656	0.337	0.517	0.253	0.402
s	0.000635	0.0001	0.000335	0.0000454	0.000138
a	0.508	0.520	0.511	0.531	0.543
Erm (MPa)	1641.2	716.3	1191.9	549	502.4

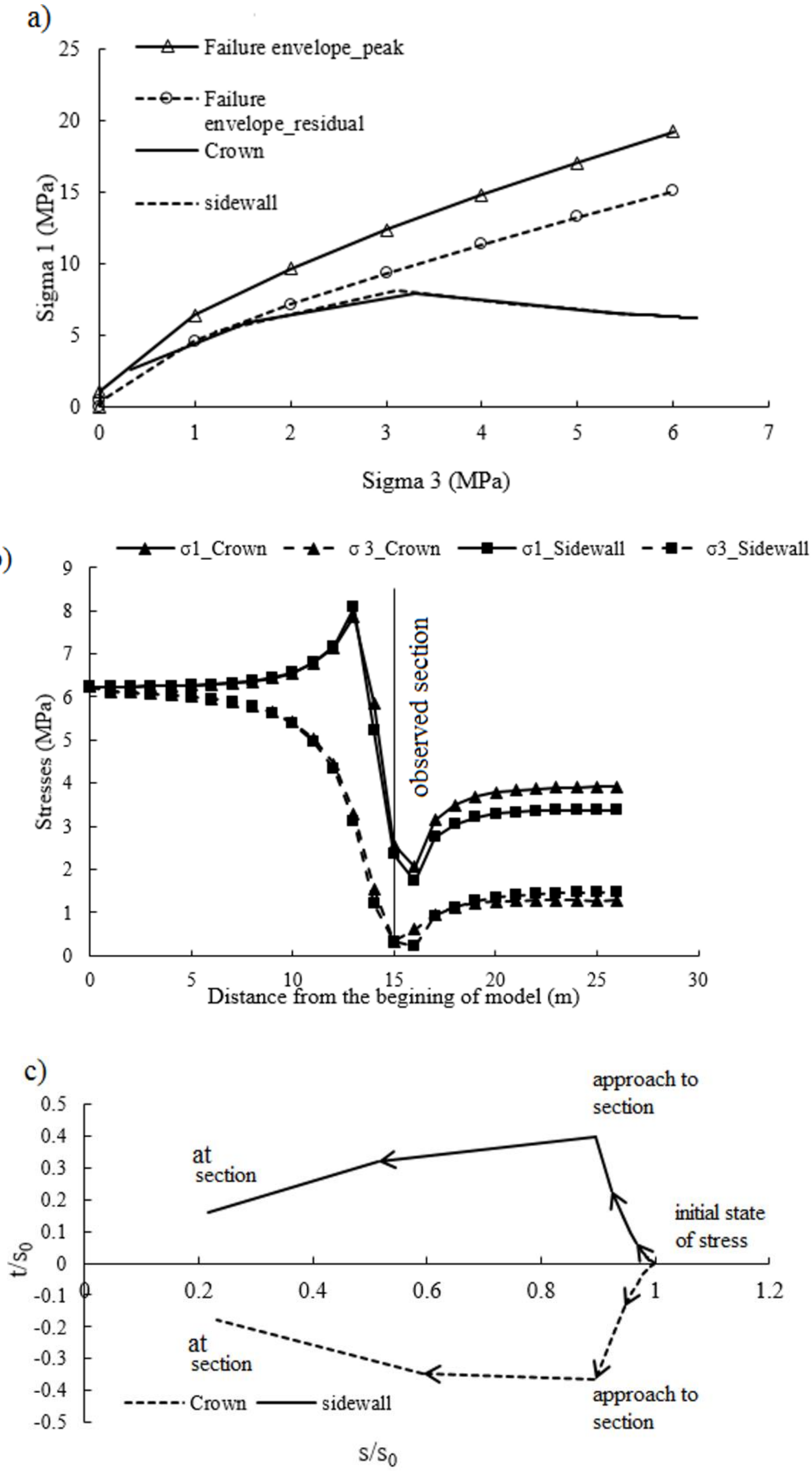

Figure 5-9 a) Relation between major and minor principal stress, b) Stresses at crown (C) and sidewall (S) considering K=1 and c) stress path during the tunnel excavation, at chainage 0+410 m , Dolomite Phyllite

Figure 5-9 represents the (calculated) stresses in the crown and side wall of the tunnel. The mean normal stress is slightly decreasing as the excavation approaches the observed section and it is gradually decreasing as the excavation reaches the observed section and remains decreasing as the excavation passes the observed section as shown in Figure 5-9 (c). In this case, when the excavation reaches the 2-3 m ahead of the observed section, the major stresses, in both crown and sidewall, is increasing and minor stress is gradually decreasing. This shows that stress path has two changes in the direction of excavation, the major principle stress increases and drastically decreases when excavation passes through the observed section, while the minor stress starts decreasing gradually when excavation proceeds towards the observed section, and remains decreasing when there is full excavation, Figure 5-9 (b).

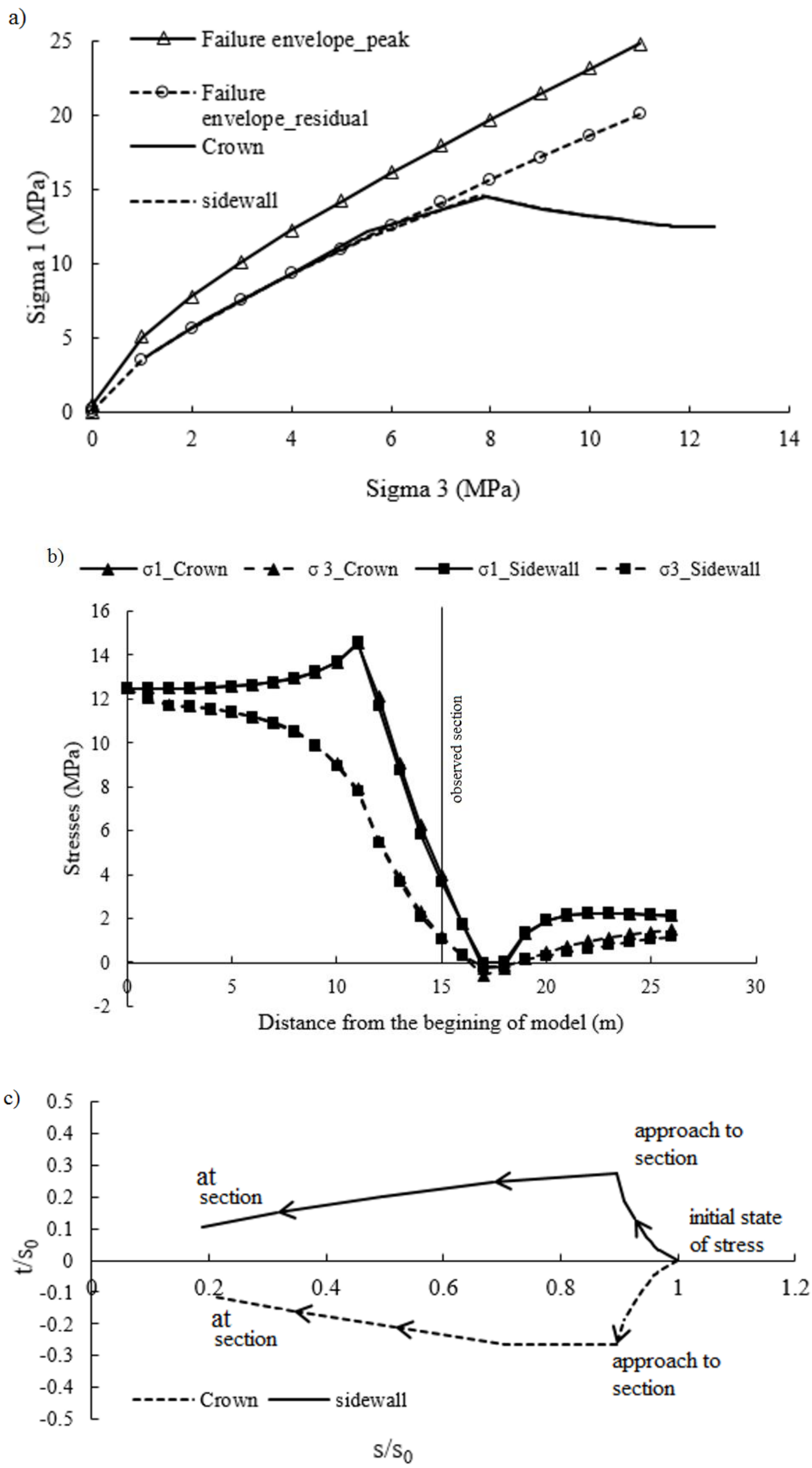

Figure 5-10 a) Relation between major and minor principal stress, b) Stresses at crown (C) and sidewall (S) considering K=1 and c) stress path during the tunnel excavation, at chainage 1+340 m, Slate

5.5.3.2 Stress path along the extremely poor rock mass

For the failure envelops used in the computation, strength is exceeded and plastic deformation around the tunnel takes place. Section at chainage 3+681m is analyzed by the elastic-perfectly plastic failure model. It is found that the normal stress drastically decreases to zero as the excavation is far away from the observed section.

The major and minor principal stresses are also examined at these typical locations, crown and sidewall, during tunnel advancement. Generalized Hoek-Brown failure criterion is used for assessing and predicting rock mass yielding in both case studies. The relation between major and minor principal stresses at crown and sidewall of Chameliya tunnel at different tunnel cross section, 0+410, 1+340 and 3+681 are shown in Figure 5-9, Figure 5-10 and Figure 5-11 respectively.

At chainage 3+681, the rock mass is modelled with an elasto perfectly plastic behavior, and considering control blasting taking as disturbance factor, D, as 0. It is found that the rock mass has not yielded during modeling, as shown in Figure 5-11, because the stress path always lies below the failure plane. In this rock type, the minor principal stress is continuously decreasing as the face reaches and passes the excavation, while the major principal stress is not significantly changing, and the rock mass does not yield.

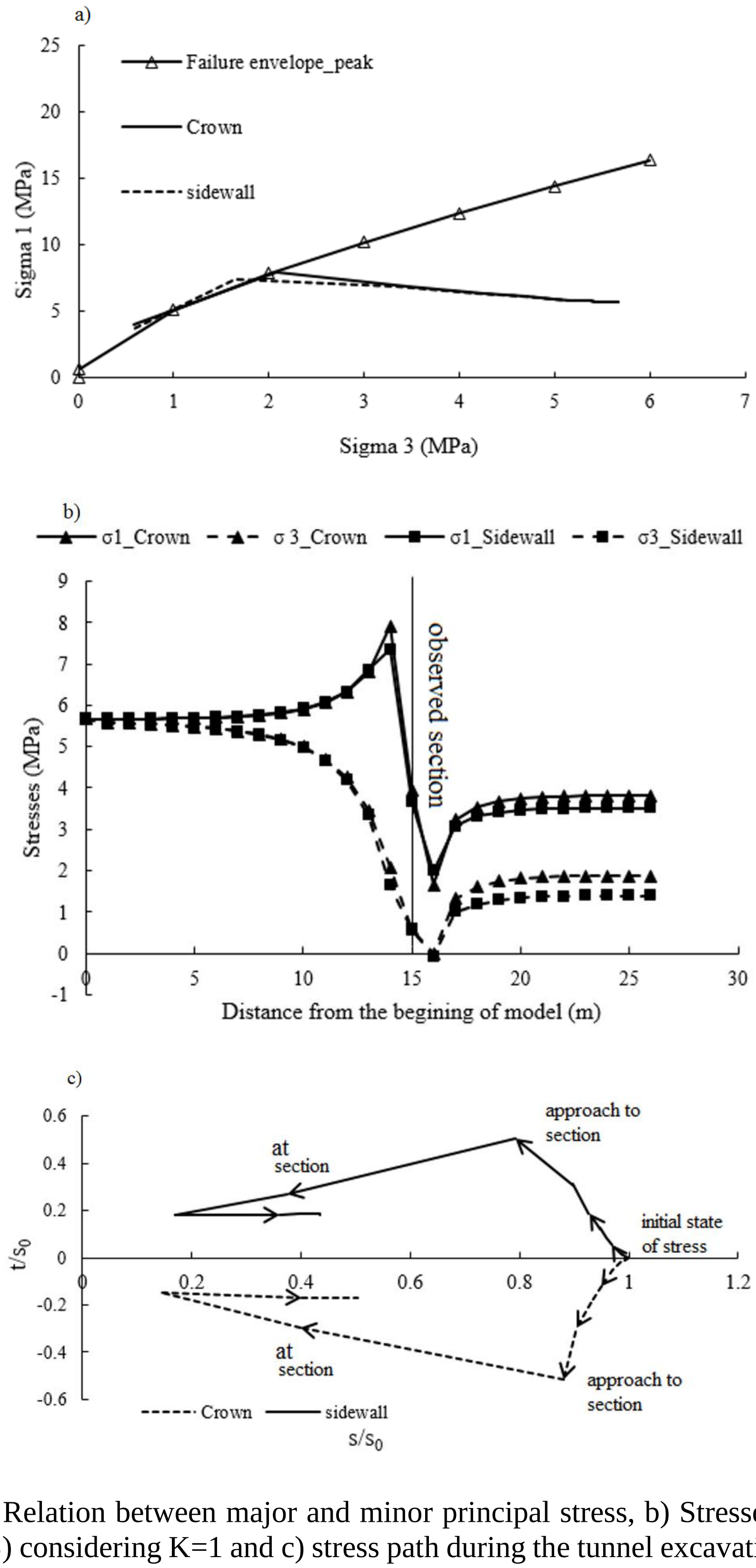

Figure 5-11 a) Relation between major and minor principal stress, b) Stresses at crown (C) and sidewall (S) considering K=1 and c) stress path during the tunnel excavation, at chainage 3+681 m, Talcosic phyllite

5.5.4 Moments and Forces in Lining Elements

5.5.4.1 Case I – Kulekhani III hydropower tunnel

The diameter of Kulekhani III tunnel is 4.0 m and passes through different types of rock mass qualities with different overburden depth. In the Lesser Himalayan region of Nepal, tunnel supports are proposed based on the rock mass classifications. The support consists of shotcrete lining, steel sets, concrete lining and rock bolts. Due to weak rock mass and high overburden, steel sets embedded in concrete lining with rock bolts are commonly used for tunnel supports.

Table 5.8 Proposed support at different tunnel section

Tunnel chainage	Support description	Peak GSI	Rock type	Overburden depth, H(m)
2+355	300 mm thick concrete lining is applied with steel ribs.	62	Quartzite	330
3+635	400 mm thick concrete lining is applied with steel ribs.	50	Phyllite	315
3+650	400 mm thick concrete lining is applied with steel ribs.	30	Shear Zone	238
3+965	400 mm thick concrete lining is applied with steel ribs.	55	Silicious Dolomite	236

Table 5.9 Material properties of concrete and steel rib

Parameters	Unit	Concrete	Steel rib
Young's modulus	GPa	30	200
Poisson's ratio		0.15	0.25
Cross sectional area	m^2		0.0379
Moment of inertia	m^4		1.72×10^{-5}
Section depth	m		0.157

Distribution of bending moment and axial force

A numerical analysis has been carried to compute the axial force and bending moment induced in the support lining. Figure 5-12 shows the trend of bending moment around the support lining

during the advancement of tunnel. It is found that the bending moment is significantly higher at the corner and invert of tunnel, if compare to the crown. It is observed that the positive moment drastically increases in the wall of tunnel, changing from positive to negative at the invert. Again, the bending moment change from negative to positive at the right side of the tunnel lining as shown in Figure 5-12. This is expected as, due to the symmetry of the tunnel, the moments are supposed to be also symmetric.

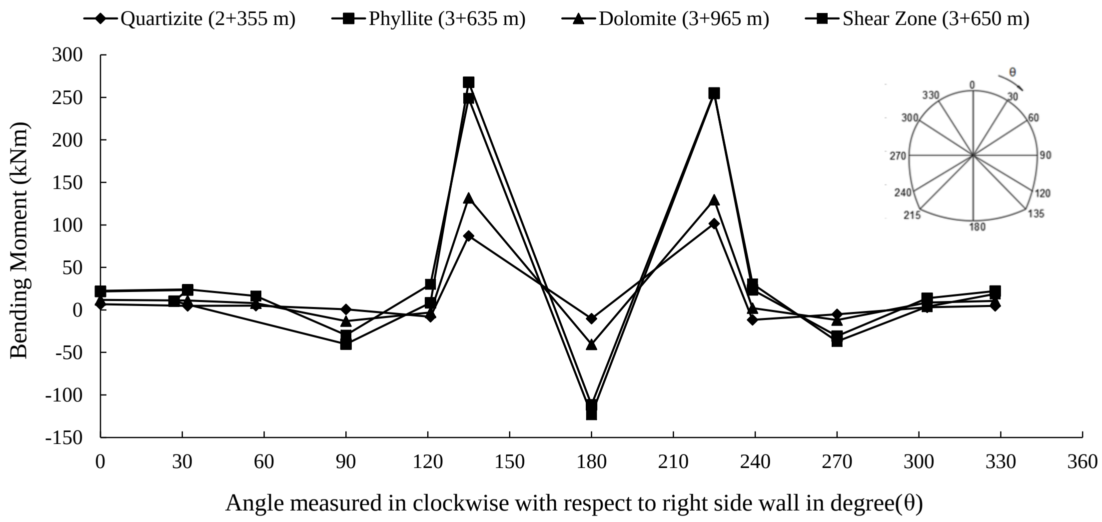

Figure 5-12 Trend of bending moment in the tunnel lining for different rock mass quality, θ is 0 on the right side of the tunnel and increasing clockwise.

There is no significant different of bending moment in crown of tunnel for all types of rock mass. But it is found that there is significantly changes in the bending moment in walls and invert of tunnel. It is observed that the positive bending moment drastically increase in the wall, and it changes from positive to negative bending moment at the center of the invert and again increases drastically in the left side of wall as shown in Figure 5-12.

The trend of bending moments along the tunnel lining, in all sections, follow the same pattern with different values due to rock mass strength and rock mass quality. At chainage

2+355 m, the rock mass with GSI= 62, and the tunnel located at a depth of 330 m, is considered as good quality of rock mass. The uniaxial compressive strength of the intact rock mass is 200 MPa. The maximum bending moment acting on the lining equal to 101 kNm at the corner of wall, while at the crown and invert are 11 kNm and -10 kNm respectively. The thickness of concrete lining is 0.3 m without steel ribs. This is naturally associated with the flattest shape of the walls.

At chainage 3+635 m, the rock mass with GSI= 50, and the tunnel located at a depth of 315 m, is considered as fair quality of rock mass. The uniaxial compressive strength of the intact rock mass is 18.4 MPa. The maximum bending moment acting on the lining is equal to 267 kNm at the corner of wall, while at the crown and invert are 21 kNm and -111 kNm respectively. The thickness of the concrete lining is 0.4 m with steel ribs. At chainage 3+650 m, the rock mass with GSI= 30, and the tunnel located at a depth of 238 m, is characterized as shear zone with crushed phyllite and considered as very poor rock mass. The uniaxial compressive strength of the intact rock mass is 18.4 MPa. The maximum bending moment acting on the lining is equal to 248 kNm at the corner of wall, while at the crown and invert are 22 kNm and -123 kNm respectively. The thickness of the concrete lining is 0.4 m with steel ribs. At chainage 3+965 m, the rock mass with GSI= 55, and the tunnel located at a depth of 236 m, is considered as good rock mass. The uniaxial compressive strength of the intact rock mass is 45.6 MPa. The maximum bending moment acting on the lining is equal to 131 kNm at the corner of wall, while at the crown and invert are 11 kNm and -40 kNm respectively. The thickness of the concrete lining is 0.4 m with steel ribs.

It is noted that rock mass strength and rock mass quality greatly effect the induced bending moment in the tunnel lining, much more significantly than the rock depth. Changes in the bending moment, from negative to positive values can be observed on the two lower sides of tunnel near the spring line region while changes from positive to negative values can be observed near the tunnel base, during the advancement of tunnel.

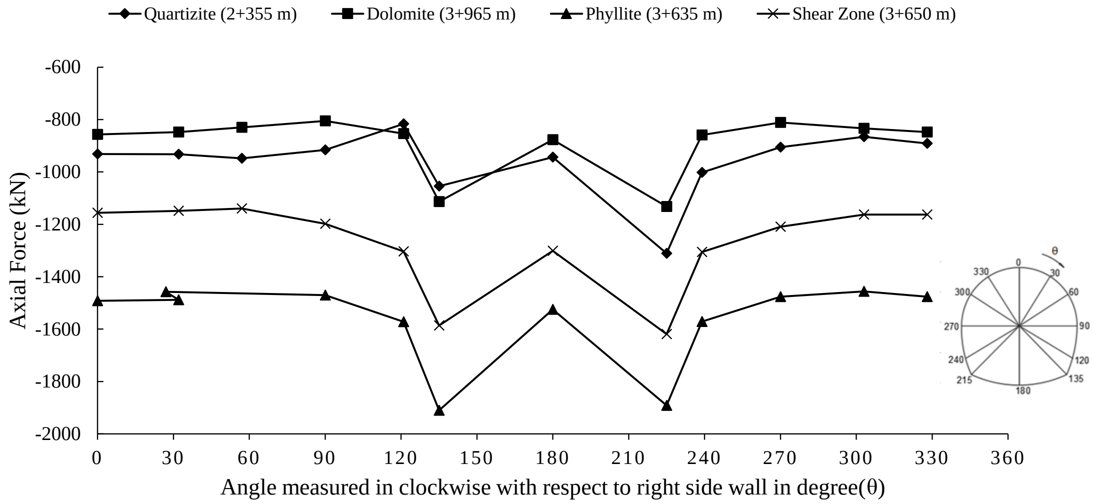

Figure 5-13 Trend of axial force in the tunnel lining for different rock mass quality, θ is 0 on the right side of the tunnel and increasing clockwise.

It is observed that tunnel lining experience more axial force based on the rock mass quality and rock mass strength than rock depth, as shown in Figure 5-13. For example, the rock depth at chainage 2+355 m has 330 m with good quality of rocks and the tunnel lining experience maximum axial force acting on the tunnel lining equal to 1.3 MN at the corner of wall. At chainage 3+635 m, the rock depth is 315 m with fair quality of rock mass with very low compressive strength of rock mass , the maximum axial force acting on the tunnel lining is equal to 1.9 MN at the corner of wall, shown in Figure 5-13.

Bending moment and axial force interaction

A bending moment and axial force interaction curve is generated based on the concrete section strength. The interaction curve gives clear idea for appropriate concrete lining thickness, based on the induced moment and axial force. A comparison between induced moments and axial force obtained from calculation and the concrete section strength is shown in Figure 5-14.

In case of chainages 3+635 m and 3+650 m, the rock mass is characterized with very poor quality, the induced bending moment and axial force lie in the border of the calculated bending moment and axial force. It shows that the given thickness of concrete lining is suitable for the given conditions. It also suggests increasing the thickness of concrete lining at the corner of the wall. But in case of the chainages 2+355m and

3+965m , where the rock masses are characterized by the good quality of rock, the induced bending moments and axial force are within the interaction curve as shown in Figure 5-14.

Deformation of tunnel support

After the numerical analysis of the four tunnel sections, the deformation in the supports are observed and found that it depends on the rock mass quality. There is no significant deformation in the concrete lining as the tunnel passes through the good quality of quartzite with GSI= 62. The thickness of concrete lining is 0.3 m and the steel ribs are also embedded inside the concrete lining. The maximum deformation in the concrete lining is 0.03 m around the tunnel as shown in Figure 5-15 (a). Similar deformation is also observed in the steel ribs as shown in Figure 5-16 (a).

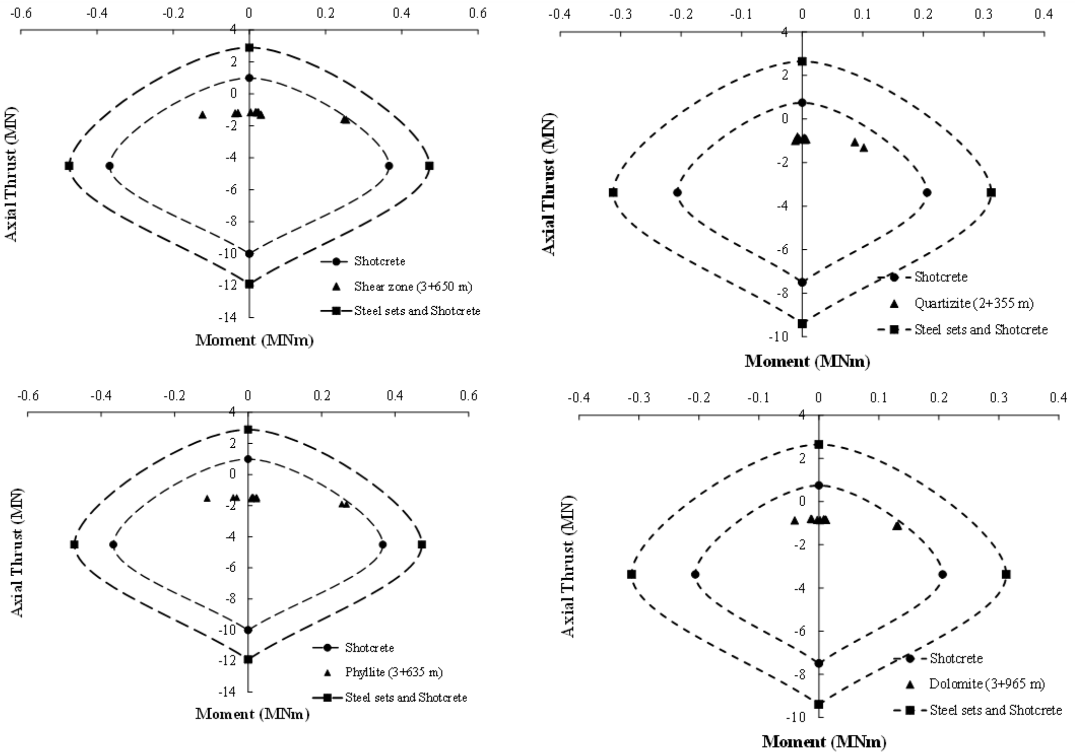

Figure 5-14 M-N interaction curves for different section and comparison of the lining stress state with the strength domain of concrete section.

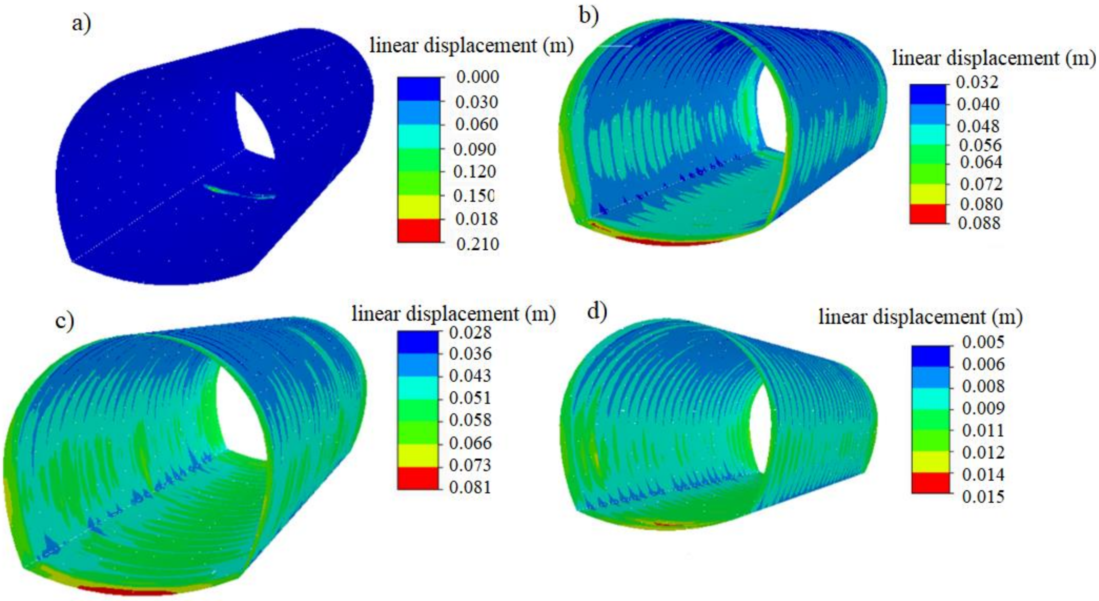

Figure 5-15 Deformation of concrete lining at different tunnel section of Kulekhani III headrace tunnel; a) 2+355 b) 3+635 c) 3+650 d) 3+965

As the tunnel passes through the poor quality of Phyllite, with GSI =50, there is no uniform deformation around the tunnel lining. It is observed that the maximum deformation occurred in the wall and invert compare to the crown, as shown in Figure 5-15 (b). The displacement in the concrete lining at the crown is 0.048 m while at the wall and crown it is 0.064 m as shown in Figure 5-15 (b). In this section, the thickness of concrete lining is 0.4 m. Similar deformation is also observed in the steel ribs Figure 5-16 (b). It is found that the tunnel support is highly deformed in the side walls and invert as compare to the crown.

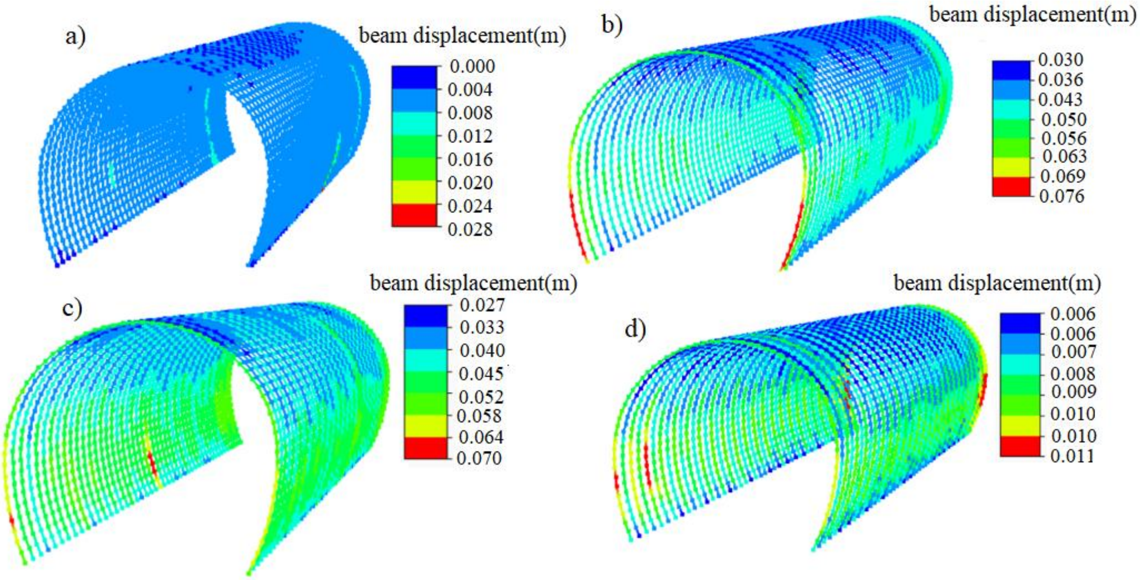

Figure 5-16 Displacement of steel ribs at different tunnel section of Kulekhani III headrace tunnel; a) 2+355 b) 3+635 c) 3+650 d) 3+965

As the tunnel passes through the very poor rock mass at chainage 3+650 m, shear phyllite, it is observed that the maximum displacement occurs in the wall and invert, if compared to the crown of the tunnel. It is found, that at the crown, the maximum displacement is 0.04 m and at the side walls and invert it is 0.066 m, as shown in Figure 5-15(c). Similar deformation also occurs in the steel ribs, Figure 5-16(c). It is observed that the maximum displacement of ribs is 0.033 m in the crown and 0.064 m at the wall and crown respectively, shown in Figure 5-16 (c). As the tunnel route passes through very poor to fair rock mass the tunnel deformation decreased. At chainage 3+965 m, Silicious

Dolomite with GSI =55 , the maximum tunnel displacement at crown is 0.006 m and at the walls and invert is 0.012 m, as shown in Figure 5-15(d). In this section the thickness of concrete lining is 0.4 m. Similarly, the deformation in the steel ribs also decreased compared to previous section, as shown in Figure 5-16 (d).

5.5.4.2 Case II – Chameliya hydropower tunnel

The route of headrace tunnel of Chameliya hydropower project passes through different types of rock masses, fair to extremely poor, described in Chapter 4. In the numerical analysis three sections are chosen, based on the rock mass quality for detail analysis shown in Table 5.10. For the support, concrete lining is provided around the tunnel in which steel ribs are embedded except in invert, i.e. steel rib is not provided in the invert level.

Table 5.10 Proposed tunnel support at different tunnel section

Tunnel chainage	Support description	Peak GSI	Rock type	Overburden depth, H(m)
0+410	400 mm thick concrete lining is applied in around tunnel, steel rib embedded into the concrete lining, no steel rib at invert	45	Dolomite	232
1+340	400 mm thick concrete lining is applied in around tunnel, steel rib embedded into the concrete lining, no steel rib at invert	50	Dolomite with slate	464
3+681	400 mm thick concrete lining is applied in around tunnel, steel rib embedded into the concrete lining, no steel rib at invert	30	Talcosic Phyllite	210

Distribution of Bending Moment and Axial Force

After the numerical analysis, the bending moment and axial forces are observed in the tunnel support at these sections. The trend of the bending moment and axial force are shown in Figure 5-17 and Figure 5-18 respectively. It is found that the bending moment is significantly higher at the corner (intersection of the sidewall with the invert) and invert of the tunnel, compared to the crown. It is observed that the positive moment is drastically increased to the wall of tunnel and changed from positive to negative moment at the invert and again changed from negative to positive moment at the right side of the tunnel lining.

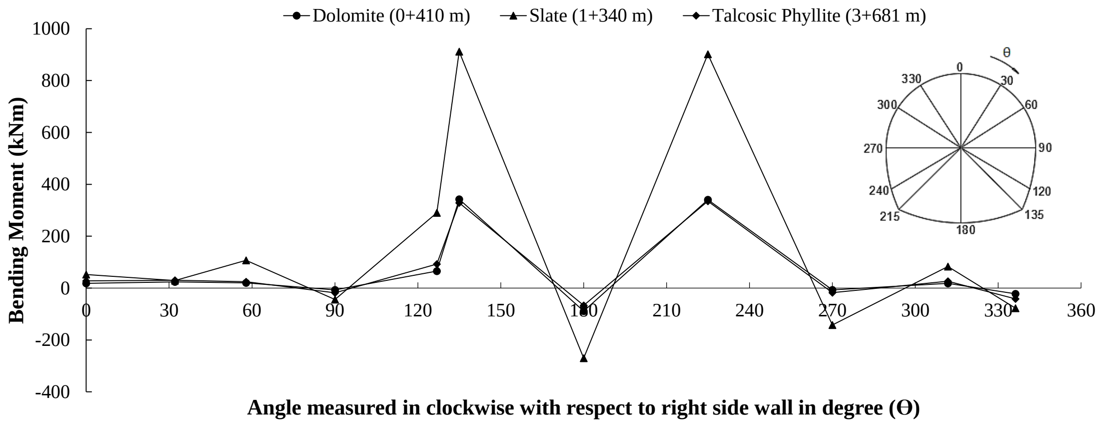

Figure 5-17 Trend of bending moment in the tunnel lining for different rock mass quality, θ is 0 on the right side of the tunnel and increasing counterclockwise

The trend of bending moment along the tunnel lining in all sections follow the same pattern with different values, due to rock mass strength and rock mass quality. At chainage 0+410 m, the rock mass with GSI= 45 at a depth of 232 m, is considered as poor quality of rock mass. The uniaxial compressive strength of the intact rock mass is 45.6 MPa. The maximum bending moment acting on the lining is equal to 342 kNm at the corner of wall -invert, while at the crown and invert are 27 kNm and -88 kNm respectively. The thickness of concrete lining is 0.4 m. At chainage 1+340 m, the rock mass with GSI= 40 at a depth of 464 m, is considered as poor quality of rock mass. The uniaxial compressive strength of the intact rock mass is 34.5 MPa. The maximum bending moment acting on the lining is equal to 911 kNm at the corner of wall, while at the crown and invert are 52 kNm and -270 kNm respectively. The thickness of concrete lining is 0.4 m with steel ribs. At chainage 3+681 m, the rock mass with GSI= 30 at a depth of 210 m, is characterized as shear zone with crushed talcosic phyllite and considered as very poor rock mass. The uniaxial compressive strength of the intact rock mass is 35 MPa. The maximum bending moment acting on the lining equal to 328 kNm at the corner of wall, while at the crown and invert are 27 kNm and -67 kNm respectively. The thickness of concrete lining is 0.4 m.

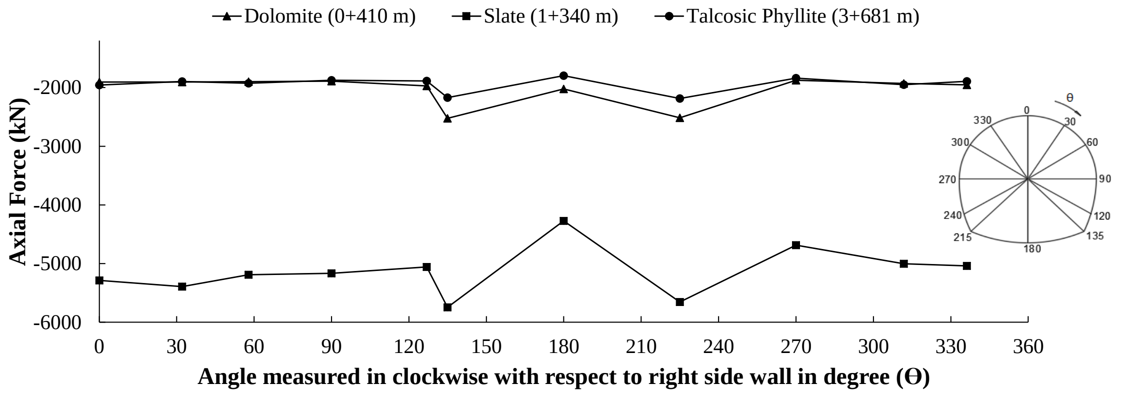

Figure 5-18 Trend of axial force in the tunnel lining for different rock mass quality, θ is 0 on the right side of the tunnel and increasing counterclockwise.

It is observed that tunnel lining experiences more axial forces as the rock cover is high. When the tunnel support has the maximum overburden depth, 464 m, at chainage 1+340 m, it presents high axial force, shown in Figure 5-18. When the tunnel support passes through chainages 0+410m and 3+681 m respectively, it experiences less axial forces as compared to chainage 1+340 m. Similarly to the previous case study, in this case also, at the corners of the wall and invert, the axial force is more than in the rest of the tunnel, as shown in Figure 5-18.

Bending moment and axial force interaction

Similarly, to the previous case study, in this case also an interaction curve is generated between bending moments and axial forces and compared with the strength of concrete section, as shown in Figure 5.19. It is found that at the high overburden depth, at chainage 1+340 m, some points lie outside the curve due to high induced bending moments, at the corner of wall and invert, as shown in Figure 5.19. Therefore, it suggests increasing the concrete lining thickness at these locations to obtain a stable lining.

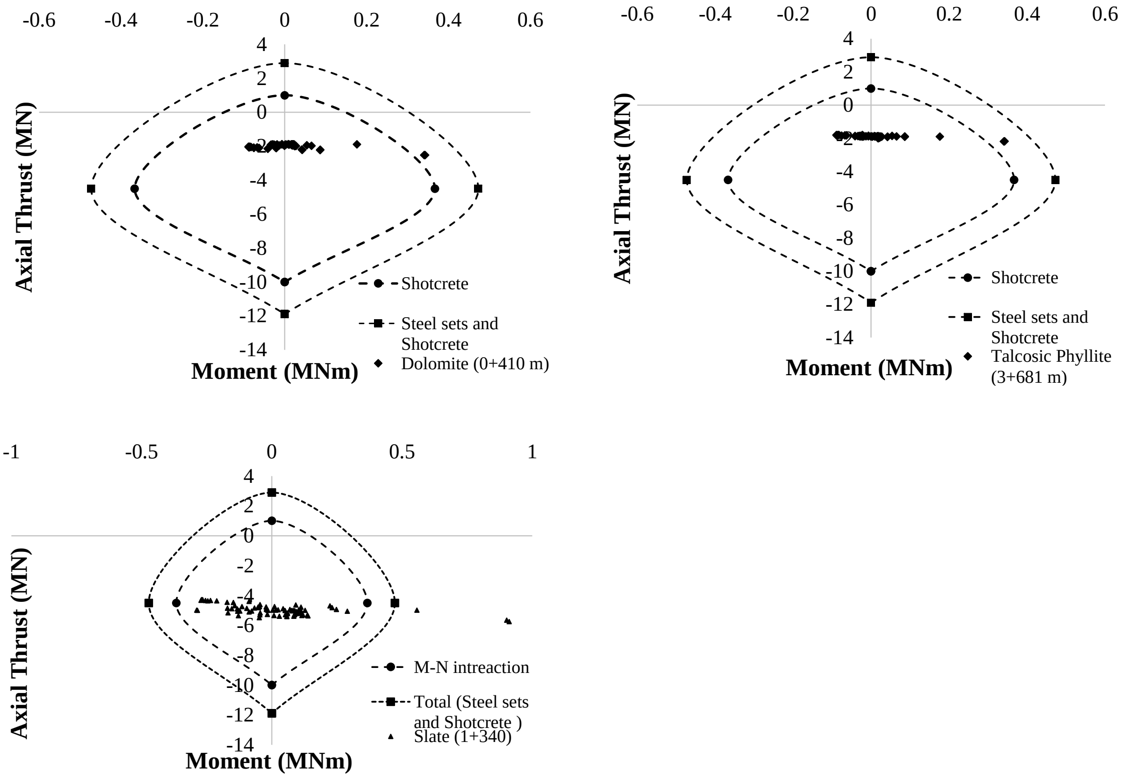

Figure 5-19 M-N interaction curves for different section and comparison of the lining stress state with the strength domain of concrete section.

Deformation of tunnel support

Similarly, the deformation in the both, concrete lining and steel ribs are observed as the tunnel passes through different quality of rock masses. At chainage 0+410 m, the maximum deformation in the concrete lining is 0.015 m at the crown and 0.027m at the wall and invert, as shown in Figure 5-20 (a). As the tunnel section passes through high overburden depth with poor rock mass, at chainage 1+340 m, the deformation in the concrete lining around the tunnel abruptly increases. It is observed that the maximum displacement in the crown is 0.125 m and at wall and invert is 0.2 m, as shown in Figure 5-20 (b).

When the tunnel passes through very poor rock mass with GSI =30, with intact rock mass compressive strength of 35 MPa and overburden depth of 210 m, the displacement in the concrete lining at the crown is 0.021 m and 0.024 m at the wall and invert, as shown in Figure 5-20. There are no significant differences in deformation around the tunnel in such case.

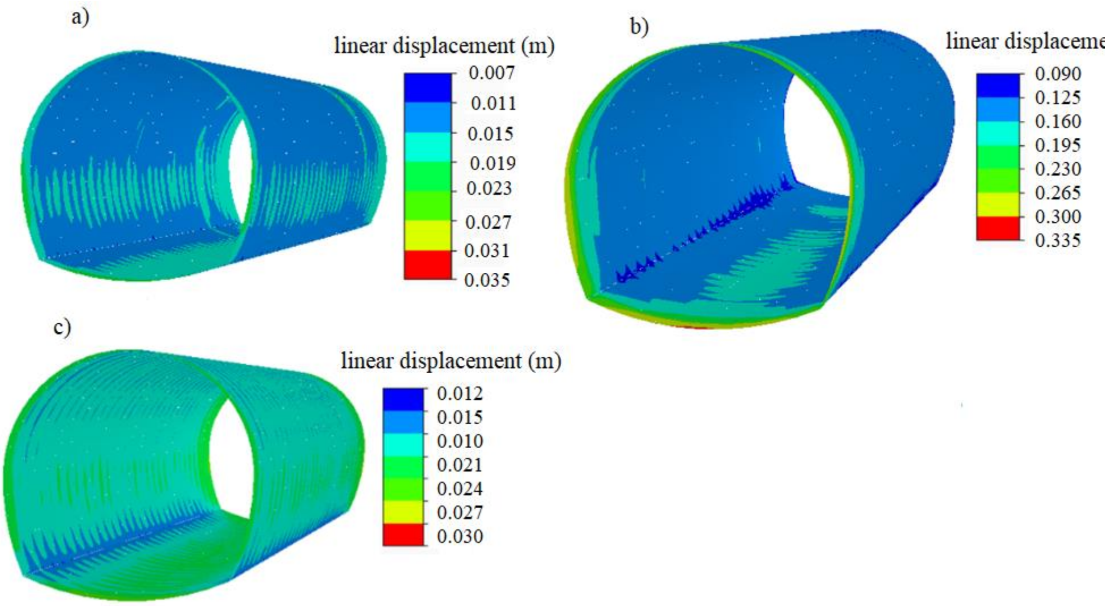

Figure 5-20 Deformation of concrete lining at different tunnel section of Chameliya headrace tunnel; a) 0+410 b) 1+340 c) 3+681

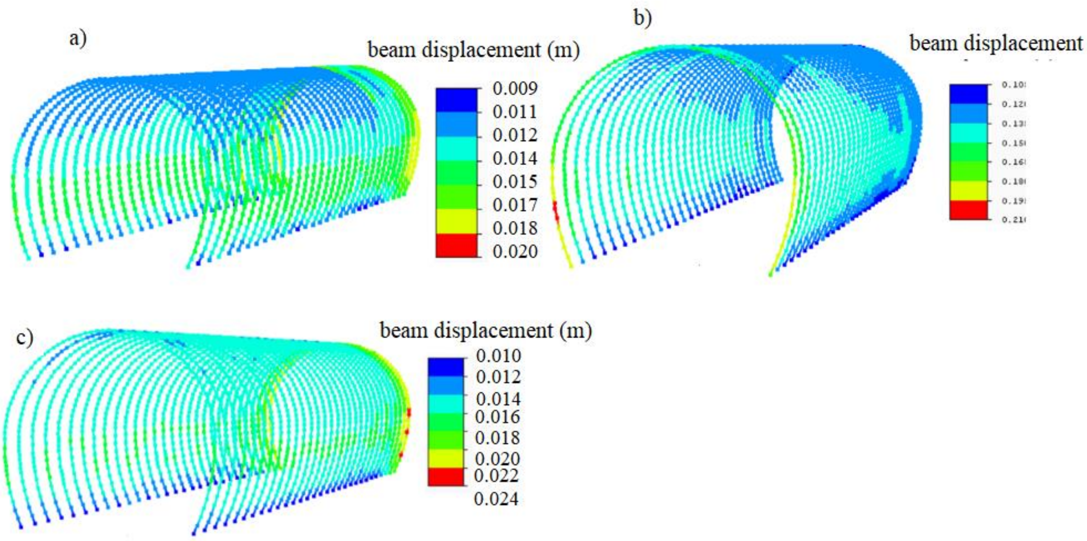

Figure 5-21 Displacement of steel ribs at different tunnel section of Chameliya headrace tunnel; a) 0+410 b) 1+340 c) 3+681

5.6 Concluding Remarks

In this chapter, a numerical analysis was carried out for the different types of rock mass of two hydropower tunnels located in the Lesser Himalayan region. These hydropower tunnels pass through the different types of the rock mass. Based on the rock mass quality, different failure criteria have been proposed for the numerical analysis, as discussed in Chapter 3. For strain-softening case, the residual parameters for modeling of such weak rock mass in this region are taken as 70 and 50 percent of the peak values for different types of the rock mass. It is found that for very poor to poor rock mass (30<GSI<50), the residual parameters for modeling is taken as 70 % of the peak values. Similarly, for fair to good rock mass (50<GSI<65), the residual parameters for modeling is taken as 50 % of the peak values.

The bending moment and axial force interaction curve give the clear idea for selection of the appropriate thickness of concrete lining. At the corners of the wall and the invert, the bending moment and axial forces are highly concentrated compared to the crown and the spring line of the tunnel. An alternative could be to soften the variation of the radius of the tunnel, with a shape closer to the circular one.

It is observed that the maximum bending moment and axial force highly concentrate at the junction of the wall and invert, especially if compared to the crown. The positive bending moment changes into negative causing, tension in the top fiber of the wall and the invert. Therefore, the heavy reinforced concrete lining should be adopted at the invert. Again, it is found that the biggest deformations of the tunnel lining are more at the junction of wall and invert if compared to deformation of the crown of the tunnel. This is in good agreement with the forces observed in the lining.

In the case of the Kulekhani III hydropower tunnel, there are no stability problems in the tunnel cross-section when it passes through the good and fair quality of rock mass. The proposed thickness of concrete lining is sufficient. When the tunnel passes through extremely poor and poor rock mass, there could have been stability problems at the lower corner of the wall and the invert. In the case of the Chameliya hydropower tunnel, the headrace tunnel passes through poor and extremely poor rock mass. The proposed support thickness is found insufficient at the lower corner of the wall and invert, which could cause support failure. Therefore, rock support from the empirical approach is not sufficient to extremely poor and poor rock mass in high overburden stress.

Rock mass classification approach suggest the uniform support around the excavation, but from the numerical analysis, it is observed that the lower corners of the wall and invert are more critical than the crown.

6 CONCLUSIONS

6.1 General

This study is focused on the tunnel closure analysis and stability of underground structures, especially hydropower tunnels, in the Lesser Himalayan region of Nepal. Weak rock mass and high overburden pressure cause excessive deformation and support failure around the tunnel.

A detailed 2D finite element analysis has been carried out for six different hydropower tunnels located in the Lesser Himalayan region. The results are analyzed in terms of tunnel closure. Different rock models are suggested which can address the real behavior of rock mass during the tunneling. For numerical analysis, field and laboratory data and measured tunnel deformation are used for validation of modeling.

The suggested rock models are used for 3D numerical analysis of two case studies of hydropower tunnels located in the Lesser Himalayan region. It is found that these rock models are suitable for numerical analysis of different quality of rock mass of the Lesser Himalayan region of Nepal.

6.2 Major Conclusions

Followings are the main conclusions from these studies:

Numerical modeling of rock mass

1. For extremely poor rock mass, i.e. GSI less than 30, the elastic-perfectly- plastic failure model is more appropriate with the disturbance factor taken as zero. It is found that the disturbance factor has great influence on the modeling of such weak rock mass in the Himalayan region.

2. For the rock mass for which the GSI value is greater than 30, the strain-softening failure model is more appropriate in this region. In this case, the disturbance factor is taken as 0.5. In strain- softening, the residual value is considered by lowering the peak GSI value which represented crushing of the intact rock and wearing joint surface roughness.

3. For very poor to moderately jointed and weathered rock mass (30<GSI<50), the residual strength parameters are taken between 60 and 70 % of peak values while for fair to good, jointed rock (50<GSI<60), the residual strength parameters are taken between 40 and 50% of peak values.

The following conclusions are drawn from the two case studies of Kulekhani III hydropower and Chameliya hydropower tunnels.

Kulekhani III hydropower tunnel

- The suggested numerical modeling discussed in chapter 3 is used for numerical analysis. The strain softening post failure characteristics is used for good, fair and poor rock mass quality at chainage 2+355 m, 3+965 m, and 3+635 m respectively. The residual strength parameters are taken as 50%, 60% and 70 % of peak strength value respectively. In this case, the disturbance factor is taken as 0.5.
- The elastic-perfectly-plastic post failure characteristics are used for the extremely poor rock mass at chainage 3+650 m. In this case, there is no reduction of the peak value. During the analysis, the disturbance factor is taken as 0, considering the controlled blasting.
- It is found that for good quality of rock mass, with GSI=62, both vertical and horizontal stresses are the same as the excavation face is far from the observed section. But when the excavation face is approaching near to the observed section, the vertical stress abruptly increases, and horizontal stress is decreasing and both stresses are remains constant as the excavation face is far from the observed section, Figure 5-5 (a).
- The stress path for very poor to poor rock mass is quite different as compares to the good rock mass. As the excavation proceeds towards the observed section, the vertical stress starts to increase and reaches its maximum when the excavation reaches 5-6 m ahead to observed section, nearly at a distance of two diameters of the tunnel ahead from the tunnel face, and continuously decreases as the excavation face reaches the observed section, and remaining constant as the excavation face is far from the observed section. Similarly, the horizontal stress is continuously decreasing and reaches its minimum value as the excavation reaches the observed section and remains constant as the excavation is far from

the observed section as shown in Figure 5-6 (b) &(c), Figure 5-7(b) &(c) and Figure 5-8 (b) &(c) respectively.

- The major and minor principal stresses are also examined around the tunnel during the advancement of the tunnel in all types of the rock mass. The relation between major and minor principal stresses around the tunnel is shown in Figure 5-5 (a). In this case, the point representing stress lies below the failure plane. It is clear that the rock mass has not yielded as the tunnel face passes through the observed section.
- Similarly, for the very poor to poor rock masses, the minor principal stress starts to decrease while major principal stress gradually increases and, as excavation passes the observed section, both the major and minor principal stress drastically decrease and follow the failure plane, as shown in Figure 5-6(a), Figure 5-7(a) and Figure 5-8 (a) respectively.
- Therefore, it is concluded that the proposed residual strength parameters hold good results for the analysis of weak rock mass in the Lesser Himalayan region of Nepal.
- There is a huge variation of bending moments and axial forces at a different location of the tunnel support. It is found that the bending moment at the lower corner of the wall and invert are much higher than at the crown.
- The axial force is also higher at the lower corner of the wall as compared to the crown. Therefore, the numerical results show invert and lower corner of the wall are more critical than the crown, regarding the design forces in the lining.

Chameliya hydropower tunnel

- For the strain-softening case, the residual strength parameters are taken as 68 % and 62 % of the peak value of poor rock mass at the chainage 0+410 m and 1+340 m respectively.
- The stress paths for advancing tunnel have been carried out, and it is found that, at the observed section, the vertical stress drastically decreases when the tunnel face reaches the observed section while the horizontal stress is gradually decreasing, as shown in Figure 5-9 (b), Figure 5-10 (b), and Figure 5-11(b) at the chainages 0+410 m, 1+340 m, and 3+681 m respectively. Similarly, the point representing the stresses lies below and follow the failure plane as shown in

Figure 5-9 (a), Figure 5-10 (b) and Figure 5-11(b) of the different rock masses. Therefore, it suggests that the proposed numerical model is suitable to model such weak rock mass in the Lesser Himalayan region of Nepal.

- Similarly, it is observed that the bending moment and shear force are much more in the lower corner of the wall and invert of the tunnel as compared to the crown. It is very useful to optimize the concrete lining thickness by using the interaction curve between the bending moment and axial force by comparing with the strength of the concrete section.
- It is found that at the high overburden at chainage 1+340 m, some points lie outside the interaction curve due to high induced bending moment at the lower corner of the wall and the invert as shown in Figure 5-19.

REFERNCES

Barla, G. (1995). Squeezing rocks in tunnels. *ISRM News Journal*, 44-49.

Barla, G. (2002). *Tunnelling under squeezing rock conditions.*

Barla, M. (1999). *Tunnels in swelling ground: simulation of 3D stress paths by triaxial laboratory testing.* PhD thesis: Politecnico di Torino.

Barton , N., Lien, R., & Lunde, J. (1974). *Engineering Classification of Rock Masses for the Design of Tunnel Support.* Rock Mechanics, vol.6, pp. 189--236.

Barton, N. (1995). The influence of joint properties in modelling jointed rock masses. *Proceedings of 8th ISRM congress, Tokyo*, (pp. 1023-1032). Balkema ,Rotterdam.

Barton, N. (2000). Some new Q-value coorelation to assist in site characterization and tunnel design. *International Journal of Rock Mechanics and Mining Sciences, 39*, 185-216.

Basnet , C. B. (2013). *Evaluation on the squeezing phenomenon at the headrace tunnel of chameliya hydroelectric project in Nepal.* Norway: Master Thesis, Norwegian University of Science and Technology.

Bieniawski, Z. T. (1989). *Engineering rock mass classifications.* John Wiley and Sons New York. 251p.

Bin Li, Hong, Y., Bo Gao, Tai Yue Qi, Zheng Zheng Wang, & Ji Ming Zhou. (2015). Numerical parametric study on stability and deformation of tunnel face reinforced with face bolts. *Tunnelling and Underground Space Technology*, 47, pp.73-80.

Cai, M., Kaiser, P. K., Tasaka, Y., & Minami, M. (2007). Determination of residual strength parameters of jointed rock masses using the GSI system. *International Journal of Rock Mechanics & Mining Sciences*, 44, pp.247-265.

Carranza-Torres, C., & Fairhurst , C. (2000). Application of the Convergence-Confinement Method of Tunnel Design to Rock Masses That Satisfy the Hoek-

Brown Failure Criterion . *Tunnelling and underground space Technology*, 15(2), pp. 187-213.

Dhawan, K. R., Singh, D. N., & Gupta, I. D. (2002). 2D and3D finite element analysis of undergroundopenings in an inhomogeneous rock mass. *International Journal of Rock Mechanics & Mining Sciences*, 39, pp.217-227.

Dwivedi , R. D., Singh , M., Viladkar , M. N., & Goel , R. K. (2013). Prediction of tunnel deformation in squeezing grounds. *Engineering Geology*, 161 , pp.55-64.

Dwivedi, R. D., Singh, M., Viladkar, M. N., & Goel , R. K. (2013). Estimation of support pressure during tunnelling through squeezing grounds. *Engineering Geology*, 168, pp.9-22.

Eberhardt, E. (2001). Numerical modelling of three-dimension stress rotation ahead of an advancing tunnel face. *International Journal of Rock Mechanics & Mining Sciences*, 38, pp.499-518.

Eberhardt, E. (2012). The Hoek–Brown Failure Criterion. *Rock Mech Rock Eng*, 45, pp. 981–988.

Galli, G., Grimaldi, A., & Leonardi, A. (2004). Three-dimensional modelling of tunnel excavation and lining. *Computers and Geotechnics*, 171-183.

Goel , R. K., Jethwa, U. L., & Paithakan, A. G. (1995). *Tunnelling through young Himalayas - a case history of the Maneri - Uttarkashi power tunnel* (Vol. 39). Engng. Geol.

Goel, R. K. (1994). *Correlations for predicting support pressures and closures in tunnels.* Ph D thesis, Nagpur University, India.

Goodman, R. E. (1989). *Introduction to Rock Mechanics.* John Wiley & Sons.

Hajiabdolmajid, V., Kaiser, P. K., & Martin, C. D. (2002). Modelling brittle failure of rock. *International Journal of Rock Mechanics & Mining Sciences*, 39, pp. 731-741.

Hoek , E. (1999). Support for very weak rock associated Support for very weak rock associated. *International Symposium on Rock Support and Reinforcement Practice in Mining.* Kalgoorlie, Australia.

Hoek, E. (2007). *Practical Rock Engineering (2007 ed.)*. Retrieved from www.rocscience.com/documents/hoek/corner/Practical-Rock-Engineering-Full-Text.

Hoek, E., & Brown, E. T. (1997). Practical estimates of rock mass strength. *International journal of rock mechanics, mining sciences, 34*, 1165-1186.

Hoek, E., & Diederichs, M. (2006). Empirical estimation of rock mass modulus. *International Journal of Rock Mechanics & Mining Sciences, 43*, 203–215.

Hoek, E., & Diederichs, M. (43 (2006)). Empirical estimation of rock mass modulus. *International Journal of Rock Mechanics & Mining Sciences*, 203–215.

Hoek, E., & Marinos, P. (2000). Predicting tunnel squeezing problems in weak. *Tunnels and Tunnelling International*, part one-November,2000 ,44-51; part two - December, 2000, p 33-36.

Hoek, E., Carranza-Torres, C., & Corkum, B. (2002). Hoek-Brown failure criterion – 2002 Edition. *Proc. NARMS-TAC Conference*, (pp. 267-273). Toronto.

Hoek, E., Kaiser , P., & Bawden , W. (1995). *Support of underground excavations in hard rock.* AABalkema.

Hoek, E., Marinos, P., & Benissi, M. (1988). Applicability of the geological strength index (GSI) classification for very weak and sheared rock masses. The case of the Athens Schist Formation. *Bull Eng Geol Env*, 57, pp. 151-160.

Hsiao, F. Y., Wang, C. L., & Chern, J. C. (2009). Numerical simulation of rock deformation for support design in tunnel intersection area. *Tunnelling and Underground Space Technology, 24,* 14–21.

Humagain , I. R. (2000). *Engineering Geological Studies in Central Nepal with emphasis on Stress Regime and Stability of Slopes and Tunnels.* 75 202 S., 88 Abb., 19 Tab.,5Anl. RWTH Aachen.

Janin, J. P., Dias, D., Emeriault, F., Kastner, R., Le Bissonnais, H., & Guilloux, A. (2015). Numerical back-analysis of the southern Toulon tunnel measurements: A comparison of 3D and 2D approaches. *Engineering Geology*, 195, pp.42-52.

Karakus, M. (2007). Appraising the methods accounting for 3D tunnelling effects in 2D plane strain FE analysis. *Tunnelling and Underground Space Technology*, 22, pp.47-56.

Khadka , S. S. (2013). Seismic Performance of tradationl Unreinforced Masonry Building in Nepal. *Kathmandu University Journal of Science, Engineering and Technology, 9*, 15-28.

Khadka, S. S., Gomes, A. T., Jeon , S., & Maskey, R. K. (2016). Comparative numerical study of 2D and 3D finite element modeling of hydropower tunnels: case study from the lesser Himalayan region of Nepal. *15th National Congress Geotechnics of Portuguese and 8th Luso – Brazilian Congress of Geotechnics.* Porto, Portugal.

Khadka, S. S., Gomes, A. T., Jeon, S., & Maskey, R. K. (2016). Numerical Modeling of weak rock mass with high in-situ stress: case studies through Himalayan hydropower tunnel of lesser Himalayan region of Nepal. *Nepal Tunnelling conference.* Kathmandu, Nepal .

Labuz, J. F., & Zang, A. (2012). Mohr–Coulomb Failure Criterion. *Rock Mech Rock Eng*, 45 , pp.975-979.

Lorig, L. J., & Varona, P. (2013). *Guidelines for numerical modelling of rock support for mines.* Australian Centre for Geomechanics,Perth: ISBN 978-0-9806154-7-0.

Marinos, V., Marinos, P., & Hoek, E. (2005). The geological strength index: applications and limitations. *Bull Eng Geol Environ*, 64, pp. 55-65.

Moller, S. C., & Vermeer, P. A. (2008). On numerical simulation of tunnel installation. *Tunnelling and Underground Space Technology*, 23, pp.461-475.

Nepal Electricity Authority (NEA). (1997). *Detail design report, Kulekhani III hydroelectric project.*

Nepal Electricity Authority (NEA). (2003). *The upgrading feasibility study on hte development of Kulekhani III hydropower project in the Kingdom of Nepal.*

Norwegian Geotechnical Insititute (NGI). (2013). *Rock mass classification and support design.* Oslo, Norway.

Oreste, P. P. (2007). A numerical approach to the hyperstatic reaction method for the dimensioning of tunnel supports. *Tunnelling and Underground Space Technology*, 22, pp.185-205.

Ozsan, A., & Basarır, H. (2003). Support capacity estimation of a diversion tunnel in weak rock. *Engineering Geology*, 68, pp.319–331.

Panthi , K. K., & Nilsen , B. (2007). Uncertainty analysis of tunnel squeezing for two tunnel. *International Journal of Rock Mechanics & Mining Sciences*, 44, pp. 67–76.

Panthi, K. K. (2006). *Analysis of engineering geological uncertainties related to tunnelling in Himalayan rock mass conditions.* Trondhein, Norway : Doctoral thesis, Norwegian University of Science and Technology.

Priest, S. D. (2005). Determination of Shear Strength and Three-dimensional Yield Strength for the Hoek-Brown Criterion. *Rock Mech. Rock Engng., 38*(4), 229-327.

Rocscience Inc. (2016). *RS2, 2D finite element analysis* . Version: 9.008 User Manual.

Rocscience Inc. (2016). *RS3, 3D finite element analysis.* Version: 1.013, Use Manual.

Sari, D., & Pasamehmetoglu, A. G. (2004). Proposed support design, Kaletepe tunnel, Turkey. *Engineering Geology* , 72, pp. 201-216.

Shrestha , P. K., & Panthi , K. K. (2014). Analysis of the plastic deformation behavior of schist and schistose mica gneiss at Khimti headrace tunnel, Nepal. *Bull Eng Geol Environ*, 73, pp. 759-773.

Shrestha , P. K., & Panthi , K. K. (2014). Groundwater Effect on Faulted Rock Mass: An Evaluation of Modi Khola Pressure Tunnel in the Nepal Himalaya. *Rock Mech Rock Eng*, 47, pp. 1021-1035.

Shrestha, G. L. (2005). *Stress induced problems in Himalayan tunnels with special reference to squeezing.* Trondheim, Norway: Doctoral thesis, Norwegian University of Science and Technology.

Shrestha, P. K., & Panthi, K. K. (2015). Assessment of the effect of stress anisotropy on tunnel deformation in the Kaligandaki project in the Nepal Himalaya. *Bull Eng Geol Environ* , 74, pp. 815–826.

Singh , B., & Goel , R. K. (2011). *Engineering Rock Mass Classification: tunnelling, foundations, and landslides.* Elsevier.

Singh, B., & Goel, R. K. (2006). *Tunnelling in Weak Rocks* . Elsevier Geo-Engineering Book Series, Volume 5 .

Singh, B., Jethwa, J. L., Dube, A. K., & Singh, B. (1992). Correlation between observed support pressure and rock mass quality. *Tunnelling and Underground Space Technology, 7*, 59-74.

Singh, M., Singh, B., & Choudhari, J. (2007). Critical strain and squeezing of rock mass in tunnels. *Tunnelling and Underground Space Technology,* 22, pp. 343-350.

Sofiano, A. I., & Nomikos, P. P. (2006). Equivalent Mohr-Coulomb and generalized Hoek-Brown strength parameters for supported axisymmetric tunnels in plastic or brittle rock. *International Journal of Rock Mechanics & Mining Sciences*, 43 , pp.683-704.

Unteregger, D., Fuchs, B., & Hofstetter, G. (2015). A damageplasticitymodelfordifferenttypesofintactrock. *International Journalof Rock Mechanics & Mining Sciences* , 80, pp. 402–411.

Upreti , B. N. (1999). An overview of the stratigraphy and tectonics of the Nepal Himalaya. *Journal of Asian Earth Sciences* , vol. 17, pp. 577-606.

World Stress Map (WSM). (2008). Retrieved from www.world-stress-map.org.

Zhao, J. (2000). Applicability of Mohr-Coulomb and Hoek-Brown strength criteria to the dynamic strength of brittle rock. *International Journal of Rock Mechanics & Mining Sciences*, 37 , pp. 1115-1121.